TECHNISCHE UNIVERSITÄT MÜNCHEN
Department Chemie, Lehrstuhl für Technische Chemie II

Aqueous Phase Reforming of Glycerol over Supported Catalysts

Aonsurang Wawrzetz

Vollständiger Abdruck der von der Fakultät für Chemie
der Technischen Universität München zur Erlangung des akademischen Grades eines
Doktors der Naturwissenschaften (Dr. rer. nat.)
genehmigten Dissertation.

Vorsitzender:		Univ.-Prof. Dr. K. Köhler
Prüfer der Dissertation:	1.	Univ.-Prof. Dr. J. A. Lercher
	2.	Univ.-Prof. Dr. U. K. Heiz

Die Dissertation wurde am 04.11.2008 bei der Technischen Universität München eingereicht und durch die Fakultät für Chemie am 04.12.2008 angenommen.

Acknowledgment

First of all I would like to thank Prof. Johannes A. Lercher for giving me the opportunity to work in his international research group. Thank you for all your great advice, patience, and beneficial discussions.

I would also like to express my great gratitude to Andreas Jentys and Prof. Angeliki Lemonidou for your guidance, fruitful discussion and your time of correcting my thesis.

Moreover, I am thankful for the financial support by the European Union in the framework of the Integrated Project TOPCOMBI (NMP2-CT-2005-515792-2).

This work could not be completed if I did not have the great help from Xavier who supported me not only on the experimental setup but also teaching me German. Thank you also Andreas Marx for supporting me on all the computer's matters. Also, I would like to thank Marianne for introducing me in the use of the electron-microscope and Martin Neukam for your great help on AAS and BET measurements.

It was nice experience at the TC-II group. It was great time that I will never forget. Thank you Wolfgang, Ana, Layhwa and Manuel who shared both enjoy and sorrow with me. Thank you for the great friendship, your care and support as giving me strength to overcome the difficulties. Special thanks to Ana for your great assistance on ATR experiment. Thank you also Roberta and Yongzhong for your tender advice, especially during lunch time, it is always encouraging and motivating me.

Last but not least, I would like to thank with all my heart to my parents, my whole family in Thailand, my loving husband, our parents and the nicest neighbours (Manfred, Helga and Schmigalle family) who always give me cheerfulness and good care.

Aonsurang Wawrzetz

October 2008

Table of Contents

Chapter 1 Introduction 4

1.1 Motivation 5

1.2 Glycerol from bio-diesel production 9

1.3 Hydrogen production processes from renewable resources 11

1.4 Catalyst development for hydrogen production 15

1.4.1 Monometallic catalysts 15

1.4.2 Bimetallic Pt and Pd catalysts 16

1.4.4 Effect of alkali metals addition on catalyst 18

1.5 Scope of the thesis 18

References 20

Chapter 2 Hydrogen production by aqueous-phase reforming of glycerol on supported metal catalysts 22

2.1 Introduction 23

2.2 Experimental Section 26

2.2.1 Catalysts preparation 26

2.2.2 Catalysts characterization 26

2.2.3 Reaction Kinetics Measurements 27

2.3 Results 28

2.3.1 Catalysts characterization 28

2.3.2 Effect of the nature of the metal supported on γ-Al_2O_3 29

2.4 Discussion 33

2.5 Conclusions 37

2.6 References 38

Chapter 3 Influence of metal particle size and reaction conditions on the reaction pathway 40

3.1 Introduction 41

3.2 Experimental Section 44
3.2.1 Catalysts preparation 44
3.2.3 Kinetic Measurements 45
3.2.4 Reaction surface study using ATR-IR spectroscopy 47
3.3 Results 48
3.3.1 Catalysts characterization 48
3.3.2 Influence of platinum particle size 49
3.3.3 Influence of reaction parameters 51
3.3.4 Reactions with liquid phase intermediate products 57
3.3.5 Surface intermediates followed by ATR-IR spectroscopy 61
3.4 Discussion 65
3.5 Conclusions 72
3.6 References 73
Chapter 4 Influence of the nature of the supports on the reaction pathway 76
4.1 Introduction 77
4.2 Experimental Section 80
4.2.1 Catalysts preparation 80
4.2.2 Catalysts characterization 80
4.2.3 Kinetic experiments 82
4.2.4 In situ ATR-IR spectroscopy during reactions 83
4.3 Results 83
4.3.1 Catalysts characterization 83
4.3.2 Catalytic activity 87
4.3.3 Surface reaction study 92
4.4 Discussion 95
4.5 Conclusions 100
4.6 References 101
Chapter 5 Summary 103
Chapter 6 Curriculum Vitae List of publications and presentations 107
6.1 Curriculum Vitae 108

6.2 List of publications 109

6.3 List of presentations..... 110

Chapter 1

Introduction

1.1 Motivation

As the world oil consumption steadily increases, the development of renewable fuels is one of the major interests to maintain the future quality of live. Bio-diesel is among the most promising renewable resources and its demand, shown in Figure 1.1, is expected to be raised until 2020 by 10%. Glycerol is the major by-product of bio-diesel production and has a high possibility of overproduction [1]. Bio-diesel is produced via transesterification of triglycerides in vegetable oil with methanol or ethanol to methyl- or ethyl- esters of fatty acid, as shown in equation 1,glycerol is the main byproduct.

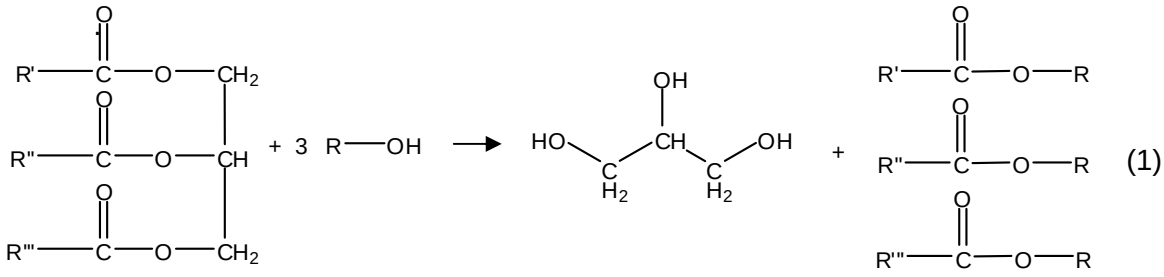

(1)

Triglycerides Methanol/Ethanol Glycerol Methyl/Ethyl Esters

In order to enhance the economy of the bio diesel production process, routes for utilizing the main byproduct glycerol are necessary. Potential reactions include the valorization of glycerol to oxygenated intermediates for the chemical industry but also the production of hydrogen [2]

Hydrogen is considered to be an ideal energy carrier in the future as clean energy source as the only by-product of hydrogen combustion is water vapor (if air is used for flame combustion of hydrogen small amounts of NO_x are produced). Hydrogen can be used as a fuel in furnaces, internal combustion engines, turbines and jet engines, and can also be converted directly to electricity in the fuel cells, with a variety of applications in transportation and stationary power generation. The only limitation in mobile applications is currently the storage of hydrogen. Hence, using glycerol to produce hydrogen is one of

the post promising alternatives for renewable energy sources in the period of diminishing petroleum reserves.

Hence, using glycerol to produce hydrogen is one of the post promising alternatives for renewable energy sources in the period of diminishing petroleum reserves.

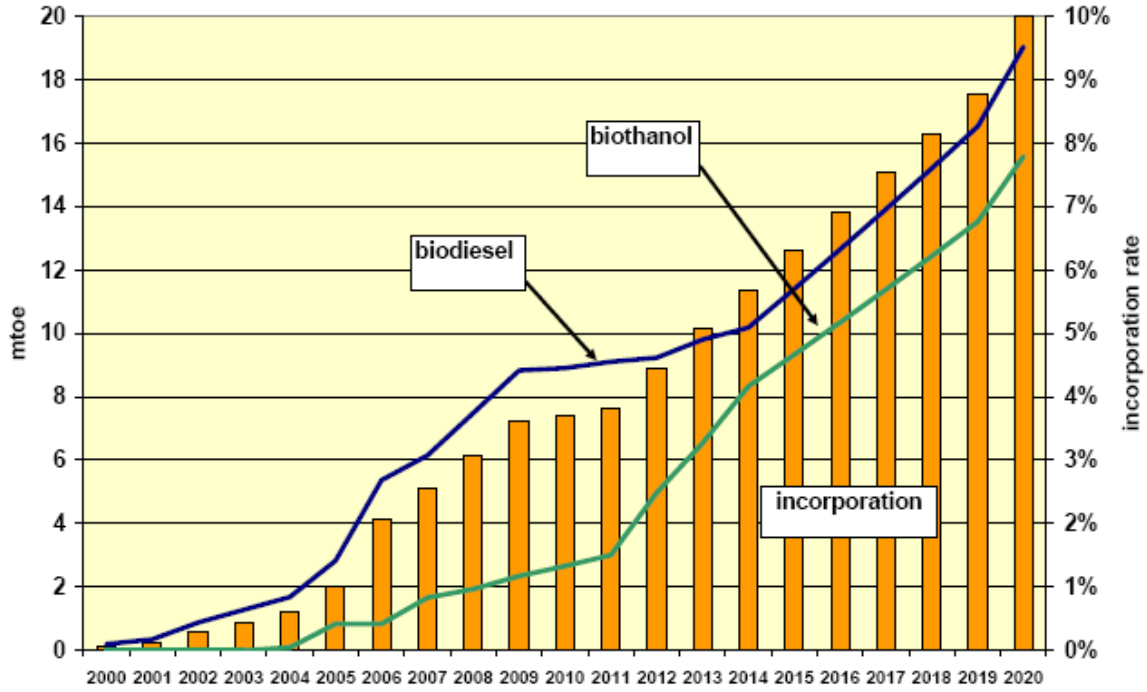

Figure 1.1: Bio-diesel demand forecast in Europe [1]

Currently hydrogen is produced from non-renewable recourses, including natural gas, naphtha and coal, but renewable resources such as biomass [2,3], bio-oil [3,4] and glycerin [3, 5-16] can also be utilized as shown in Figure 1. 2.

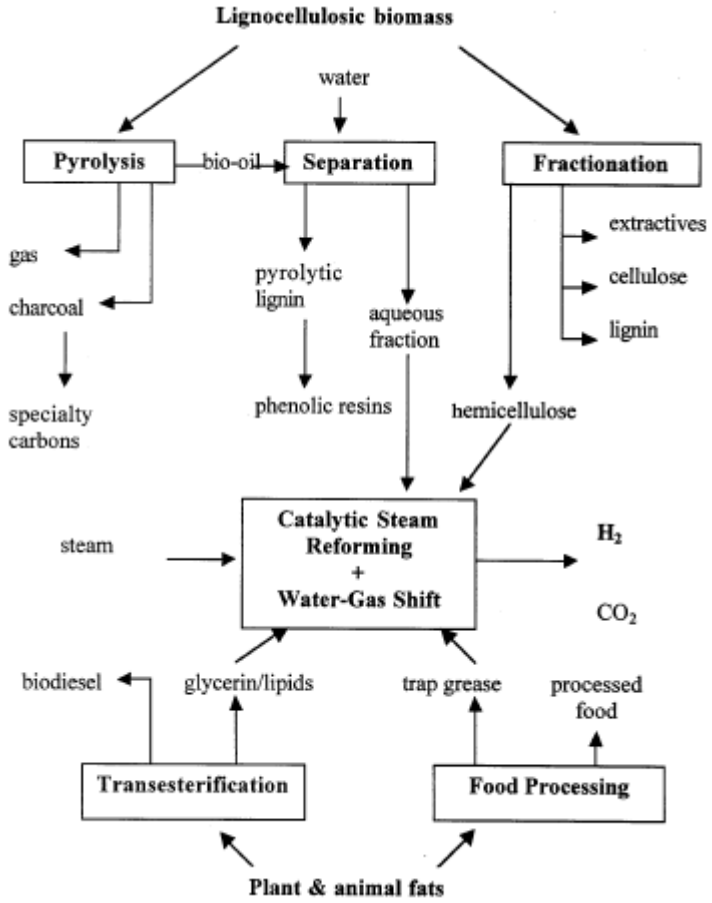

Figure 1.2: Biomass to hydrogen process concepts [2].

The initial concept to produce hydrogen from biomass was introduced by Wang et. al. [2]. In their pioneering work, acetic acid and hydroxyacetaldehyde were chosen as target molecules, which are major liquid products derived from the pyrolysis of carbohydrates in biomass. In their experiments, a series molecules was subjected to steam reforming catalyzed by commercial Ni-based catalysts. Steam reforming of hydroxyacetaldehyde proceeded rapidly over these catalysts without coke formation on the surface of the catalyst at 873 K. The yield to hydrogen from hydroxyacetaldehyde was about 80%, which is slightly higher than from acetic acid (75% hydrogen yield). However, the methane yield from hydroxyacetaldehyde was less than from acetic acid. Wang et.al. [2] also examined the reforming of ethanol, ethylene glycol, glycerol, and acetol over the commercial nickel based catalyst called UCI G-90C. These reactants were almost

completely converted at 673 K in a fixed bed reactor, the hydrogen yield varied between 94 and 100%.

Chornet and co-workers [3] studied hydrogen production from biomass based liquids including pyrolysis bio-oil from sawdust, hemicellulose, trap grease and crude glycerin,. Crude glycerin from transesterification of vegetable oil contains 55% glycerin and methyl esters of fatty acids. The hydrogen yield from crude glycerin was around 77% of the stoichiometric amount. The total conversion of CO in the gas through water gas shift reaction would increase the hydrogen yield to 95% of the theoretically value. Moreover, the steam reforming of waste vegetable oils, particularly “trap grease”, was examined by Chornet and co-worker [5] recently in a fluidized bed reactor using a commercial nickel based catalyst. The conditions of steam reforming were temperatures slightly above 1073 K, a steam-to-carbon (S/C) ratio of 3-5 and a methane-equivalent space velocity of 900-1200 h^{-1}. Under such conditions, 100% of the tap grease was converted to gas. The hydrogen yield during the first 120 hours was 25 g per 100 g of grease, which is 74% of the possible stoichiometric conversion.

Several vegetable oils, for instance, sunflower, rapeseed, corn and soybean oils were also investigated for the production of hydrogen by steam reforming. Marquervich et.al. [18] performed the experiments in an isothermal fixed-bed tubular reactor at steam-to-carbon (S/C) ratios of 9, 6, and 3, at temperatures between 773 and 903 K and at a pressure of 1-2 bar. Both laboratory and commercial Nickel based catalysts were employed. The hydrogen yields from sun flower oil were between 72% - 87%. Results for the steam reforming of sunflower, rapeseed, corn, and soybean oils at the same catalyst temperature and S/C ratio showed that oil conversion to gases and hydrogen yields were not depended on the type of vegetable oil.

The most recent approach of hydrogen production from glycerol was initiated by Dumesic et al. [5-16]. The most effective catalysts on aqueous-phase reforming of oxygenated hydrocarbon solutions were Pt/Al_2O_3, $NiSn/Al_2O_3$, Raney-Ni, and Raney-NiSn

catalysts using temperatures of 473 – 533 K and pressures of 15-50 bar. The major advantage of this process is minimizing the energy which is needed to vaporize both water and the oxygenated hydrocarbon. The oxygenated compounds are non-flammable and non-toxic, allowing them to be stored and handled safely. In addition, aqueous phase reforming (APR) occurs at temperatures and pressures where the water-gas shift reaction is thermodynamic favorable, thus it is possible to generate hydrogen with low amounts of CO in a single stage reactor. Moreover, low temperatures minimize undesirable decomposition reactions which typically occur at high temperatures. Production of H_2 and CO_2 from carbohydrates [5-16] may be accomplished in a single-step, low-temperature process, in contrast to the multi-reactor steam reforming system required for producing hydrogen from hydrocarbons. The current studies reveal the feasibility of hydrogen production from renewable various oxygenated compounds in aqueous phase reforming condition.

1.2 Glycerol from bio-diesel production

Glycerol is the main by-product formed during bio-diesel production. Bio-diesel mainly contains fatty acid methyl or ethyl esters from vegetable oils or animal fats which are produced by the transesterification (also called methanolysis when methanol is used) of vegetable oils and fats with methanol in the presence of acid or base catalysts. In addition, the process yields glycerol. The overall transesterification reaction [19] can be described by three reactions:

$$\text{Triglyceride} + \text{ROH} \xleftrightarrow[\text{catalyst}]{} \text{Diglyceride} + R^{I}\text{COOR} \quad (1)$$

$$\text{Diglyceride} + \text{ROH} \xleftrightarrow[\text{catalyst}]{} \text{Monoglyceride} + R^{II}\text{COOR} \quad (2)$$

$$\text{Monoglyceride} + \text{ROH} \xleftrightarrow[\text{catalyst}]{} \text{Glycerol} + R^{III}\text{COOR} \quad (3)$$

where R^{I}, R^{II} and $R^{II}I$ are long-chain hydrocarbons which may be the same or different with R= $–CH_3/C_2H_5$.

The first step is the conversion of triglycerides to diglycerides, followed by the conversion of diglycerides to monoglycerides and of monoglycerides to glycerol, yielding one methyl ester molecule per mole of glyceride at each step [20, 21]. Catalysts used for the transesterification of triglycerides are classified as alkali, acid, enzyme or heterogeneous catalysts. Most commonly sodium hydroxide, sodium methoxide and potassium hydroxide are used as catalysts, which cause formation of several by-products such sodium salts in the crude glycerol. If the oil has a high content of free fatty acids and water, acid catalyzed transesterification is suitable. The common acids are sulfuric acid, phosphoric acid, hydrochloric acid or organic sulfonic acid.

The general industrial process of bio diesel production is shown in Figure 1.3 [22]. The transesterification of the vegetable oils with methanol catalyzed by basic catalysts (NaOH) in a CSTR or plug flow reactor is the first step in the process. The reaction is carried out at 333 K under atmospheric pressure with a residence time of about 1 hour. The products from the reaction are in two phases: a glycerol-rich phase and a methyl ester-rich phase, which are separated in a settling tank and a centrifuge. The glycerol stream contains mixture of approximately 50 wt % glycerol, the base catalyst and soap. The soap formation from base catalysts can be form via equation 4.

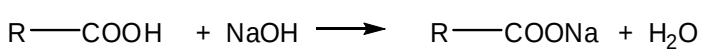

(4)

This fraction is neutralized with acid and the soap forms fatty acids, which are later separated from the glycerol stream. The fatty acid can be recycled and used for bio-diesel production. A vacuum flash process separates the methanol and glycerol phases, yielding 85 wt % crude glycerol. The methyl ester-rich stream, which also contains 2-3 wt % methanol, a small amount of base and small amounts of di- and monoglycerides, is

neutralized prior to methanol removal, which removes the remaining catalyst and soap. The methanol in the methyl ester stream is then stripped by vacuum flash or in a falling film evaporator. Subsequent water washing removes salts and fatty acid from the methyl ester stream. The water remaining in the bio-diesel is removed during a final drying step in a vacuum flash process. Water is also removed from the methanol stream and the remaining methanol is recycled in the process.

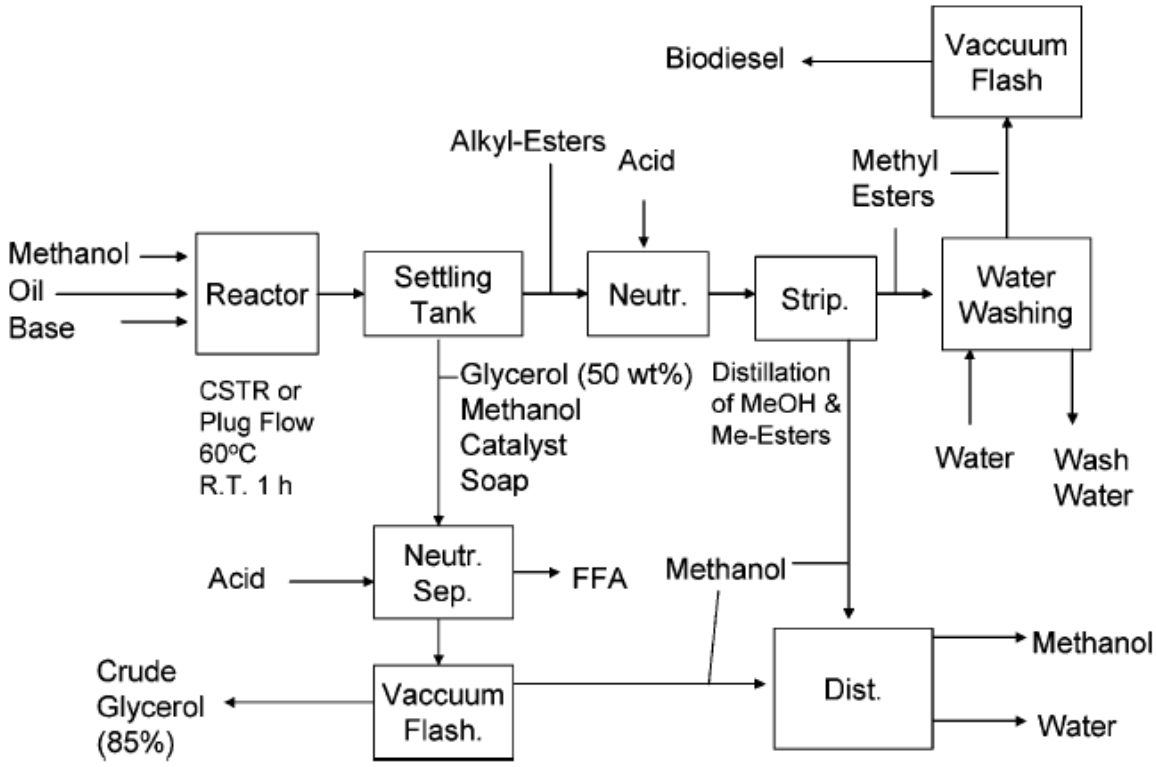

Figure 1.3: Basic technology of bio diesel process [22]

1.3 Hydrogen production processes from renewable resources

The hydrogen production by reforming can be categorized into 2 major approaches: steam reforming and aqueous phase reforming. Steam reforming is a process operated at atmospheric pressure at high temperature (> 673 K) using catalysts based on nickel, cobalt or noble metals, which are typically too expensive for reaction on industrial scale. The most important parameters in the steam reforming process are

temperature, steam-to-carbon (S/C) ratio and catalyst-to-feed ratio. Steam reforming of natural gas is carried out in the range of 1073-1173 K, with a molar S/C ratio in the range of 3-5 and a space velocity of 1500-2000 h^{-1}. High temperature and excess steam favorably shift the equilibrium and increase the rate of the reforming reaction. The reaction between CO and H_2O to H_2 and CO_2 (Water gas shift reaction) is carried out in a separate reactor operating at a lower temperature. Oxygenated organic compounds such as methanol or acetic acid are more reactive than hydrocarbons and therefore, reforming can be carried out at lower temperatures [2].

Steam reforming of oxygenated compounds has been described by Wang et.al. [2], who studied the reforming of ethanol and other alcohols at 673 -973 K and pressures slightly above atmospheric pressure in a fixed-bed micro reactor. The industrial catalysts used, UCI G-90C, contained 15% Ni on a ceramic support ($Al_2O_3/CaAl_2O_4$). At 673 K they observed almost the complete conversion of ethanol, ethylene glycol, glycerol, and acetol at a GHSV = 2240 h^{-1}(0.25 ml catalyst), S/C = 5 and a residence time of 0.02 s. The catalyst showed serious deactivation after a short period of high activity at this temperature.

Chornet and co-workers [3] studied on steam reforming of biomass-derived liquids with a fluidized-bed reactor which provide the better mixed regime than fixed bed reactor. The superheated steam at a pressure slightly above atmosphere was used as a fluidizing gas as well as a reactant in the reforming process. A nickel based catalyst from Sud-Chemie, designed naphtha reforming in a fix bed reactor was used at 1123 K. A high hydrogen yield from crude glycerin was achieved and a deactivation of the catalyst durindg the glycerol steam reforming process was not observed.

The steam reforming reaction of oxygenated organic compounds [2] proceeds via reactions shown in (5) and (6):

• Complete steam reforming:

$$C_nH_mO_k + (n - k)\, H_2O \longrightarrow n\, CO + [(n + m/2 - k)]\, H_2 \qquad (5)$$

• Partial thermal decomposition: (or cracking)

$$C_nH_mO_k \longrightarrow C_xH_yO_z + \text{gas } (H_2, CO, CO_2, CH_4 \ldots) + \text{coke} \quad (6)$$

Because of the excess of steam used in the process, carbon monoxide further undergoes the water gas shift reaction (7):

• Water gas shift reaction:

$$n\ CO + n\ H_2O \longrightarrow n\ CO_2 + n\ H_2 \quad (7)$$

The sum of reaction in equation (5) and (7),

$$C_nH_mO_k + (2n - k)\ H_2O \longrightarrow n\ CO_2 + [(2n + m/2 - k)]\ H_2 \quad (8)$$

Thus, the maximum (stoichiometric) yield of hydrogen that can be obtained by reforming and water gas shift (corresponding to the complete conversion of organic carbon to CO_2) equals 2 + m/2n – k/*n* moles per mole of carbon in the feed. In the case of glycerol, $C_3H_8O_3$, the yield of hydrogen is 2.33 moles per mole of carbon in the feed as described in reaction (9):

$$C_3H_8O_3 + 3\ H_2O \longrightarrow 3\ CO_2 + 7\ H_2 \quad (9)$$

In reality, this yield will always be lower than the stoichiometric maximum because both the steam reforming and water gas shift reactions are reversible, resulting in the presence of some carbon monoxide and methane in the product. In conclusion, steam reforming process leads to higher CO production, rapid catalysts deactivation and higher energy consumption compared to the aqueous phase reforming process in which the energy to vaporize the feed can be eliminated.

The aqueous phase reforming (APR) process is a unique method that generates hydrogen from aqueous solutions of oxygenated compounds in a single step process compared to the three or more reaction steps required for the conventional gas phase reforming processes. The major advantage of the APR process is that the reforming is done in the liquid phase at significant lower temperatures (473 – 533 K) where the water-gas shift reaction is favorable, making it possible to generate hydrogen with low amounts

of CO in a single reactor. Furthermore, the APR process is possible at pressures from 15 to 50 bar where the hydrogen-rich effluent can be effectively purified.

The catalytic pathway for the production of H_2 and CO_2 by aqueous-phase reforming (APR) of oxygenated hydrocarbons involves the cleavage of C–C bonds as well as C–H and/or O–H bonds (Figure 1.4, adapted from reference [10]). Pathway I is the C–C cleavage to form CO adsorbed. The cleavage of these bonds occurs readily over metal compoents of the supported catalysts [6]. The adsorbed CO species can be removed from the surface by the water-gas shift reaction to form CO_2 and H_2.

The byproducts can be formed from parallel and consecutive pathways (Figure 1.4). Parallel reactions proceed via cleavage of C–O bonds followed by hydrogenation to alcohols, or by rearrangement reactions to form organic acids. Alcohol and organic acids can undergo further C-C and C-O cleavage to from alkanes and CO_2. The other side reactions is the hydrogenation of adsorbed CO and CO_2 to form alkanes as shown in the route IV a) and b). It can be concluded that hydrogen can be obtained from route I and water gas shift reaction whereas it can be consumed in route II via C-O cleavage and the methanation reaction. Hence, to develop the catalysts for enhancing hydrogen production, catalysts should have the high activity in C-H, C-C and water gas shift and less activity in C-O cleavage and hydrogenation of CO/CO_2.

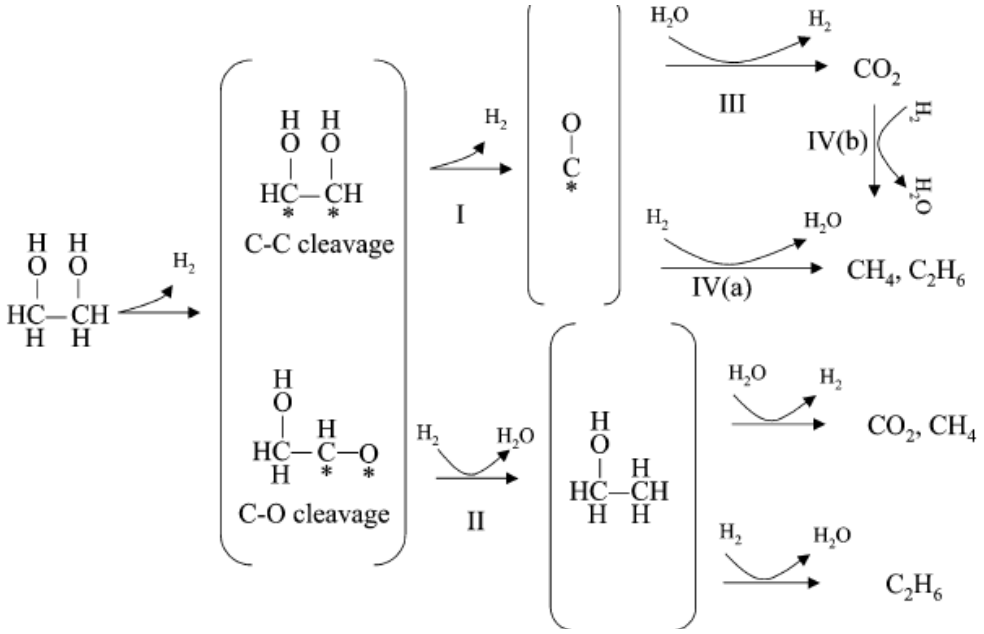

Figure 1.4: Schematic representation of reaction pathways and selectivity challenges for production of H_2 from conversion of ethylene glycol with water [10].

1.4 Catalyst development for hydrogen production

The catalysts developments for reforming of oxygenated compound have been recently studied. In the following a short summary about catalysts for generating hydrogen by steam reforming [28-31] and aqueous phase reforming [5-17] of biomass derived oxygenated compounds, such glycerol ethylene glycol and ethanol is given.

1.4.1 Monometallic catalysts

Aqueous-phase reforming of ethylene glycol over silica-supported Group VIII metal catalysts was conducted in an up flow fixed bed reactor at 483K and 22 bar. The rate of ethylene glycol reforming based on the CO_2 production decreases in the following order Pt~Ni>Ru>Rh~Pd>Ir (as shown in Figure 1.5) [6]. The catalytic activities of Pt and Ni were similar, however, Ni/SiO_2 deactivated fast at 498 K. Pt and Pd provided the highest H_2 selectivity, whereas Rh, Ru and Ni showed a higher selectivity to alkanes. For

the hydrogen production with less alkenes formation, Pt-based catalysts were most promising.

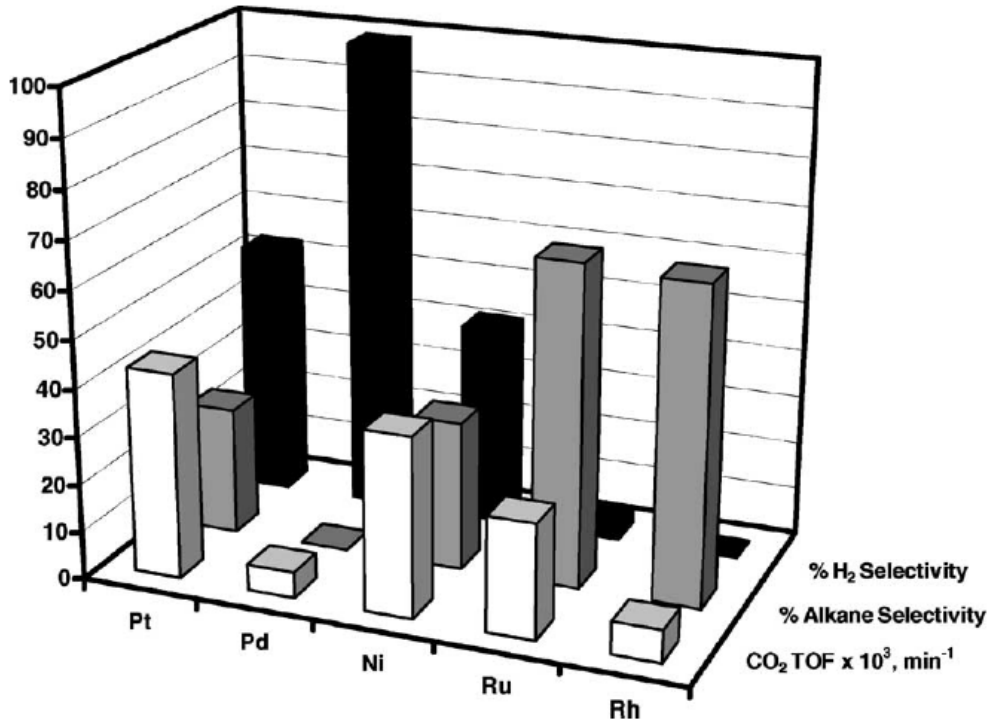

Figure 1.5: Comparison of catalytic performance of metals for aqueous-phase reforming of ethylene glycol at 483 K and 22 bar (grey bar: CO_2 TOF × 10^3 (min^{-1}); white bar: % alkanes selectivity; black bar: % H_2 selectivity) [6].

1.4.2 Bimetallic Pt and Pd catalysts

The activity of Pt catalysts can be improved further by adding Ni, Co or Fe to a Pt/Al_2O_3 catalyst [11]. PtNi and PtCo catalysts supported on Alumina with varying atomic ratios from 1:1 to 1:9 provided hydrogen formation rates of 2.8-5.2min^{-1} for APR of ethylene glycol solutions at 483 K which is higher than that for Pt/Al_2O_3 (1.9 min^{-1}) under the same reaction conditions. Moreover, Pt_1Fe_9/Al_2O_3 catalyst showed higher hydrogen turnover frequencies of approximately 4.3 min^{-1} at 483 K. It is suggested that bimetallic catalysts of Pt combined with Ni, Co or Fe improves the activity for H_2 production by decreasing in the heat of adsorption for CO and H_2 due to lowering the d-band center of

Pt which results in a higher availability of the surface for reaction with ethylene glycol. The similar results on steam reforming were found by Song et.al. [28], whostudied steam reforming of bio-ethanol at temperatures less than 723 K over Rh-Ni bimetallic catalyst supported on CeO_2. It was discovered that the role of Rh is to form H_2 and CO_x via the cleavage of the C–C and C–H bonds of ethanol, while addition of Ni enhanced the water gas shift reaction. In general, bimetallic catalysts have a significantly higher activity than monometallic catalysts on hydrogen production of APR and steam reforming process by adding the proper metal which helps enhancing through the water gas shift reaction.

1.4.3 Catalysts support

Aqueous-phase reforming of 10wt% ethylene glycol solutions was studied at temperatures of 483 and 498K at pressure of 22.4 and 29.3 bar over Pt supported on TiO_2, Al_2O_3, carbon, SiO_2, SiO_2-Al_2O_3, ZrO_2, CeO_2 and ZnO [12] as well as Pt-black. Platinum catalysts were prepared by incipient wetness impregnation of various supports with aqueous solutions. The different supports exhibited a strong influence on rate for hydrogen formation due to the different of acid-base properties which promotes the side reaction (C-O cleavage). Based on the turnover frequency for H_2 Pt black, Pt supported on Al_2O_3 TiO_2 and carbon exhibited high activity for aqueous-phase reforming of ethylene glycol. In contrast, Pt supported on carbon, TiO_2, SiO_2-Al_2O_3 and Pt-black produced higher amounts of gaseous alkanes and liquid-phase compounds (ethanol, acetic acid and acetaldehyde).

Suzuki et al. [29] compared catalysts with Group 8-10 metals supported on Y_2O_3, ZrO_2, CeO_2, La_2O_3, SiO_2, MgO and Al_2O_3 prepared by the impregnation method. The reforming process of glycerol was conducted at atmospheric pressure and temperature above 623 K. The products were mostly gaseous including hydrogen, carbon dioxide, carbon monoxide and alkanes. The steam reforming reaction of glycerol is influenced by catalysts carriers on glycerol conversion due to its surface area and metal dispersion

properties. Suzuki and coworker found that Ru supported on Y_2O_3 gave the highest glycerol conversion and hydrogen selectivity (85%) compared to ZrO_2, CeO_2, La_2O_3, SiO_2, MgO and Al_2O_3. The results of the stability test of 3wt%Ru/Y_2O_3 showed only a slight decrease in the glycerin conversion on the reaction time, and little carbon was deposited on the catalyst. These results indicate that the performance of the Ru/Y_2O_3 catalyst in the steam reforming of glycerin is very high.

1.4.4 Effect of alkali metals addition on catalyst

Carbon deposition has been shown as the main reason to cause deactivation of catalysts in steam reforming of oxygenated hydrocarbons. The addition of alkali metals can decrease the deactivation rate [30,31]. King and coworker [30] have reported that Rh/CeO_2-ZrO_2 is selective to H_2 at temperatures of 623 K for ethanol steam reforming. However, the catalyst deactivates fairly rapidly. An improvement of catalyst stability was achieved by adding of 0.5% K (as KOH), however, it decreased in the catalyst activity by about 20% compared to the un-promoted catalyst. In addition, sodium addition on cobalt-based catalysts for steam reforming (623–723 K) of bio-ethanol was demonstrated [ref]. The catalysts preparation was done by co-precipitation method from nitrate salts and sodium carbonate. an increase of H_2 yield (5-8%) and catalyst stability were found compared to the unpromoted materials.. With the highest loading of sodium (about 1 wt%) exhibited the best activity and the highest stability for more than 240 hours.

1.5 Scope of the thesis

The production of hydrogen for fuel cell and other industrial application for renewable biomass-derived resources is a major challenge as global energy generation moves towards a hydrogen society. Nowadays the worldwide trend of increasing production of these fuel results in the overproduction of glycerol. The ideal alternative

would be to produce hydrogen and chemical from glycerol in the single stage at the moderated reaction conditions. Thus, aqueous phase reforming of glycerol is an attractive technique due to low temperature requirements, less CO production and possible value added by-products formation.

The catalysts and process development for aqueous phase reforming of glycerol were studied with respect to the effects of different metals supported on γ-Al_2O_3 (chapter 2), the effect of reaction conditions, particle size as well as reaction pathway study of potential catalysts (Pt/Al_2O_3) by ATR-IR spectroscopy (chapter 3) and the influence of different support materials (chapter 4).

Chapter 2 focuses on the feasibility of hydrogen production from glycerol by aqueous phase reforming on Pt, Pd, Ni, Ru and Rh supported on γ-alumina and the effect of the different metals on the selectivity. Pt/Al_2O_3 showed the highest hydrogen production rate with low CO content as well as a high potential for the formation of value added products, especially, 1,2-propanediol. Further studies of the reaction pathway and the influences of operating conditions over Pt supported on Al_2O_3 catalyst were investigated in chapter 3. The effects of Pt particle size and reaction conditions led to an understanding of the reaction network and to the identification of the intermediates. The details of the reaction pathway were revealed by studying aqueous phase reforming of intermediates (Lactic acid and Hydroxyacetone) and by investigating the surface of the catalysts under reaction conditions by attenuated total reflection infrared (ATR-IR) spectroscopy Chapter 4 illustrates the influence of acid-base and reducibility properties of various supports on the reaction network. The summary of the major results and conclusions of this thesis are described in Chapter 5.

References

1. Economic analysis of EU agriculture, Brussels, April 2007.
2. D. Wang, D. Montane´ ,E. Chornet , Appl. Catal. A 143 (1996) 245.
3. S. Czernik, R. French, C. Feik, E. Chornet, Ind. Eng. Chem. Res. 41 (2002) 4209.
4. K. Takanabe, K. I. Aika, K. Seshanb, L. Lefferts, J. Catal. 227 (2004) 101.
5. R. D. Cortright, R. R. Davda, J. A. Dumesic, Nature 418 (2002) 964.
6. R. R. Davda, J. W. Shabaker, G. W. Huber, R. D. Cortright, J. A. Dumesic, Appl. Catal. B Environmental 56 (2005) 171.
7. J. W. Shabaker, G. W. Huber, J. A. Dumesic, J. Catal. 222 (2004) 180.
8. G. W. Huber, J. W. Shabaker, J. A. Dumesic, Science 300 (2003) 2075.
9. R. R. Davda, J. W. Shabaker, G. W. Huber, R. D. Cortright, J. A. Dumesic, Appl. Catal. B Environmental 56 (2005) 171.
10. G. W. Huber, J. A. Dumesic, Catal. Today 111 (2006) 119.
11. J. W. Huber, J. W. Shabaker, S. T. Evans, J. A. Dumesic, Appl. Catal. B Environmental 62 (2006) 226.
12. R. R. Davda, J. W. Shabaker, G. W. Huber, R. D. Cortright, J. A. Dumesic, Appl. Catal. B Environmental 43 (2003) 13.
13. J. W. Shabaker, G. W. Huber, R. R. Davda, R. D. Cortright, J. A. Dumesic, Catal. Lett. 88 (2003) 1.
14. J. W. Shabaker, D. A. Simonetti, R. D. Cortright, J. A. Dumesic, J. Catal. 231 (2005) 67.
15. J. W. Shabaker, R. R. Davda, G. W. Huber, R. D. Cortright, J. A. Dumesic, J. Catal. 215 (2003) 344.
16. J. W. Shabaker, J. A. Dumesic, Ind. Eng. Chem. Res. 43 (2004) 3105.
17. S. Czernik, R. J. French, K. A. Magrini-Bair, E. Chornet, Energy & Fuels 18 (2004) 1738.

18. M. Marquevich, X. Farriol, F. Medina, D. Montane´,
Ind. Eng. Chem. Res., 40 (2001) 4757.

19. J. Otera, Transesterification. Chem. Rev. 93(4) (1993) 1449.

20. B. Freedman, R. O. Butterfield, E. H. Pryde,
J. Am. Oil. Chem. Soc. 63(10) (1986) 1375.

21. H. Noureddini , D. Zhu, J. Am. Oil. Chem. Soc. 74 (11) (1997) 1457.

22. J. V. Gerpen, G. Knothe, Biodiesel Handbook, AOCS Press Champaign, IL,
(2005).

23. J. H. Sinfelt, D. J. C. Yates, J. Catal. 8 (1967) 82.

24. D. C. Grenoble, M. M. Estadt, D. F. Ollis, J. Catal. 67 (1981) 90.

25. M. A. Vannice, J. Catal. 50 (1977) 228.

26. H. V. Fajardo, L. F. D. Probst, Appl. Catal. A General 306 (2006) 134.

27. J. Rostrup-Nielsen, Phys. Chem. 3 (2001) 283.

28. J. Kugai, S. Velu, C. Song, Catal. Lett. 101(2005) 255.

29. T. Hirai, N. Ikenaga, T. Miyake, T. Suzuki, Energy & Fuels 19 (2005) 1761.

30. H. S. Roh, A. Platon, Y. Wang, D. L. King, Catal. Lett. 110 (2006) 1.

31. J. Llorca, N. Homs, J. Sales, J. G. Fierro, P. R. Piscina, J. Catal. 222 (2004) 470.

Chapter 2

Hydrogen production by aqueous phase reforming of glycerol on supported metal catalysts

Abstract

Hydrogen produced from renewable feedstocks such as crude glycerol, which is the main by-product formed during bio-diesel production, will develop into an attractive alternative energy source in the near future. Hydrogen production by a low temperature process is studied by using transition metal catalysts supported on gamma alumina. The highest H_2 rate was achieved over Pt followed by Pd, and decreased for Pd > Pt > Rh > Ru > Ni (all supported on γ-Al_2O_3). Moreover, the alkane selectivity of Pd and Pt were the lowest (<1%), however, Pd catalyst produced highest amount of CO. The major liquid phased product is 1, 2-propanediol which is formed in the high quantity from Ru (42%) and Pt (30%) catalysts. Thus, Pt/γ-Al_2O_3 is the potential catalyst for aqueous phase reforming of glycerol due to high amount of hydrogen and 1,2-propanediol formation with low CO content.

2.1 Introduction

In recent years, the interest in hydrogen production from sustainable resources has been grown significantly as the future economics will depend on alternatives in the coming era of limited availability of fossil based fuels. Glycerol is the main biomass-derived by-product formed in bio-diesel production and the worldwide trend of increasing production of bio-fuels results already in an overproduction of glycerol. In Europe, the production of glycerol in 2004 reached 350,000 tons [13], thus, using glycerol to produce hydrogen is an attractive route for the production of renewable hydrogen. However, economic routes for the production of hydrogen from renewable biomass-derived resources still remain to be developed.

Hydrogen production from glycerol has been studied through aqueous-phase reforming [4-11], conventional steam reforming [1-3] as well as by thermal processes utilizing metal complexes as homogenous catalysis. Cole-Hamilton studied the hydrogen

production from oxygenated compounds [14-17] catalyzed by ruthenium and rhodium complexes in the presence of sodium hydroxide at 393 K. The rate (catalysts turnover) of hydrogen formation from glycerol [14] was in the range of 12.4 – 37.6 hourly, which was much less efficient compared to other substrates such as, e.g. 1,2-ethanediol. Steam reforming of glycerol Using a commercial nickel-based catalysts was studied in the gas phase in fixed bed reactors by Chornet et.al. [1,2]. The catalysts showed a serious deactivation at 673 K after a short period of high activity at a high steam to carbon ratio of 5 [1]. Suzuki and co-workers [3] investigated the steam reforming of glycerol by ruthenium supported on different oxide supports and reported almost 100% glycerol conversion over Ru on Y_2O_3 and ZrO_2 with a hydrogen selectivity around 80%. The Ru/Y_2O_3 catalysts did not deactivate during 24 hours, however, the concentration of CO in the gas was higher for steam reforming [1-3] compared to the aqueous phase reforming process [4-11]. The general advantage of this single stage reaction to hydrogen is the lower formation of CO (less than 1000 ppm) due to thermodynamic favorable equilibrium of the water gas shift reaction at low temperatures. Moreover, the energy consumption is lower as the reaction is carried out in the liquid phase and, hence, the feed is not needed to be vaporized. Therefore, aqueous phase reforming reaction is a fascinating approach for the production of hydrogen from renewable sources.

Aqueous-phase reforming process of oxygenated hydrocarbons was described by Dumesic and co-workers [4-11] mainly using 1, 2 ethanediol as a model reactant for higher oxygenated hydrocarbons such as glycerol and sorbitol.

The overall reaction of aqueous-phase reforming of glycerol can be described by equation (3)

C-C bond cracking of glycerol:

$$C_3H_8O_3 \longrightarrow CO + 4H_2 \qquad (1)$$

Water gas shift reaction:

$$CO + H_2O \longleftrightarrow H_2 + CO_2 \quad (2)$$

Overall reaction of aqueous phase reforming (1) + (2)

$$C_3H_8O_3 + 3\,H_2O \longleftrightarrow 3CO_2 + 7\,H_2 \quad (3)$$

For aqueous phase reforming of glycerol was studied using Pt/Al_2O_3 and Raney-NiSn as catalysts [4, 5, 7] with glycerol concentrations of 1wt % at temperatures between 489 and 538 K and pressures of 29 to 56 bar by Cortright et al. [4]. Note that the pressure in the aqueous phase reforming reaction is typically adjusted to be only slightly above the vapor pressure of the reactant. In these experiments Raney-Ni catalysts showed the higher selectivity for H_2 (~81%) compared to the Pt catalysts (~ 75%) at conversions of glycerol above 90 % The addition of Sn to Raney Ni catalysts significantly reduced the rate of methane formation, while maintaining high rates for C–C cleavage. However, it was necessary to operate only slightly above the vapor pressure of the feed and at moderate space times to achieve high selectivities for production of H_2 over Raney-NiSn catalysts whereas for the Pt catalyst a wider range of operation conditions could be used.

Hydrogen production from glycerol by aqueous phase reforming is a promising technique, however, further catalyst development in order to lower the CO formation as well as high value added by-products formation are required. In the present work the influence of the nature of different metals supported on γ-Al_2O_3 (Pt/Al_2O_3, Pd/Al_2O_3, Ni/Al_2O_3, Ru/Al_2O_3 and Rh/Al_2O_3) on the activity and selectivity for aqueous-phase reforming of glycerol is described. The role of different metal on the reaction pathways of aqueous phase reforming of glycerol will be discussed.

2.2 Experimental Section

2.2.1 Catalysts preparation

A series transition metals including Pt, Pd, Ru, Rh and Ni were supported on γ-Al_2O_3 by incipient wetness impregnation. The precursor salts were palladium (II) nitrate solution 10 wt% in nitric acid (Aldrich), platinum (II)-ammonium nitrate (Strem chemicals), ruthenium (III) nitrosyl nitrate solution (Strem chemicals), rhodium (III) nitrate solution (Strem chemicals) and nickel (II) nitrate (Aldrich). The support was γ-Al_2O_3 from Degussa with a surface area of 150 m²/g (Aerosil). After impregnation of the support with the minimum amount of aqueous precursor solution (2.2 g solution / g support), the catalysts were dried under air at 393 K for 12 hours and subsequently calcined in synthetic air for 2 hours at 573 K with the rate of 1K/min. Prior to the reaction kinetic tests and characterization, Ni, Ru and Rh supported on Al_2O_3 were reduced in H_2 at 723 K and Pt and Pd supported on Al_2O_3 were reduced in H_2 at 623 K [31] for 2 hours using a heating rate of 0.5 K/min.

2.2.2 Catalysts characterization

Atomic absorption spectroscopy (AAS)

The concentration of the metal was determined by atomic absorption spectroscopy using a UNICAM 939 AA-Spectrometer. Typically 20-40 mg of the sample was dissolved in a mixture containing 0.5 ml of hydrofluoric acid (48%) and 0.1 ml of nitro hydrochloric acid at the boiling point of the mixture (ca. 383 K).

Hydrogen Chemisorption

The fraction of accessible Pt, Pd, Ni, Ru and Rh atoms was determined by H_2 chemisorption measurements using a Sorptomatic 1990 Series sorptometer (Porotec Sorptomatic 1990 Automated BET). Approximately 1g of catalyst was reduced in H_2 at

588 K (Pt and Pd) or at 673 K (Ni, Ru and Rh) for 1h and subsequently evacuated overnight. All isotherms were measured at 308 K. The amount of chemisorbed hydrogen was determined after removing physisorbed hydrogen from the sample by evacuation at 35°C. The hydrogen uptake on the sample was determined by extrapolating the linear part of the adsorption isotherm to zero pressure assuming a H/Pt ratio of 1 [12].

Nitrogen physisorption

The BET surface area and pore size distribution were determined by N_2 adsorption–desorption at 77 K using a Sorptomatic 1990 Series instrument after activation of the sample in vacuum at 573 K.

2.2.3 Reaction Kinetics Measurements

The activity of the catalysts for the aqueous-phase reforming of glycerol was studied in a laboratory reactor system, the scheme is shown in Figure 2.1. The reactor was a stainless-steel tubular reactor (5 mm-id) containing a packed bed of the pressed and crushed catalyst (50-200 mg) with a particle size of 300 - 500 µm. A liquid solution of 10wt % glycerol (spectrophotometer grade, ≥99.5%, Aldrich) in deionized water was introduced in an up-flow configuration with a HPLC pump. The liquid and gaseous products leaving the reactor were cooled in a heat exchanger to liquefy condensable vapors. The effluent was mixed with nitrogen and the two phases were separated after the 16-port sampling valve by condensation. The liquid samples were analyzed in a gas chromatograph with FID/GCMS detector and CP-Wax 57 CB column. To ensure the detection of all carbon containing species in the liquid products, the liquid samples were additionally analyzed by elemental analysis (Elementar Vario EL). Gaseous products were analyzed on line by a gas chromatograph with TCD detector and two capillary columns (MS-5S and Para Plot Q). The catalytic activity tests were carried out at 498 K and 29 bar using an aqueous solution containing 10 wt% glycerol. The LHSV was between 44-83 h^{-1} in order to maintain conversion levels at similar range 5%, which

allows treating the data with a differential kinetics model. Prior to the reaction the catalysts were reduced in H_2 and before the reaction the system was purged and pressurized with nitrogen. The carbon products selectivity was calculated by following equation 1. The carbon balance is in ±5% errors.

$$Carbon\ Selectivity\ of\ species\ i\ (\%) = \frac{C\ atom\ in\ species\ i\ of\ products}{Converted\ glycerol\ based\ on\ carbon\ atom} \times 100 \quad (1)$$

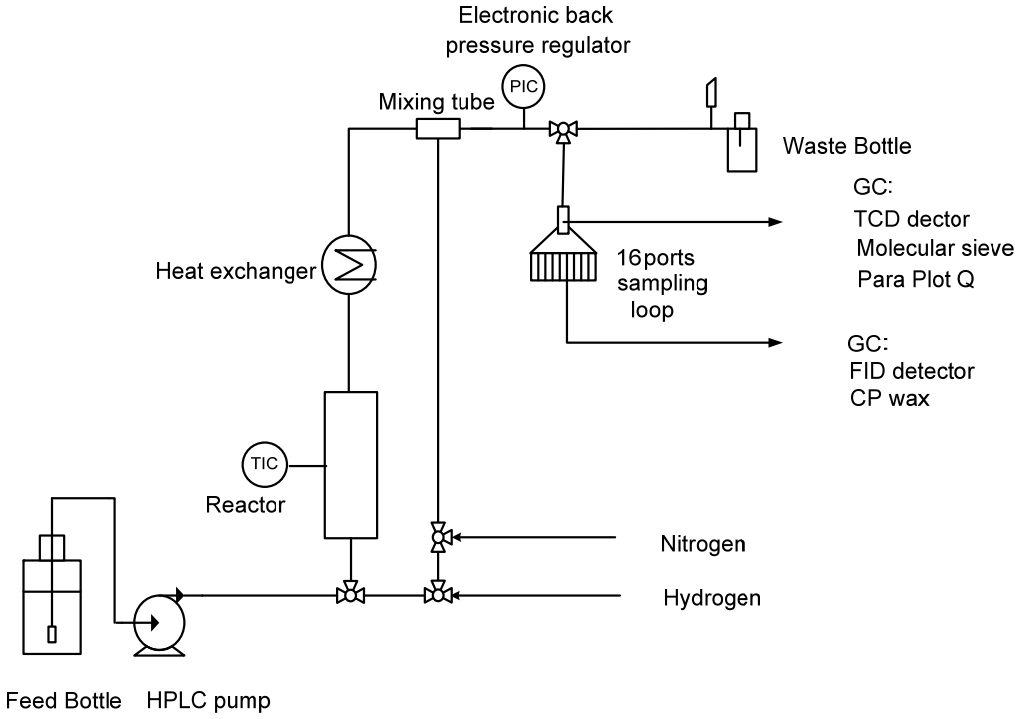

Figure 2.1: Reactor used for kinetic experiments

2.3 Results

2.3.1 Catalysts characterization

The specific surface area and the metal dispersion of the catalysts are summarized in Table 2. 1. The surface areas of all catalysts are in the same range, while the metal dispersion of the Pt/Al_2O_3 was the highest (98 %) and decreased down to 7%

for the Ni/Al_2O_3 catalyst. The loading of the metal is about 150 mmol/g catalysts except nickel which contains 2.5 mmol/g.

Table 2.1 Properties of the catalysts used

Catalysts	Surface area (m^2/g)	H/Metal ratio
2.97 wt% Pt/Al_2O_3	116	0.75
14.7 wt% Ni/Al_2O_3	95	0.08
1.6 wt% Pd/Al_2O_3	108	0.46
1.6 wt% Ru/Al_2O_3	104	0.82
1.6 wt% Rh/Al_2O_3	118	0.94

2.3.2 Effect of the nature of the metal supported on γ-Al_2O_3

The H_2 rate of the catalysts (as shown in Figure 2.2) followed the order Pt > Pd > Rh > Ru > Ni at 498 K and 29 bar whereas the alkane selectivity (Figure 2.3) which mainly methane generally decreased in the following order Ni > Rh > Ru >Pt > Pd.

The main carbon containing products from Pt, Ni, Rh and Ru catalysts in the gaseous product stream were mainly CO_2 (20-35%). Only over the Pd catalyst a significant formation of CO was detected, while the CO/CO_2 ratios of the other catalysts, decreased in the order Ru > Rh >Ni> Pt as shown in Figure 2.4.

The liquid products contained alcohol (methanol, ethanol and propanol), aldehyde (acetaldehyde and propanal), acid (lactic acid, propanoic acid and acetic acid) hydroxyacetone, 1,2-propanediol, 1,2-ethanediol and 1,2-ethanediol. The products

selectivity based on carbon atom of by-products in the liquid phase at 498 K and 29 bar over the different catalysts are compared in table 2. 2. The carbon balance of liquid and gas products could be determined within ± 5% error. All catalysts produced hydroxyacetone and 1, 2-propanediol. In general, Pd and Pt catalysts produced more C1 and C2 oxygenated compounds (1, 2-ethanediol, methanol, acetic acid and ethanol) compared to Ni, Ru and Rh, while Rh and Ru generated mostly C3 oxygenated hydrocarbons (hydroxyacetone, 1, 2 propanediol, 1, 3 prodanediol and lactic acid). The acid production (mainly acetic acid) is produced in high extent over Pd catalysts. Pure alumina formed low quantity of ethanol and mostly C3 oxygenated products including hydroxyacetone, propanol, propanoic acid and small amount of propanal. Gaseous product from alumina is mainly carbon dioxide and small amount of ethane.

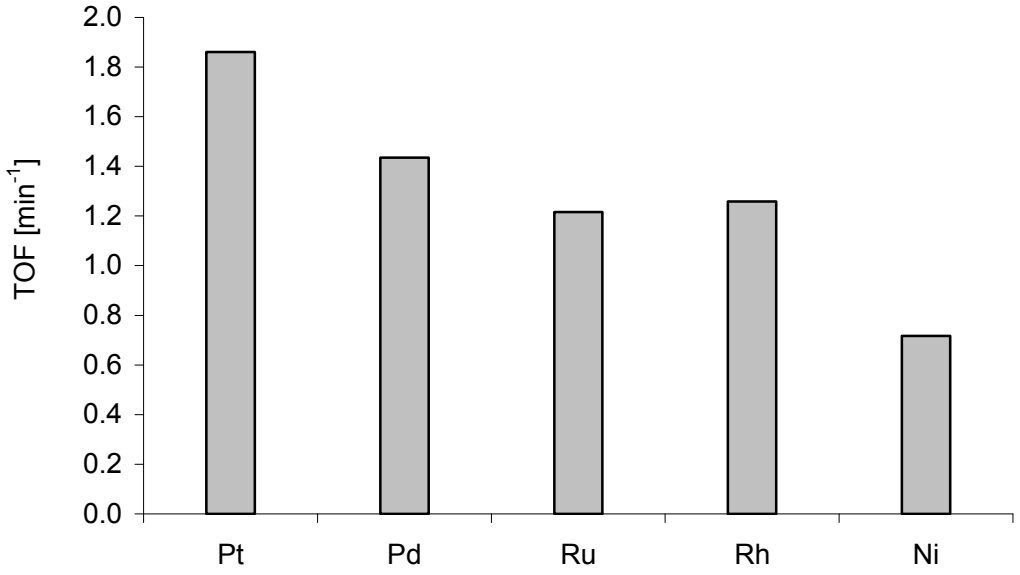

Figure 2.2: Turnover frequency based on hydrogen (Experimental conditions: T= 498 K, total pressure = 29 bar, Glycerol concentration = 10wt %)

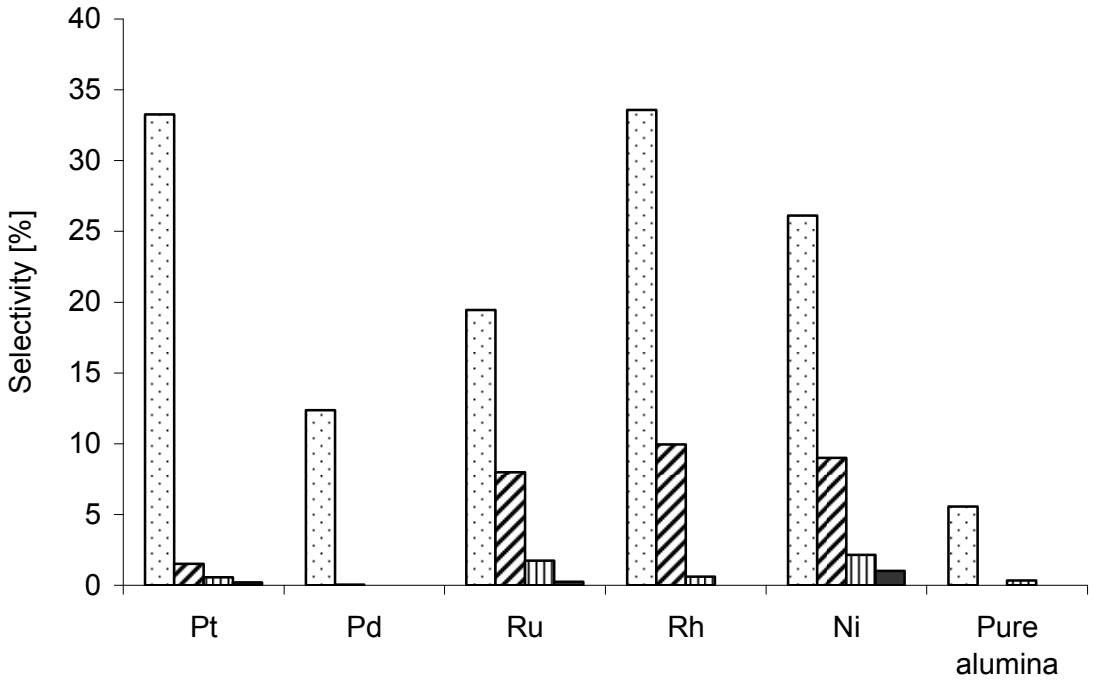

Figure 2.3: Gaseous products selectivity based on carbon atom carbon dioxide (⬚), methane (▨) ethane (▥) and propane (■). (Experimental conditions: T= 498 K, total pressure = 29 bar, Glycerol concentration = 10wt %)

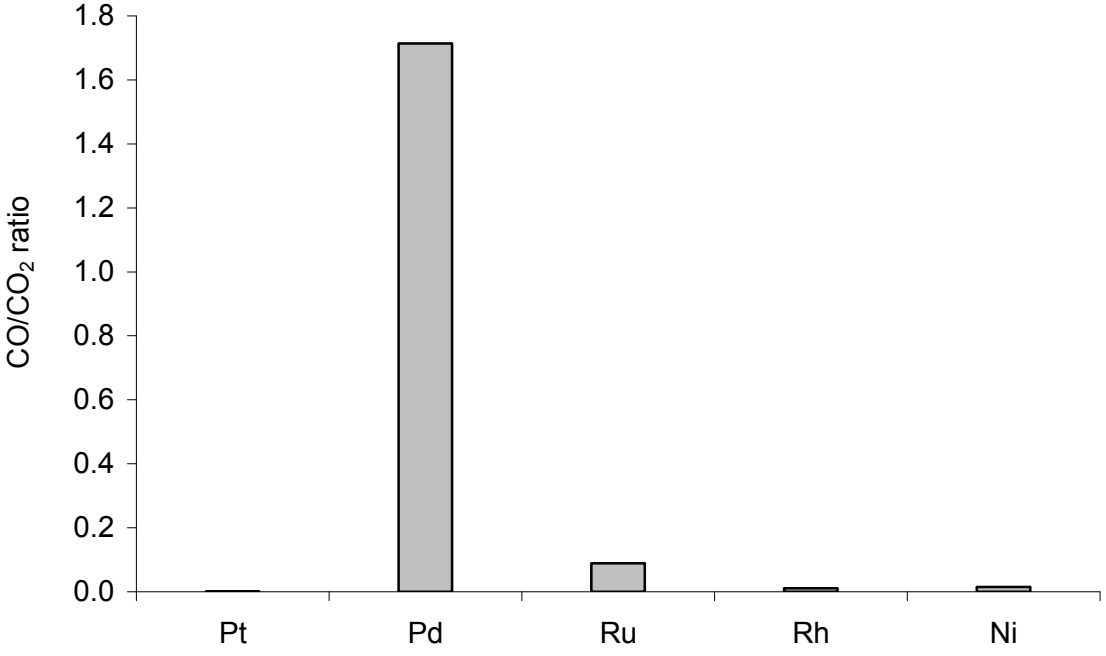

Figure 2.4: CO/CO_2 ratio from different catalysts 498 K and 29 bar

Table 2.2 Liquid product selectivity based on carbon atom (Experimental conditions: T= 498 K, total pressure = 29 bar, Glycerol concentration = 10wt %)

Catalysts	1,2-Propane diol	1,3-Propane diol	1,2-Ethane diol	Methanol	Ethanol	Propanol	Hydroxy acetone	Ald.	Acid	Gas
Pt/Al_2O_3	30	1	9	1	8	1	7	3	2	36
Pd/Al_2O_3	26	-	2	-	6	-	20	-	13	34
Ru/Al_2O_3	42	5	1	-	-	-	23	-	-	31
Rh/Al_2O_3	28	-	-	-	-	-	29	-	-	45
Ni/Al_2O_3	25	-	1	-	3	9	14	0	3	39
Al_2O_3	-	-	1	1	4	17	67	1	3	11

Ald: Summation of acetaldehyde and propanal

Acid: Summation of acetic acid, propanoic acid and lactic acid

Gas: Summation of carbon dioxide, alkane (C1-C3) and carbon monoxide

2.4 Discussion

The products detected in the in gaseous and liquid streams can be formed via different reaction routes. Glycerol can undergo hydrogenolysis (C-C bond braking) on the metal surface and hydrogen, 1, 2 ethanediol, carbon dioxide and carbon monoxide can be produced as shown in equations (7)-(10).

$$C_3H_8O_3 \longrightarrow 3CO + 4H_2 \quad (7)$$

$$C_3H_8O_3 \longrightarrow C_2H_6O_2 + CO + H_2 \quad (8)$$

1, 2 ethanediol is a reaction intermediate, which can react to hydrogen and carbon monoxide by hydrogenolysis

$$C_2H_6O_2 \longleftrightarrow 2CO + 2H_2 \quad (9)$$

The low concentration of CO in the product indicates that the activity of the catalysts for the water-gas shift reaction (equation 10) is generally high.

$$CO + H_2O \longleftrightarrow H_2 + CO_2 \quad (10)$$

Alternatively, Hydrogen is also produced from dehydrogenation (C-H cleavage) to form glyceraldehyde [19,20] and it is further converted to Lactic acid via cannizzaro type reaction [21,22] (equation 11). This route is the route of acid formation as Lactic acid is then reduced to form propanoic acid (equation 12) [23,24].

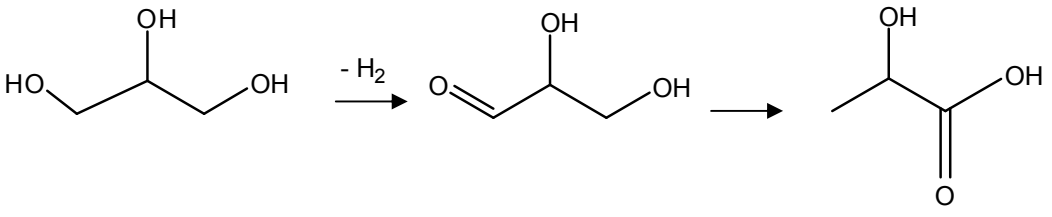

(11)

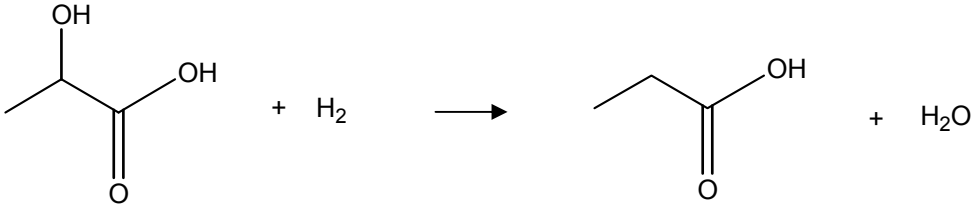

(12)

Methane can be formed via methanation form CO, leading to a loss of H_2 rate formation and higher alkanes are possibly formed by a Fischer-Tropsch like reaction (equation 13 – 15)

$$CO + 3H_2 \longleftrightarrow CH_4 + H_2O \quad (13)$$

$$CO + 5H_2 \longleftrightarrow C_2H_6 + 2H_2O \quad (14)$$

$$CO + 7H_2 \longleftrightarrow C_3H_8 + 3H_2O \quad (15)$$

An alternative route is the dehydration and hydrogenation via a bifunctional (metal/acid) mechanism [25]. The main product from dehydration at low conversion is hydroxyacetone, which can be hydrogenated to 1,2-propanediol as shown in equations (16)-(17).

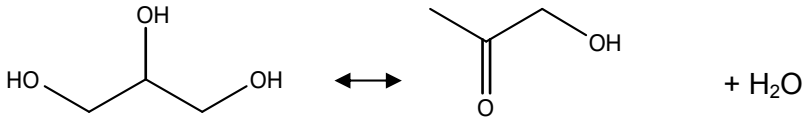

Glycerol Hydroxyacetone (16)

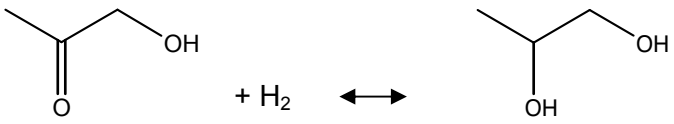

Hydroxyacetone 1,2-propanediol (17)

Influence of the nature of the metals on selectivity

Hydrogen and Alkanes

Hydrogen can be formed via C-H (dehydrogenation) and C-C cleavage of glycerol and intermediate oxygenated compounds as well as via the water gas shift reaction. On the other hand, hydrogen can be consumed by hydrogenation of intermediate (CO and hydroxyacetone) and dehydration reactions. The high hydrogen selectivity achieved over Pt and Pd catalysts at low conversion indicates the generally lower activity of these metals in hydrogenation for CO compared to Ru, Rh and Ni. The low concentration of CO

in the reactant is a result of the high activity of Pt for the water gas shift reaction under these reaction conditions.

The alkanes formed, which were mainly methane and some traces of ethane and propane, can either results from the hydrogenation of CO, or alternatively from the cleavage of C-C and/or C-O in alcohols and acids. The Pd and Pt catalysts produced the intermediated liquid by-products including acetic acid, ethanol and propanoic acid whereas they produced less alkane. On the other hand, the Ru, Rh and Ni catalysts generated more alkanes such as ethane and propane in the gaseous product. The order of activity of the catalysts for alkane formation (Ni > Rh > Ru > Pt >Pd) agrees well with the methanation activity of these metals in a similar temperature range [26]. The reason that Rh, Ru and Ni catalysts showed the higher selectivity of alkanes than Pt and Pd catalysts could be the more preferable of methanation reaction and C-O cleavage of acid and alcoholic compound compared to Pt and Pd.

Carbon monoxide

The main reaction pathway to carbon monoxide is the C-C bond cleavage of glycerol or of intermediate oxygenated compounds such as 1,2-ethanediol. The (theoretical) ratio of H_2:CO form the reforming reaction of glycerol is 4:3. The significant lower levels of CO detected indicate that the subsequent water gas shift reaction of CO to form H_2 is fast under the conditions of the aqueous phase reforming reaction. Among the series of metals studied, the highest formation of CO was observed on the Pd catalyst (see figure 2.5). Note that this follows the order Pd < Ru< Rh < Pt on Al_2O_3 , with Pt being 15-20 times more active than Rh and Ru and 50 times more active than Pd in the water gas shift reaction at 513 K reported by Dumesic et. al. [8] and Kondarides et. al. [28].

Liquid intermediated products

The highest concentration of intermediate products formed in the liquid phase (mainly oxygenated C1 and C2 compounds such as 1,2-ethanediol, acetaldehyde, ethanol and acetic acid) via C-C bond cleavage was observed on Pd and Pt (figure 2.4)

as a result of the higher activity of these metals for the C-C bond cleavage compared to C-O cleavage. Recent DFT calculations [15] comparing the stability of the Pt-C and the Pt-O bonds of surface species derived from ethanol on Pt (111) confirmed the higher activity for C-C bond cleavage of platinum catalysts. Rh, Ru and Ni catalysts do not produce C1 and C2 oxygenated compounds, while they generate more ethane and propane than Pt and Pd. This indicates that Ru, Rh and Ni catalysts are more active in C-O cleavage of intermediates (alcohol aldehyde) than Pt and Pd. For C3 oxygenated compounds hydroxyacetone and 1, 2 propanediol were the main products in the liquid phase, which could be generated by dehydration/hydrogenation in the metal and the support [25,27]. Oxygenated acid production is favored on Pd catalyst, it could be from via cannizzaro type reaction as the reaction of benzaldehyde to benzoic acid [24]. Hydroxyacetone is the common product not only from all metal supported on alumina but also pure alumina. The dehydration route of glycerol take place on the alumina support subsequently hydrogenated further to 1, 2 propanediol on the metal site which is most preferable over Pt and Ru catalysts followed by Rh, Ni and Pd. Pt and Ru catalysts are generally active for hydrogenation of ketone to diol compounds as reported by Rylander and Steele [29]. The reaction on alumina surface is then mainly dehydration of glycerol to hydroxyacetone and propanol.

2.5 Conclusions

Hydrogen production from glycerol by aqueous phase reforming on Pt, Pd, Ni, Ru and Rh supported on γ-alumina at a temperature around 500 K is feasible. To achieve high hydrogen rate formation, the catalyst must possess high activity in C-C cleavage and the water gas shift reaction, while the activity for hydrogenation of CO and oxygenated intermediate reactions should be low. The Pt/γ-Al_2O_3 catalyst performed the best in the aqueous phase reforming reaction due to highest hydrogen formation with low CO content. Although the hydrogen rate from the Pd/γ-Al_2O_3 catalysts was relatively high due to its low hydrogenation activity of hydroxyacetone and CO, the significant CO formation on Pd resulting form the lower activity in the water gas shift reaction makes this catalyst less suitable for H_2 production for fuel cell applications. The intermediate compound to 1,2-propanediol formation is hydroxyacetone which is the product from dehydration route on alumina site. Metal/support bi-functional reaction route is defined for 1,2 propanediol formation from glycerol. The future work will be focused on the study of reaction network which lead to hydrogen and liquid phased products of aqueous phase reforming of glycerol over pt catalysts.

2.6 References

1. D. Wang, D. Montane, E. Chornet, Appl. Catal. A 143 (1996) 245.
2. S. Czernik, R. French, C. Feik, E. Chornet, Ind. Eng. Chem. Res. 41 (2002) 4209.
3. H. Toshihide, I. Na-oki I., M. Takanori, S. Toshimitsu, American Chemical Society (2005).
4. R. D. Cortright, R. R. Davda, J. A. Dumesic, Nature 418 (2002) 964.
5. G. W. Huber, J. W. Shabaker, J. A. Dumesic, Science 300 (2003) 2075.
6. J. W. Shabaker, G. W. Huber, R. D. Cortright, Ind. Eng. Chem. Res. 43 (2004) 3105.
7. J. W. Shabaker, G. W. Huber, J. A. Dumesic, J. Catal. 222 (2004) 180.
8. R. R. Davda, J. W. Shabaker, G. W. Huber, R.D. Cortright, J. A. Dumesic, Appl. Catal. B Environmental 56 (2005) 171.
9. R. R. Davda, J. W. Shabaker, G. W. Huber, R. D. Cortright, J. A. Dumesic, Appl. Catal. B Environmental 43 (2003) 13.
10. G. W. Huber, J. A. Dumesic, Catal. Today 111 (2006) 119.
11. J. W. Shabaker, G. W. Huber, R. R. Davda, R. D. Cortright, J. A. Dumesic, Catal. Lett. 88 (2003) 1.
12. P. Chou, M. A. Vannice, J. Catal. 104 (1987) 1.
13. http://www.fas.usda.gov/pecad2/highlights/2003/09/biodiesel3.
14. D. Morton, D. J. Cole-Hamilton, J. Chem. Soc., Chem. Commun. (1988) 1154.
15. D. Morton, D. J. Cole-Hamilton, J. A. Schofleid, R. J. Pryce, Polyhedron 6 (1987) 2187.
16. D. Morton, D. J. Cole-Hamilton, I. D. Utuk, M. Paneque-Sosa, M. Lopez-Povede, J. Chem. Soc. Dalton Trans (1989) 489.
17. D. Morton, D. J. Cole-Hamilton, J. Chem. Soc., Chem. Commun. (1987) 248.
18. P. H. Lewis, J. Catal. 11 (1968) 162.

19. E. P. Maris, R. J. Davis, J. Catal. 249 (2007) 328.

20. E. P. Maris, W. C. Ketchie, M. Murayama, R. J. Davis, J. Catal. 251 (2007) 281.

21. C. Keresszegi, D. Ferri, T. Mallat, A. Baiker, J. Phys. Chem. B 109 (2005) 958.

22. A. E. T. Kuiper, J. Medema, J. J. G. M. Bokhoven, J. Catal. 29 (1973) 40.

23. M. S. Tam, R. Craciun, D. J. Miller, J. E. Jackson,
Ind. Eng. Chem. Res. 37 (1998) 2360.

24. M. K. Bernard, A. Tadafumi, M. M. Roberto, A. Kunio,
Ind. Eng. Chem. Res. 38 (1999) 2888.

25. T. Miyazawa, K. Kunimori, K. Tomishige, J. Catal. 240 (2006) 213

26. M. A. Vannice, J. Catal. 37 (1975) 37.

27. M. A. Dasari, P. Kiatsimkul, W. R. Sutterlin, G. J. Suppes,
Appl. Catal. A General 281, (2005) 225.

28. P. Panagiotopoulou, D. I. Kondarides, Catal. Today 112 (2006) 49.

29. P. N. Rylander, D. R. Steele, Engelhard Ind. Tech. Bull. 5 (1965) 113.

30. R. Alcalá, M. Mavrikakis, J. A. Dumesic, J. Catal. 218 (2003) 178.

31. G. R. Wilson, W. K. Hall, J. Cat 17 (1970) 190.

32. J. R. Rostrup-Nielsen, B. J. J. Handsen, Catal. 144 (1993) 38.

Chapter 3

Influence of metal particle size and reaction conditions on the reaction pathway

Abstract

The influence of the metal particle size of Pt/Al_2O_3 catalysts and of the reaction conditions including pressure, reactant concentration and space velocity on the formation of hydrogen and oxygenated compounds in the aqueous phase reforming of glycerol are reported. The potential reaction intermediates were identified by ATR-IR spectroscopy under reaction conditions and used as reactants to elucidate the reaction pathways leading to gaseous and liquid products. For the aqueous phase reforming reaction, four reaction routes were identified, one mainly leading to gaseous products (H_2 and CO_2) and three in the liquid phase leading to 1,2-propanediol, 1,3-propanediol and to acetic and propanoic acid. The rate of hydrogen formation was found to increase over small Pt particles, due to the enhanced activity of C-C cleavage. On the contrary, the selectivity to oxygenated products in the liquid phase is enhanced by larger metal particles and reactions at higher pressure.

3.1 Introduction

Hydrogen, being used in fuel cells or directly in combustion engines, is a key transport fuel for zero CO_2 emission vehicles in the future. Therefore, routes for hydrogen production from renewable sources such as biomass pyrolysis oil, bio-ethanol, trap grease [1, 2] and glycerol [2-11] are in the focus of the current interest. Among these materials glycerol is an attractive resource due to its present ample availability being the main by-product formed in bio-diesel production.

Hydrogen rich streams can be produced from glycerol by reactions in the gas phase in the presence or absence of steam or in the aqueous phase. Gas phase steam reforming of glycerol is typically carried out at temperatures above 623 K and at atmospheric pressure [3-5]. Hydrogen is produced via two reactions, i.e.

Decomposition of glycerol:

$C_3H_8O_3$ (g) ⟶ CO (g) + $4H_2$ (g) (1)

Water gas shift reaction:

CO (g) + H_2O (g) ⟷ H_2 (g) + CO_2 (g) (2)

A significant number of publications focus on glycerol reforming in the gas phase. The catalysts studied include noble and base metals such as Ru [3], Ir [3, 4], Co [3, 4] and Ni [2, 3, 4, 5] and various metal oxides i.e., Y_2O_3, ZrO_2, CeO_2, La_2O_3, SiO_2, MgO and Al_2O_3 as supports. Among the noble metal catalysts, Ru/Y_2O_3 [3] showed highest hydrogen yield of 85% at 773 K. However, under these conditions high concentrations of CO (selectivity 21%) are formed. Complete conversion of glycerol was reported for Ir/CeO_2 at 673 K with selectivity to hydrogen of 85% [4]. Ni based catalysts were the most frequently studied although the hydrogen selectivity achieved was about 75% and a temperature of at least 873 K was required to reach the complete conversion. For a commercial Ni based catalysts Chornet et. al. [2] reported a hydrogen selectivity of 77 % at 1123 K. For Ni supported on CeO_2 Haryanto et al. reported that the complete conversion to be achieved at 873 K with maximum hydrogen selectivity of 75 %, a CO selectivity of 25% and a methane selectivity of 5% [5].

In general, it can be summarized that glycerol can be effectively converted to synthesis gas in the gas phase, but due to the high temperatures required relatively high concentrations of CO were formed due to the unfavorable equilibrium of the water gas shift reaction at high temperatures. Therefore, the synthesis gas produced needs to be further processed in order to meet the requirements for direct use in fuel cell applications (i.e., CO < 50 ppm).

In comparison, the reforming of glycerol in the aqueous phase (APR) requires lower temperatures (423-523 K) but higher pressures (15-60 bar) [6-16]. Besides the advantage of the reduced energy consumption as the evaporation of the water is not necessary, the lower reaction temperature leads to drastically reduced CO formation due

to the more favorable equilibrium of the water gas shift reaction. Apart from the reactions already mentioned for the reforming of glycerol in the gas phase, further reactions are feasible in the aqueous phase at low temperature such as the hydrogenation of carbon monoxide (Reaction 3) as well as the dehydrogenation (Reaction 4) and hydrogenolysis of glycerol to diols (Reaction 5).

Hydrogenation of carbon monoxide

$$CO + 3H_2 \longleftrightarrow CH_4 + H_2O \quad (3)$$

Dehydrogenation of glycerol:

$$C_3H_8O_3 \longleftrightarrow C_3H_6O_3 + H_2 \quad (4)$$

Dehydration/Hydrogenation:

$$C_3H_8O_3 + H_2 \longleftrightarrow C_3H_8O_2 + H_2O \quad (5)$$

Aqueous phase reforming of biomass derived alcohols has been studied in depth by Dumesic et al. using ethylene glycol as a model compound [6-16]. Among the different metals studied (Pt, Ni, Ru, Rh, Pd and Ir supported on SiO_2), Pt was the most selective catalyst for hydrogen formation [12] and among the different supports investigated (ZrO_2, ASA, C, CeO_2, TiO_2, SiO_2, ZnO, Al_2O_3) [13], Pt supported on Al_2O_3 showed the highest hydrogen selectivity (>90%). In addition, liquid products were also observed including methanol and ethanol with a selectivity of 57% and 29%, respectively (based on the number of carbon atoms in the liquid products).

Catalysts active for APR should have high catalytic activity for water gas shift reaction and sufficiently high catalytic activity for C-C bond cleavage, while significant activity in methanation and Fischer-Tropsch reactions lead to lower hydrogen selectivity. Acidic supports in combination with a metal favor dehydration/hydrogenation reactions consuming hydrogen [12].

On this basis, alumina Pt based catalysts were chosen as most promising candidates for APR reactions of glycerol in the present work. Under all reaction conditions the alumina support remained stable although it was transformed from γ-Al_2O_3 to a

boehmite structure. The influence of the particle size of Pt and the reaction conditions on the formation of products in the gas and the liquid phase were studied. The reaction pathways for the conversion of glycerol to hydrogen and oxygenated liquid products were investigated by *in situ* ATR IR spectroscopy and related to the products observed in the catalytic reactions.

3.2 Experimental Section

3.2.1 Catalysts preparation

The catalysts (Pt/γ-Al_2O_3) with a Pt loading 1, 3, and 5 wt% were prepared by incipient wetness impregnation. Platinum (II)-ammonium nitrate (Strem chemicals) was used as precursor, the support was γ-Al_2O_3 (Aeroxide Alu C-Degussa) with a surface area of 150 m^2/g. After impregnation of the support with the aqueous precursor solution the catalysts were dried in air at 393 K for 12 hours and calcined in synthetic air for 2 hours at 573 K. Prior to reaction and characterization the catalysts were reduced in H_2 at 623 K for 2 hours.

3.2.2 Catalyst characterization

Atomic absorption spectroscopy (AAS)

The concentration of the metal was determined by atomic absorption spectroscopy using a UNICAM 939 AA-Spectrometer. Typically, 20-40 mg of the sample was dissolved in a mixture of 0.5 ml of hydrofluoric acid (48%) and 0.1 ml of nitro-hydrochloric acid at the boiling point of the mixture (about 383 K).

Hydrogen and nitrogen chemisorption

The fraction of accessible Pt atoms was determined by H_2 chemisorption using a Sorptomatic 1990 Series sorptometer (Porotec Sorptomatic 1990 Automated BET). Approximately 1g of catalyst was reduced in H_2 at 588 K for 1 hour, followed by outgassing in vacuum at 308 K for 4 hours after reduction. The sorption isotherms were measured at 308 K. The amount of chemisorbed hydrogen was obtained after removing physisorbed hydrogen from the sample by evacuation at 308 K for 2 hours. The metal dispersion was determined by assuming H/Pt ratio of 1 [17]. The particle sizes of Pt of all samples were calculated by the relationship between dispersion and crystallite size in equation [18] assuming spherical particles. The BET surface area and pore size distribution were determined by N_2 adsorption–desorption at 77 K using a Sorptomatic 1990 Series instrument after activation of the sample in vacuum at 573 K for 2 hour.

3.2.3 Kinetic Measurements

A laboratory reactor system was used for testing the catalyst performance in the aqueous-phase reforming of glycerol (schematically shown in Figure 3.1). The stainless steel tubular reactor (1/4 inch o.d.) was loaded with a bed of the pressed and crushed catalyst (50-160mg) with a particle size between 300-500 μm. After the reduction of the catalysts in H2 at 623 K for 2 hours, the system was purged and pressurized with nitrogen before starting the reaction. A liquid solution of glycerol (spectrophotometer grade, ≥99.5%, Aldrich) in deionized water was introduced in an up-flow configuration with a HPLC pump. The liquid and gaseous products leaving the reactor were cooled in a heat exchanger to liquefy condensable vapors. The effluent was mixed with nitrogen and the two phases were separated after the 16-port sampling valve by condensation.

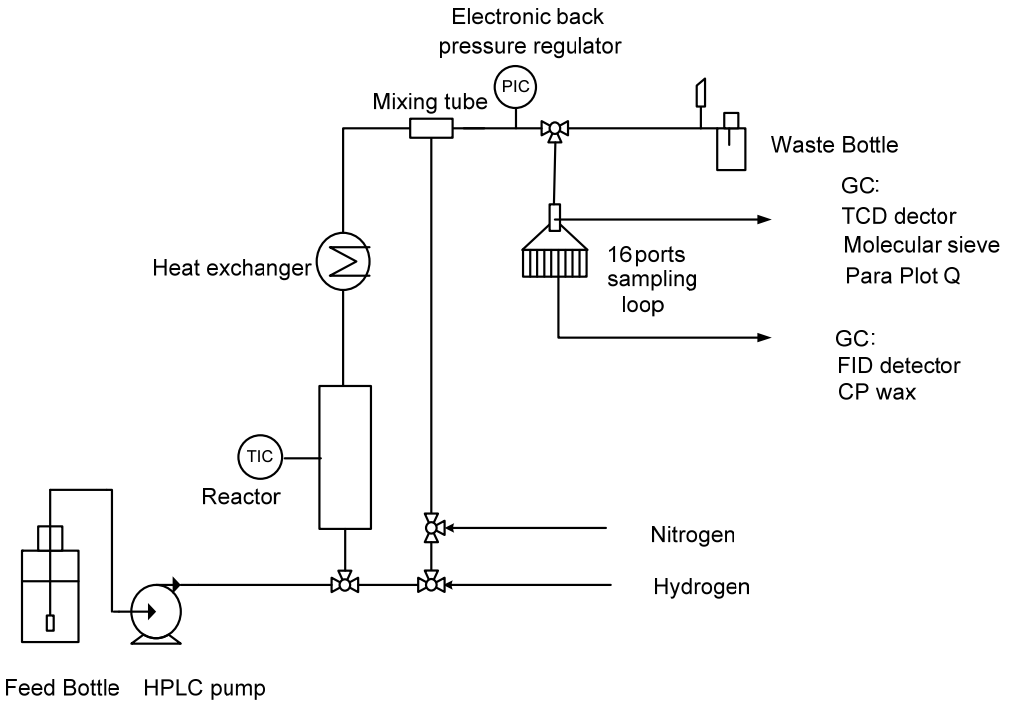

Figure 3.1: Scheme of the reactor used for kinetic experiments

The liquid samples were analyzed in a gas chromatograph equipped with FID/MS detector and CP-Wax 57 CB column. To ensure the detection of all carbon containing species in the liquid products, the liquid samples were additionally analyzed by elemental analysis (Elemental Vario EL). Gaseous products were analyzed on line by a gas chromatograph with TCD detector and two capillary columns (MS-5S and Para Plot Q).

The influence of the metal particle size and the pressure (26 to 45 bar) was studied using a 20 wt% glycerol solution (H2O/C = 6.8) at 498 K. The effect of the glycerol concentration was investigated in the concentration range 10-30 wt% at 498 K and 29 bar. The conversion levels were kept in the same range (7-10 %) by varying the WHSV in order to allow a differential analysis of the rate. Furthermore, a series of experiments was conducted at 498 K and 29 bar by varying the WHSV between 0.45 - 22.70 h-1 of a 30 wt% glycerol solution (molar ratio of $H_2O/C = 4$) to attain high glycerol conversion levels. The reaction routes from the potential intermediates of aqueous phase reforming (lactic acid and hydroxyacetone) were performed at concentration of 10 wt%

with the space velocity of at 3.7 and 24.3 h-1 to maintain conversion levels of 4 - 8% and in the space velocity in the range of 0.23 - 24.3 h-1.

3.2.4 Reaction surface study using ATR-IR spectroscopy

The surface of a ZnSe internal reflection element (IRE area 4x16mm) was coated with an aqueous suspension of the 3 wt% Pt/γ-Al_2O_3 catalyst (50 mg catalyst and 500 mg deinoized water prepared in an ultrasonic bath at 318 K). The water in the suspension was evaporated at room temperature for 6 hours and the thin film catalyst coated on the IRE was reduced in hydrogen at 513 K with 1K/min for 1 h. The thickness of the film was around 4 μm based on alumina density of 3.27 g/cm^3. The evanescent wave was generated at the interface with the penetration depth in the average at 1 μm which calculated according to equation (6) [19]

$$d_p = \frac{\lambda_1}{2\pi\left(\sin^2\theta - n_{21}{}^2\right)^{\frac{1}{2}}} \qquad (6)$$

where λ_1 is the wavelength in the more dense medium and n_{21} is the ratio of the refractive indices at the interface given by: $\lambda_1 = \frac{\lambda}{n_1}$ and $n_{21} = \frac{n_2}{n_1}$.

where: λ – wavelength of IR radiation

θ – angle of incidence (60 °)

n_1 – refractive index of internal reflection element (ZnSe =2.406)

n_2 – refractive index of sample (alumina = 1.63 and glycerol = 1.47)

The ATR-IR spectra were recorded by using a stainless steel flow through cell, the scheme is shown in Figure 3.2. The ATR cell unit was placed in the spectrometer (Nicolet 5700 with a liquid nitrogen-cooled MTC-A detector). A trapezoidal crystal of ZnSe (size 27.7x10x2 mm) with an angle of incidence of 60° (three active reflections) was used. The coated IRE was mounted into the stainless steel flow cell and sealed with a carbon

gasket. During the reaction, spectra were taken at a resolution of 4 cm^{-1} by accumulating 32 interferograms. After the reduction of the catalysts, a liquid glycerol solution (30wt %) was fed into the ATR cell with a HPLC pump at a rate of 0.01 ml/min. The pressure of the system adjusted to 29 bar and the temperature was increased from room temperature to 498 K with the rate of 3 K/min.

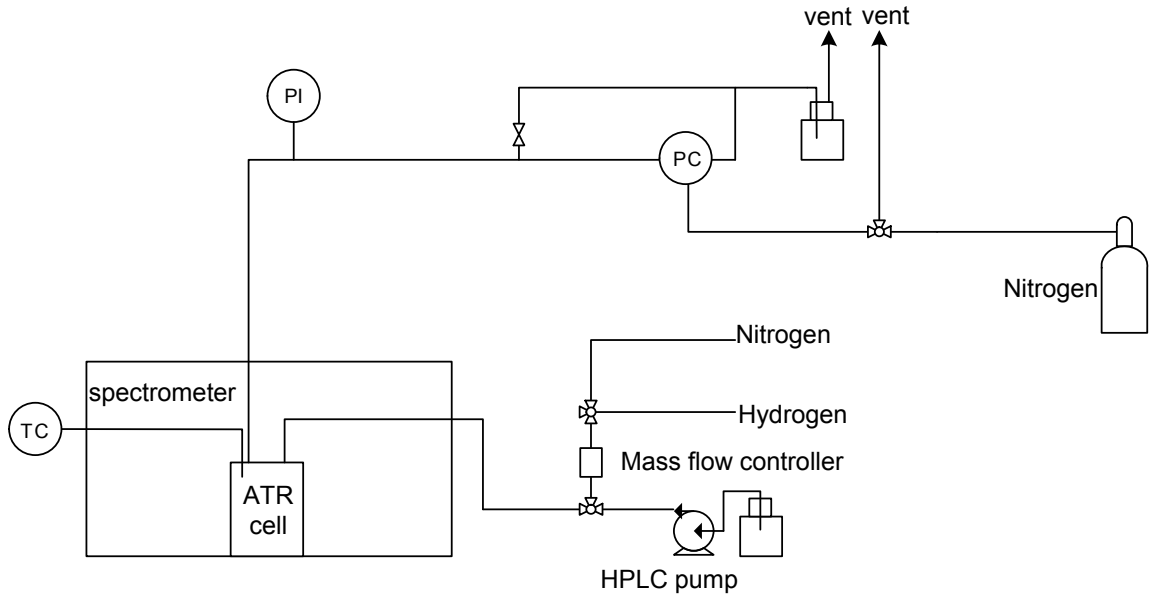

Figure 3.2: Scheme of the reactor used for *in situ* ATR-IR spectroscopy

3.3 Results

3.3.1 Catalysts characterization

The characteristic properties of the Pt catalysts are summarized in Table 3.1. The amount of Pt did not affect the specific surface area of the final catalyst, while the dispersion of the Pt particles decreased with the metal loading from 98% to 42%. The smallest particles with a size of 1.1 nm were observed on the catalyst with the lowest Pt loading (1 wt %) and with increasing Pt loading the size of the metal particles increased to 1.5 nm and to 2.6 nm for the catalysts with a Pt loading of 3 wt% and of 4.9 wt%, respectively.

Table 3.1 Properties of the catalysts

Pt Loading (wt%)	Surface area (m^2/g)	Average Particle size (nm)	Dispersion
0.98	104	1.1	0.98
2.97	105	1.5	0.75
4.88	102	2.6	0.42

3.3.2 Influence of platinum particle size

The role of the Pt particle size on the activity in aqueous phase reforming of glycerol was studied at 498 K using a 20 wt% glycerol solution. Gaseous and liquids products were formed. The products in the gas phase included hydrogen, alkanes (C1 to C3), carbon dioxide and carbon monoxide. The C1 oxygenated liquid product was mainly methanol, the C2 oxygenated liquid products included acetaldehyde, acetic acid, ethanol and 1,2-ethanediol and the C3 oxygenated liquid products included hydroxyacetone, propanol, 1,2-propanediol, 1,3-propanediol, lactic acid, propionaldehyde and propanoic acid. The major product of C3 oxygenated products group was 1,2-propanediol, while the main C2 products were ethanol and 1,2-ethanediol.

The reaction rates for glycerol consumption and product formation as function of the particle size are presented in Figure 3.3. While the rate of glycerol converted was hardly influenced by the metal particle size, a pronounced effect on the formation of products was observed. For hydrogen and CO_2, which are the main products of the reforming reaction, the rate decreased with increasing particle size of the metal clusters, while it increased in the same sequence for the formation of gaseous alkanes. CO was only formed in traces with the three catalysts studied (400 – 1200 ppm), but it increased with the particle size in parallel with the formation of light alkanes. The formation of the

C2 and C3 liquid oxygenated products only slightly increased with the Pt particle size, while it decreased for the C1 liquid oxygenated products.

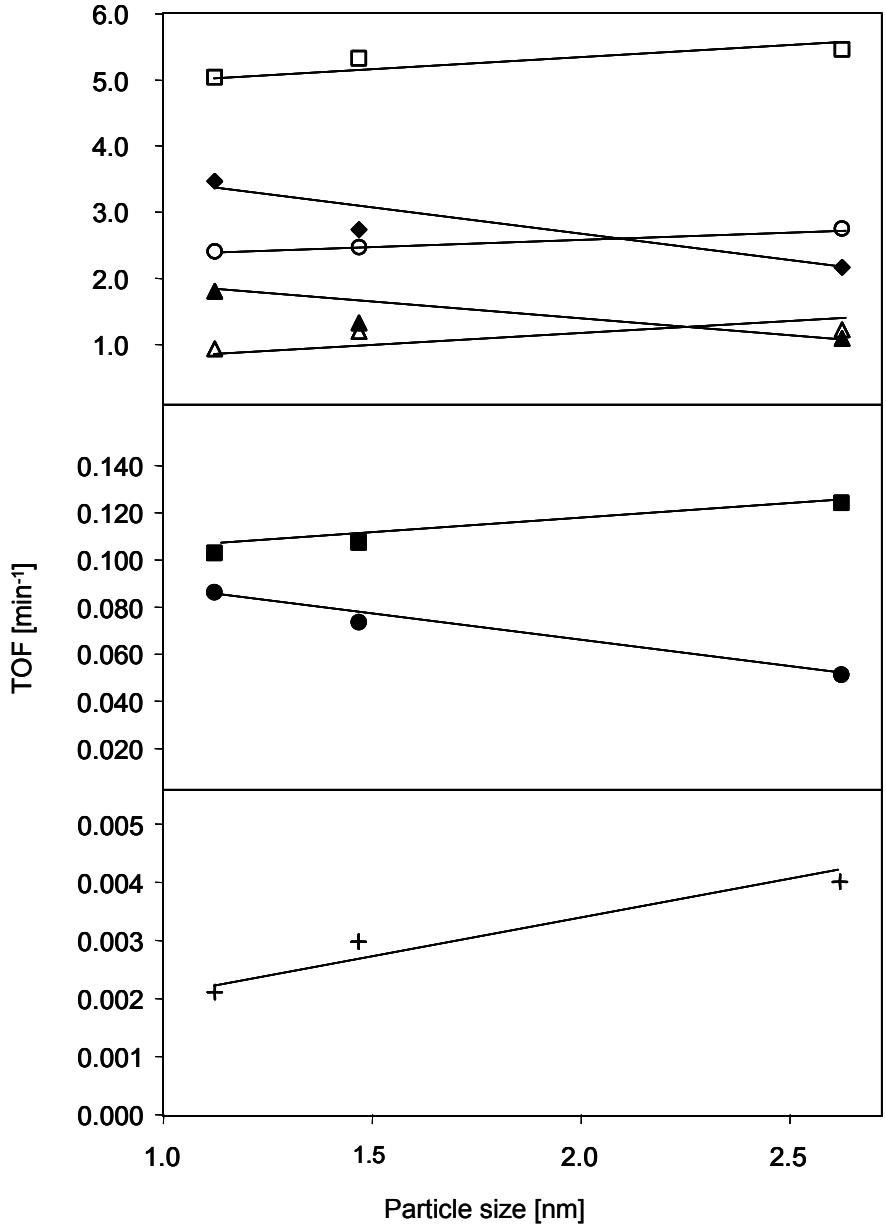

Figure 3.3: Turnover frequencies for the conversion of glycerol (□) and the formation of hydrogen (◆), carbon dioxide(▲), alkanes (■), carbon monoxide (+), C1 oxygenated product (●), C2 oxygenated products (△) and C3 oxygenated products (○) (Experimental conditions: T=498 K, total pressure 29 bar, glycerol concentration 20 wt %).´

3.3.3 Influence of reaction parameters

The rates of glycerol conversion and for the formation of the gaseous and liquid products as function of the total pressure over the 3 wt% platinum catalyst are shown in Figure 3.4. The conversion of glycerol was not affected by the total pressure. The rates of hydrogen, gaseous products (CO, alkane and CO_2) and C1 oxygenated liquid phase products decreased, while the rates of C2 and C3 oxygenated products increased with increasing pressure.

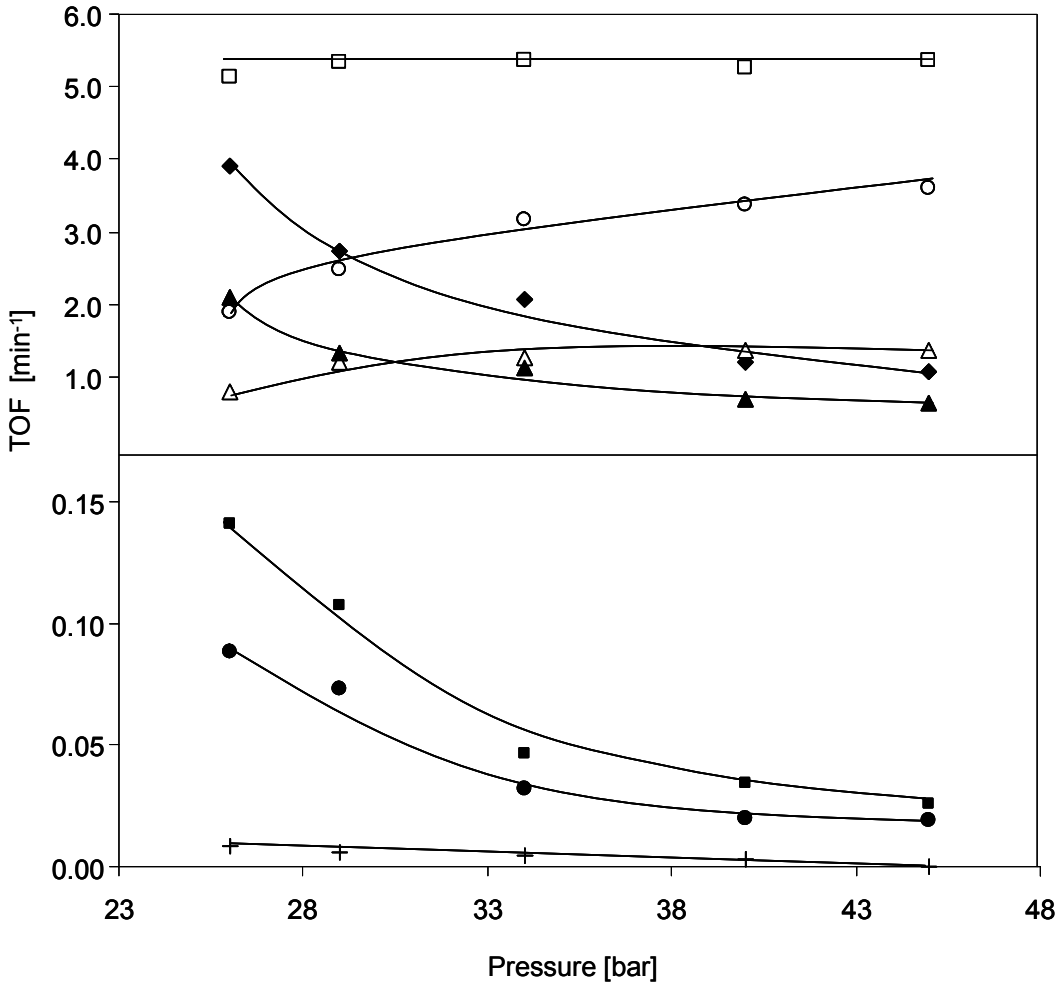

Figure 3.4:Turnover frequencies for the conversion of glycerol (□) and the formation of hydrogen (◆), carbon dioxide (▲), alkanes (■), carbon monoxide (+), C1 oxygenated product (●), C2 oxygenated products (△) and C3 oxygenated products (○) on 3 wt% Pt/Al_2O_3 (Experimental conditions: T 498 K, glycerol concentration 20 wt %)

The effect of glycerol concentration was studied with 3 wt% Pt/Al_2O_3 at 498 K, 29 bar and space velocities between 4.7 and 22.7 h^{-1}. The turnover frequencies for glycerol and for the formation of the main products are shown in Figure 3.5. The rate increased for all products with the glycerol concentration. The reaction orders (summarized in Table 3.2) for the formation of C1-C3 liquid oxygenated products were approximately 0.8, while for the gaseous products (H_2, CO_2, CO and alkanes) they were slightly lower (about 0.6).

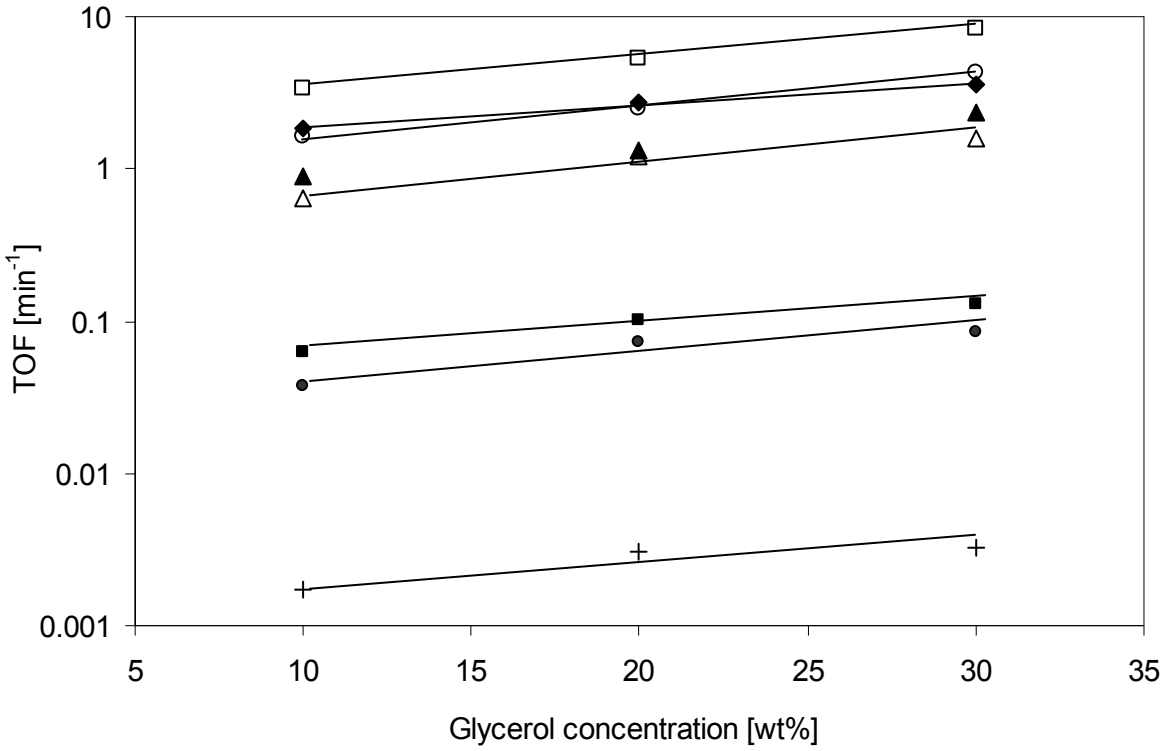

Figure 3.5: Turnover frequencies for the conversion of glycerol (□) and the formation hydrogen (◆), carbon dioxide (▲), alkanes (■), carbon monoxide (+), C1 oxygenated product (●), C2 oxygenated products (△) and C3 oxygenated products (○) on 3 wt% Pt/Al_2O_3 (Experimental conditions: T 498 K, total pressure 29 bar).

Table 3.2 Reaction orders for the products formed (Experimental conditions: T 498 K, total pressure 29 bar, glycerol concentration 10, 20 and 30 wt %)

Reactant /Products	reaction order with respect to glycerol
Glycerol	0.79
Hydrogen	0.59
Carbon dioxide	0.64
Alkanes	0.67
Carbon monoxide	0.63
C1 oxygenate compounds	0.77
C2 oxygenate compounds	0.82
C3 oxygenate compounds	0.85

The yield of the main products as function of the glycerol conversion is shown in Figure 3.6. The highest yield was observed for the C1-C3 oxygenated products, which approach 45% at a glycerol conversion of 90%. The positive initial slope indicates that the formation of these products occurs directly from glycerol. CO_2, the main carbon containing gaseous product of the reforming reaction, was formed with a similar yield at high conversion levels, however the zero initial slope and the lower yields at low conversion levels indicate that CO_2 is formed via consecutive reactions. The yield for light alkanes and CO increased only moderately with the conversion. The detailed distribution of liquid products is shown in Figures 3.7-3.8. The products are categorized according to their functional groups in acids, mono-alcohols, diols and aldehydes. Among the liquid phase products only ethanol was formed as secondary product, while the positive slopes of the yields at initial conversion levels for all other liquid phase products indicate that these products were directly formed from glycerol. For 1,2-ethanediol, 1,2-propanediol ,

1,3-propanediol, (C2-C3) acids and (C2-C3) aldehydes a maximum in the yield at around 50% conversion was observed, at higher conversion levels these products undergo secondary reactions.

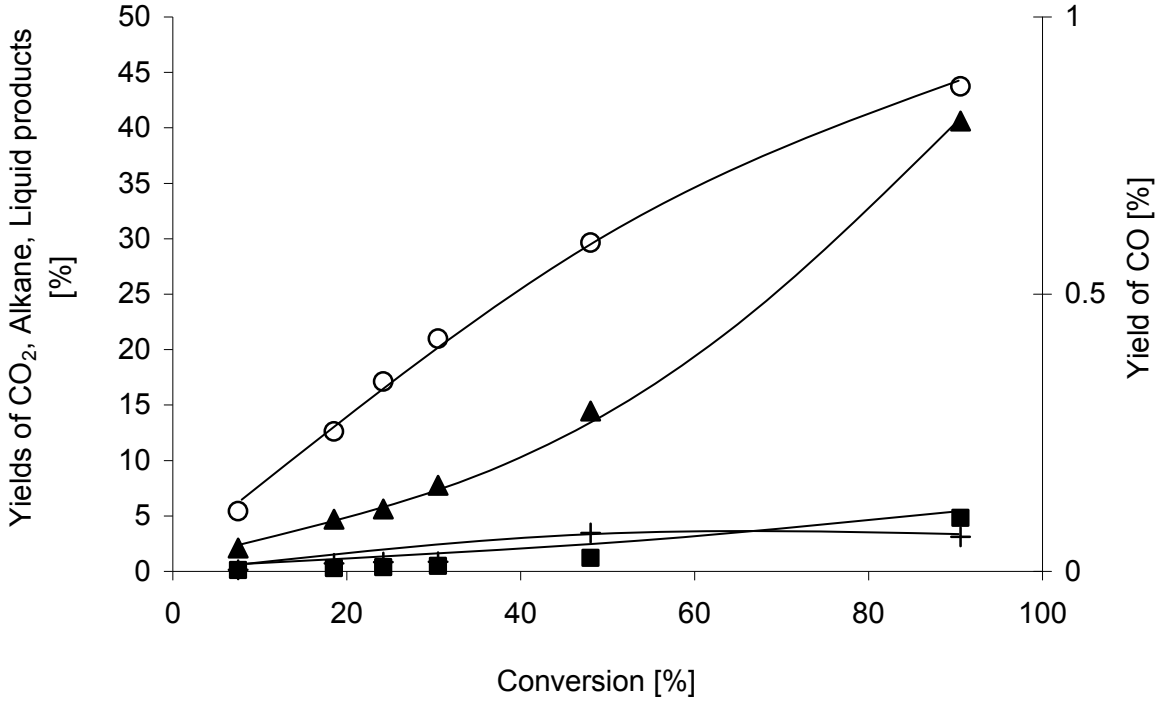

Figure 3.6: Yield of carbon containing products as a function of conversion;
carbon dioxide (▲), alkane (■), carbon monoxide (+),
C1-C3 oxygenate product (○) (Experimental conditions: 2.97 wt% Pt/Al_2O_3, T= 498 K, total pressure = 29 bar, glycerol concentration = 30wt %)

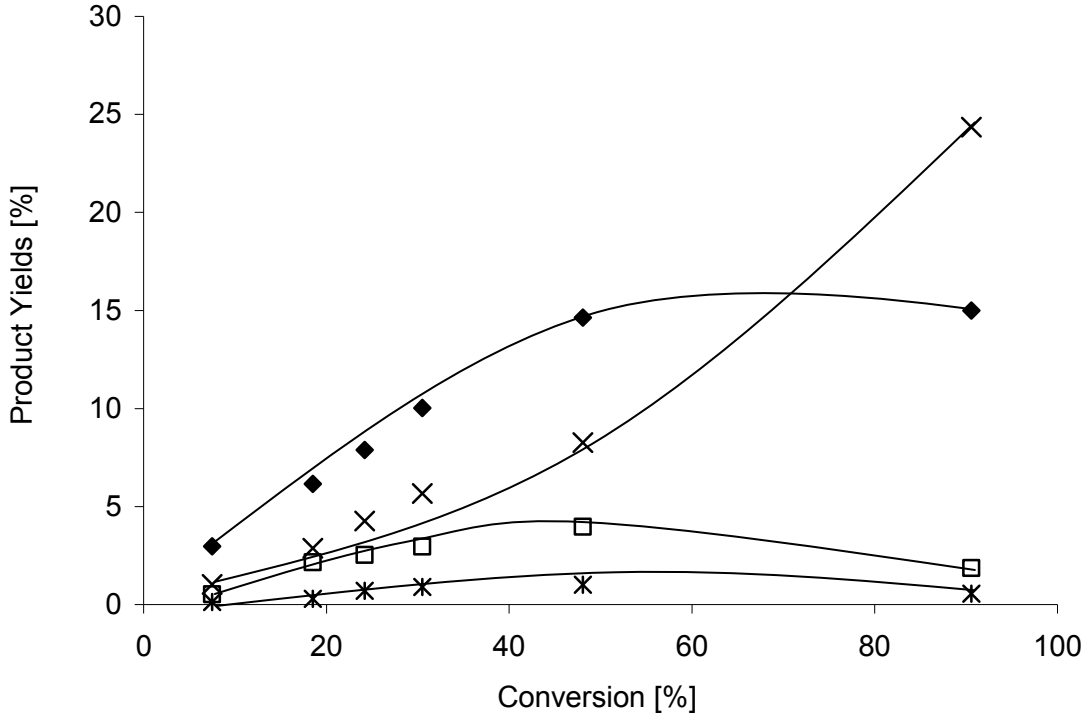

Figure 3.7: Yields of carbon containing liquid products as a function of conversion;
1, 2-propanediol (◆), monoalcohols (methanol, ethanol and propanol) (x),
1, 2-ethanediol (□) and acids (lactic acid, acetic acid and propanoic acid) (✳)
(Experimental conditions:3 wt% Pt/Al_2O_3, T 498 K, total pressure 29 bar,
glycerol concentration 30 wt %)

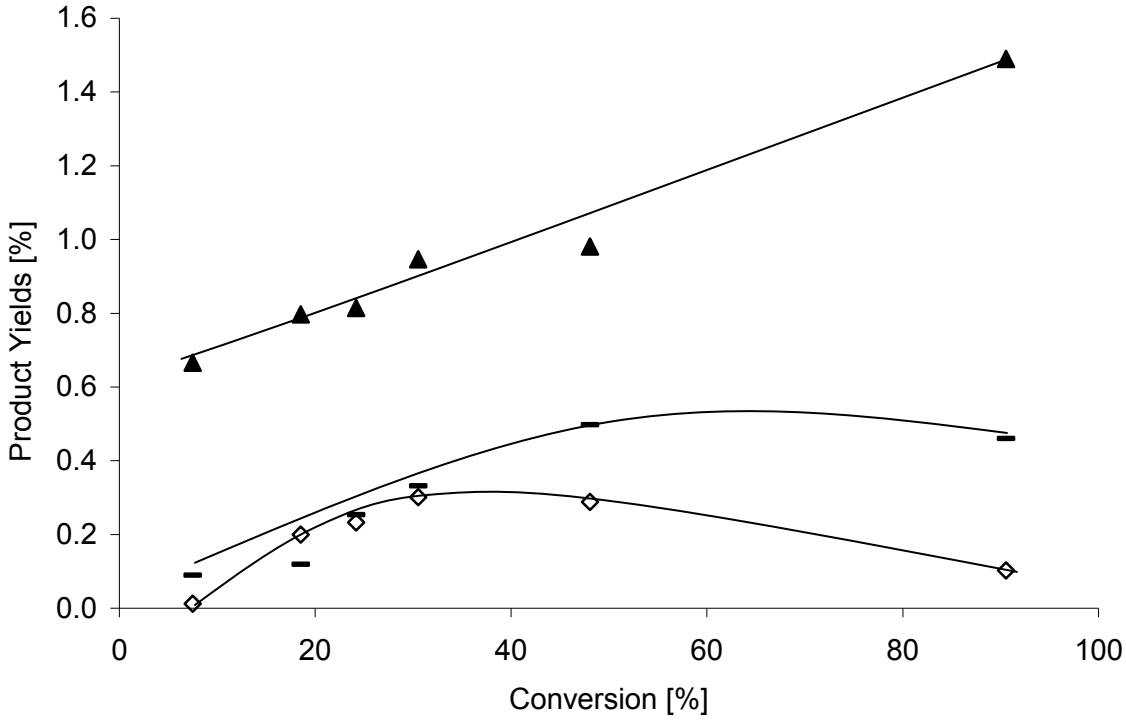

Figure 3.8: Yields of carbon containing liquid products as a function of conversion; hydroxyacetone (▲), aldehyde (acetaldehyde and propanal) (-), and 1, 3-propanediol (◇) (Experimental conditions:3 wt% Pt/Al_2O_3, T 498 K, total pressure 29 bar, glycerol concentration 30 wt%)

3.3.4 Reactions with liquid phase intermediate products

To study the reaction pathways for the formation of the C3 oxygenated products, the conversion of the intermediates including hydroxyacetone and lactic acid was studied in aqueous solution. The rates for the formation of gaseous and liquid products are shown in Table 3.3 and 3.4, respectively. The primary gas phase carbon containing products from lactic acid and hydroxyacetone were carbon dioxide and methane. In the liquid phase 1, 2-propanediol was the main product from reaction with hydroxyacetone (similar to glycerol), while propanoic acid was the main product from lactic acid conversion.

Table 3.3 Rates for the formation of gaseous products from glycerol, lactic acid and hydroxyacetone (Experimental conditions: T 498 K, total pressure 29 bar, catalysts 3 wt% Pt/Al_2O_3)

Reactants	Gaseous Products (rate based on carbon atom) [min^{-1}]						Converted reactants [min^{-1}]
	CO_2	C_2H_6	H_2	CH_4	CO	C_3H_8	
Glycerol (30wt%)	2.315	0.040	3.533	0.079	0.003	0.012	8.231
Lactic acid (10wt%)	0.090	0.004	0.060	0.034	-	4.81E-05	0.189
Hydroxyacetone (10wt%)	1.366	0.037	0.766	0.751	-	-	7.804

Table 3.4 Rates for the formation of liquid products from lactic acid and hydroxyacetone

Reactant	Liquid Products (rate based on carbon atom, min^{-1})												
	1	2	3	4	5	6	7	8	9	10	11	12	13
Glycerol (30wt%)	0.03	0.07	0.08	0.91	0.001	0.09	0.73	0.07	0.03	3.27	0.57	0.01	0.04
Lactic acid (10wt%)	-	-	-	0.007	-	-	-	0.003	0.027	-	-	-	-
Hydroxy acetone (10wt%)	0.623	-	-	1.467	-	0.132	-	0.035	0.054	3.125	0.064	-	-

Liquid products: (1) acetaldehyde, (2) propanal, (3) methanol, (4) ethanol, (5) 2-propanol, (6) 1-propanol, (7) hydroxyacetone, (8) acetic acid, (9) propanoic acid, (10) 1,2-propanediol, (11) 1,2-ethanediol, (12) 1, 3-propanediol and (13) lactic acid

The yields of gas phase and liquid phase products for the conversion of hydroxyacetone are shown in Figures 3.9 and 3.10, respectively. The C1-C3 oxygenated products were formed directly form hydroxyacetone, while alkanes, CO_2 and CO appear to be formed via intermediate products. Among the oxygenated products, acetaldehyde and propanal were formed first, while mono alcohols and the diols were formed as secondary products.

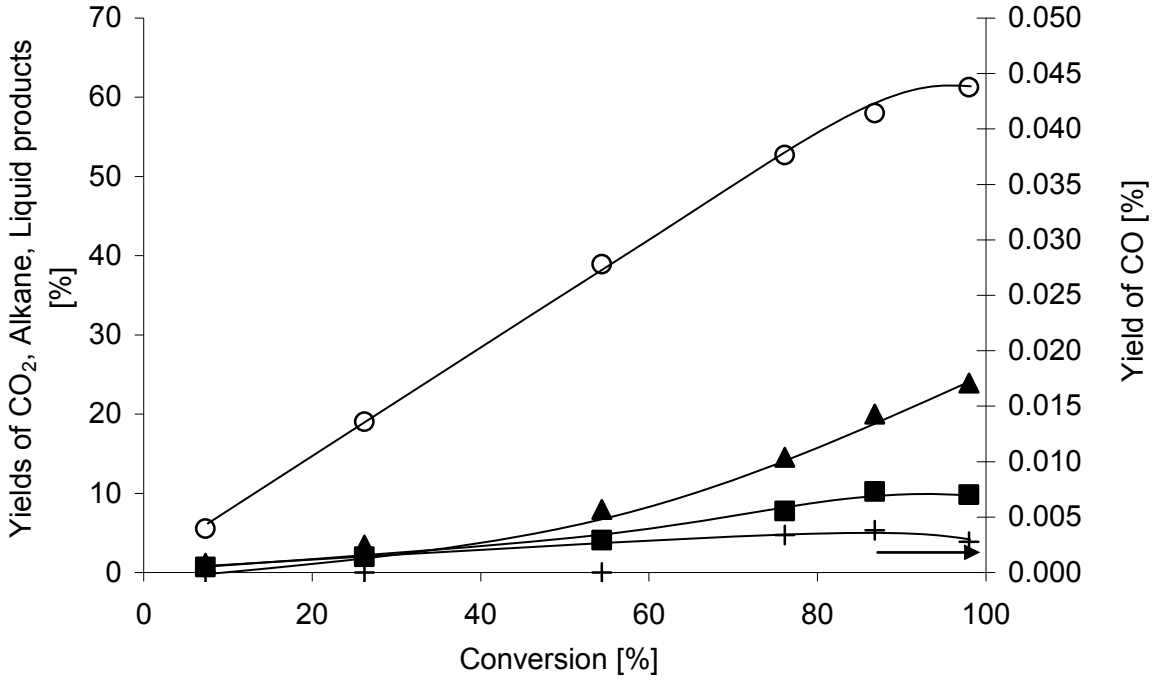

Figure 3.9: Yields of carbon containing products as a function of conversion;
carbon dioxide (▲), alkanes (■), carbon monoxide (+),
C1-C3 oxygenated products (○), (Experimental conditions: 3 wt% Pt/Al_2O_3, T 498 K, total pressure 29 bar, Hydroxyacetone concentration 10 wt %)

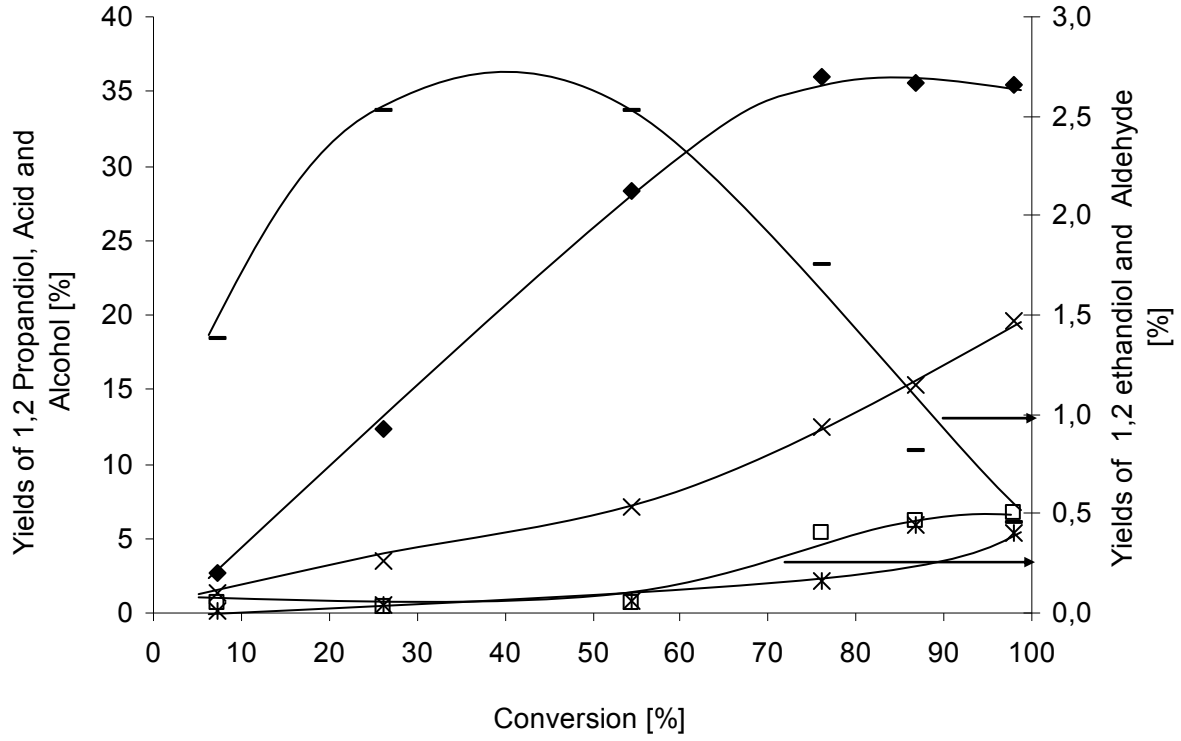

Figure 3.10: Yields of carbon containing liquid products as a function of hydroxyacetone conversion; 1,2-propanediol (◆), aldehydes (acetaldehyde and propanal) (-), monoalcohols (methanol, ethanol and propanol) (x), 1,2-ethanediol (□) and acids (lactic acid, acetic acid and propanoic acid) (∗) (Experimental conditions:3 wt% Pt/Al_2O_3, T 498 K, total pressure 29 bar, Hydroxyacetone concentration 10 wt %)

3.3.5 Surface intermediates followed by ATR-IR spectroscopy

The ATR-IR spectra of the surface species during the reforming of glycerol in the aqueous phase on the Pt/Al_2O_3 catalyst at temperatures between 303 and 498 K and a pressure of 29 bar are shown in Figure 3.11. The assignment of the characteristic bands to the reactant and intermediates is summarized in Table 3.5.

Table 3.5 Band assignments for oxygenated compounds

Wave number [cm $^{-1}$]			Bands Assignment
Glycerol 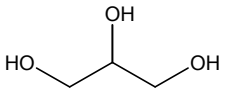	Glyceraldehyde 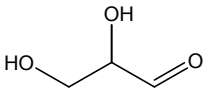	Hydroxyacetone 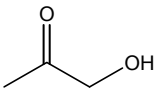	
-	1745	1718	C=O stretching
1402	1370	1417	COH deformation
1322	1300	1361	CH_2 twisting
1203	1254	1228	CH_2 twisting
1108	1142	-	C-O stretching (α - hydroxyl)
1035	1038	1085	C-O stretching (β - hydroxyl)
989	987	960	CH_2 rocking
975	979	-	CH_2 rocking

The bands at 1347, 1290, 1180, 966, 960 cm^{-1} can be assigned to the deformation vibration of COH and to twisting and rocking vibrations the CH_2 groups, which are present in glycerol as well as in the intermediates [20]. Glycerol can be identified by the stretching vibration of C-O at alpha and beta positions at 1085 and 1012 cm^{-1}. The position of the carbonyl bands allows identifying glyceraldehyde (1745 cm^{-1}) and hydroxyacetone (1718 cm^{-1}). The band at 1640 cm^{-1} is assigned to the bending vibration of OH groups in water.

Up to 443 K only water and glycerol were observed in the IR spectra. The two bands at 1745 and 1718 cm^{-1} present above 443 K indicate the formation glyceraldehyde and hydroxyacetone, respectively. At reaction temperatures between 463 and 498 K two broad bands 2045 and 1918 cm^{-1} were additionally observed, which are related to the linear and bridged bonded CO on Pt [21, 22]. Simultaneously to the sorption of CO on the catalyst, two bands 1510 and 1434 cm^{-1} were detected, which are assigned to the asymmetric and symmetric stretching vibrations of the surface carboxylate structure of ethanol and propanol adsorbed on alumina [23]. The large negative band at 1130 cm^{-1} resulted from an incomplete compensation of the band at 1085 cm^{-1} due to its shift to lower wavenumbers with increasing temperature.

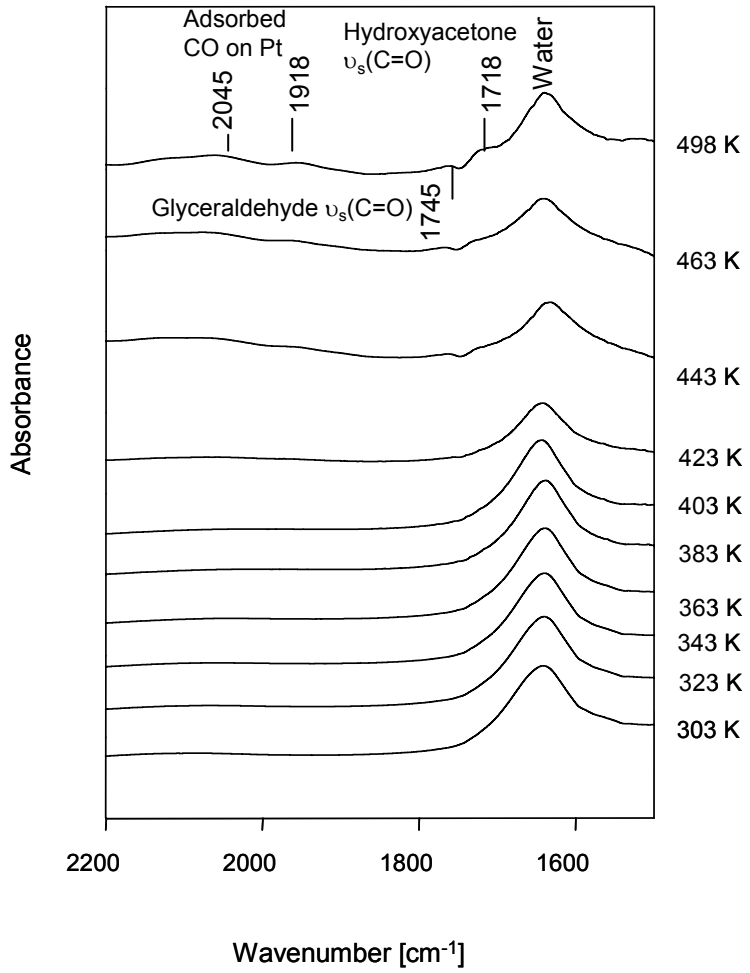
Adsorbed
CO on Pt
2045
1918
Hydroxyacetone
υs(C=O)
1718
Water
Glyceraldehyde υs(C=O)
1745
498 K
463 K
443 K
423 K
403 K
383 K
363 K
343 K
323 K
303 K
Absorbance
2200
2000
1800
1600
Wavenumber [cm-1]

Figure 3.11a

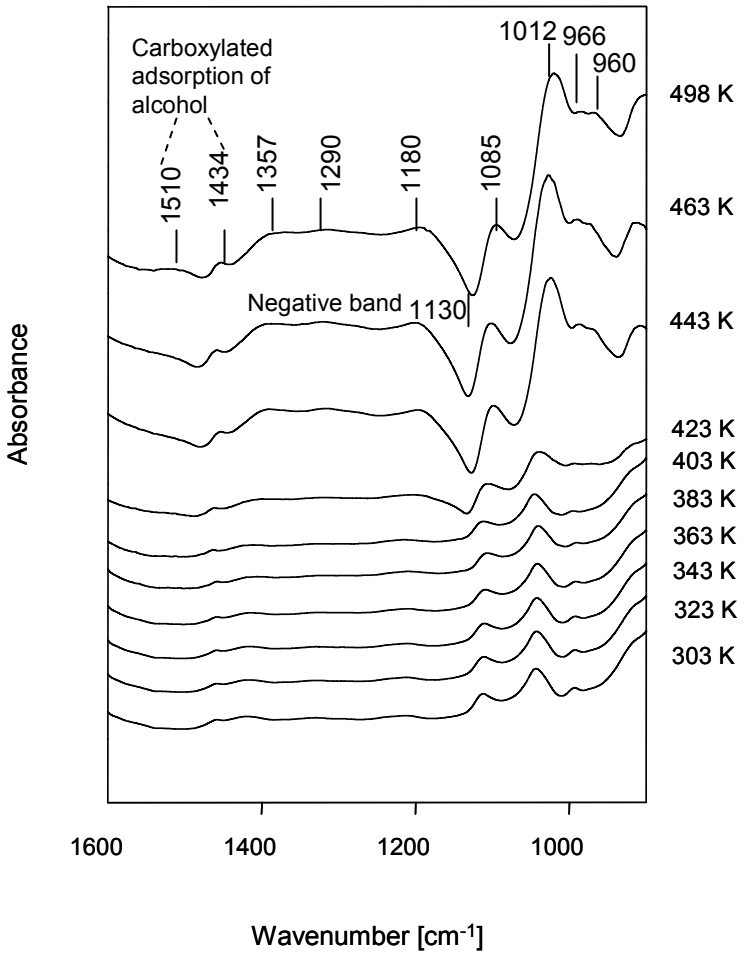

Figure 3.11b

Figures 3.11a/b: ATR-IR spectra during reforming of 20 wt% glycerol on 3 wt% Pt/Al_2O_3, at 29 bar and temperatures indicated

3.4 Discussion

To understand the role of the metal particle size and of the hydrogen partial pressure on the formation of products in the gas and liquid phase the reaction mechanism will be discussed first.

The overall reaction network proposed for the aqueous phase reforming of glycerol to gaseous and liquid products is shown in Figure 3.12. This reaction network is based on the present experimental results and earlier work reported in the literature [5-12, 27-30]. The reaction network contains 4 parallel reaction routes, which were confirmed by the formation of hydroxyacetone (1718 cm^{-1}), glyceraldehyde (1745 cm^{-1}) and CO (1918 and 2045 cm^{-1}) on the catalyst under reaction conditions as observed in the ATR-IR experiments. Route I is the main route for the formation of the gaseous products, the formation of oxygenated compounds containing 2 or 3 carbon atoms in the liquid phase occurs via the reactions in routes II to IV.

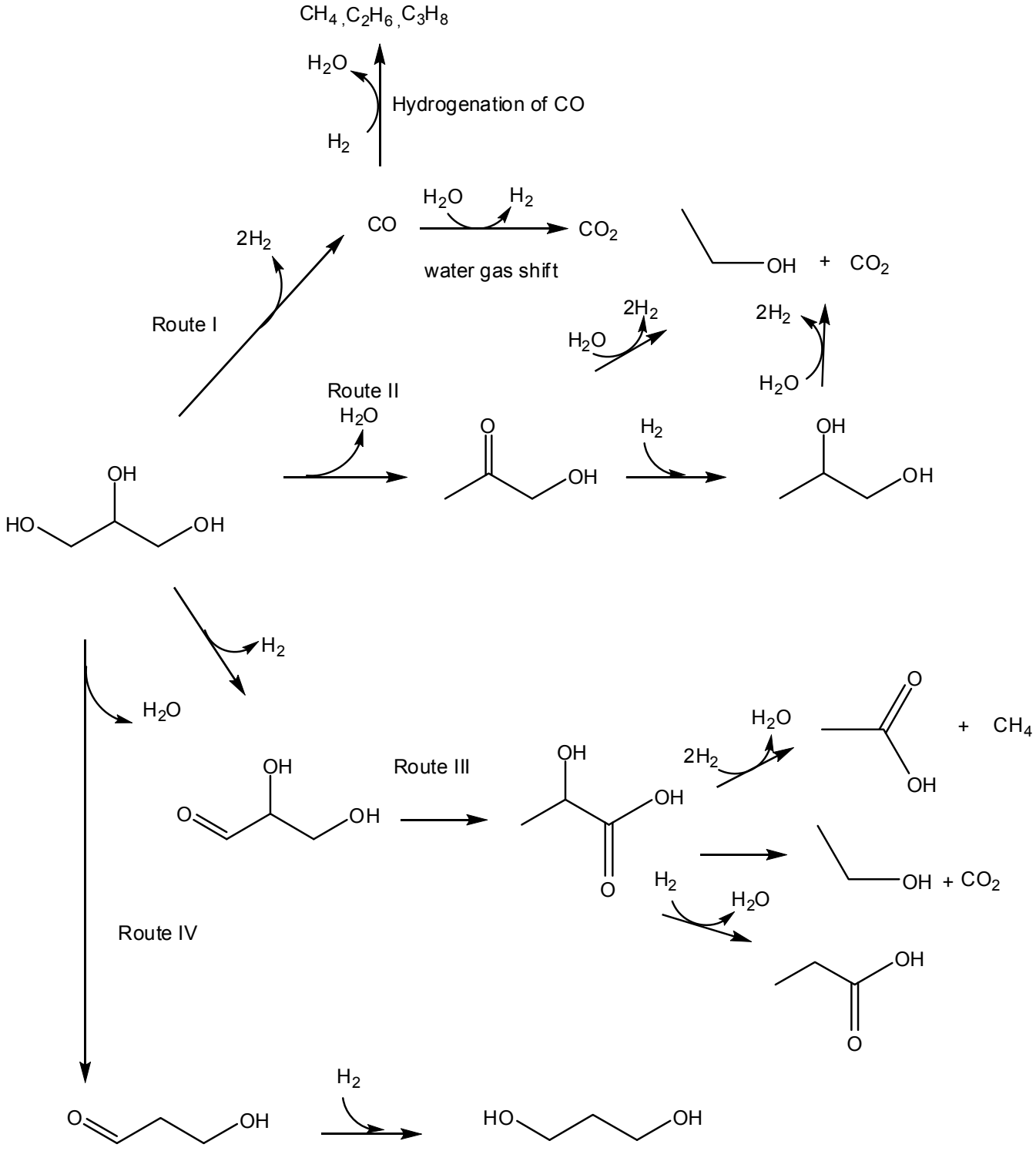

Figure 3.12: Reaction pathways for aqueous phase glycerol reforming

Route I describes the cleavage of the C-C bonds leading to hydrogen and CO, which subsequently reacts via a water gas shift reaction to hydrogen and CO_2. Alternatively, CO can undergo hydrogenation to methane and to higher alkanes, which

were found in significant concentrations compared to methane, via Fischer-Tropsch type reactions. However, using lactic acid and hydroxyacetone as reactants we have shown that methane can be also formed via the demethylation of these intermediates.

Route II describes the formation of 1,2-propanediol via the dehydration of glycerol to hydroxyacetone as intermediate, followed by a subsequent hydrogenation. However, from this intermediate different reactions are feasible. For the reforming of hydroxyacetone [2, 26] a hydrogen to CO_2 ratio of 0.55 was observed, which is significantly lower than stoichiometric ratio expected (H_2/CO_2 = 2.33). This indicates that most of the hydrogen produced was consumed in the hydrogenation of hydroxyacetone to 1,2-propanediol as shown in reaction (7). The present results are in agreement with earlier work of glycerol hydrogenolysis over the metal group VIII supported catalyst [27-29], which also described hydroxyacetone as the major intermediate for 1,2-propanediol formation. Additionally, ethanol can be formed as a (secondary) product via the decarbonylation of hydroxyacetone as shown in equation (8). At high conversion levels the yield of 1,2-propanediol decreases while the yields of ethanol and carbon dioxide increase sharply, which indicates that 1,2-propanediol can undergo further decarbonylation to form ethanol and CO_2.

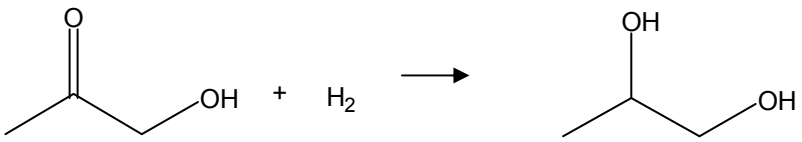

(7)

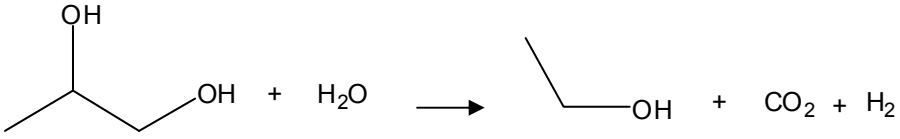

(8)

Route III describes the dehydrogenation of glycerol to hydrogen and glyceraldehyde, which is further converted to lactic acid through a Cannizzaro type reaction by the basic sites of alumina [30-31]. For reaction using lactic acid as reactant methane, CO_2 and propanoic acid were found as main product in the gas and liquid phase, respectively. For the overall reforming reaction of lactic acid a hydrogen to carbon dioxide ratio of 0.52 was observed, which is less than stoichiometric ratio (H_2/CO_2 = 2) expected.

This deviation results from the consumption of hydrogen in reactions leading the methane and the liquid oxygenates via the reduction and demethylation of lactic acid to propanoic acid (reaction 9) and acetic acid (reaction 11) respectively. Also the decarboxylation of lactic acid to ethanol was observed, however this reaction does not consume hydrogen (reaction 10).

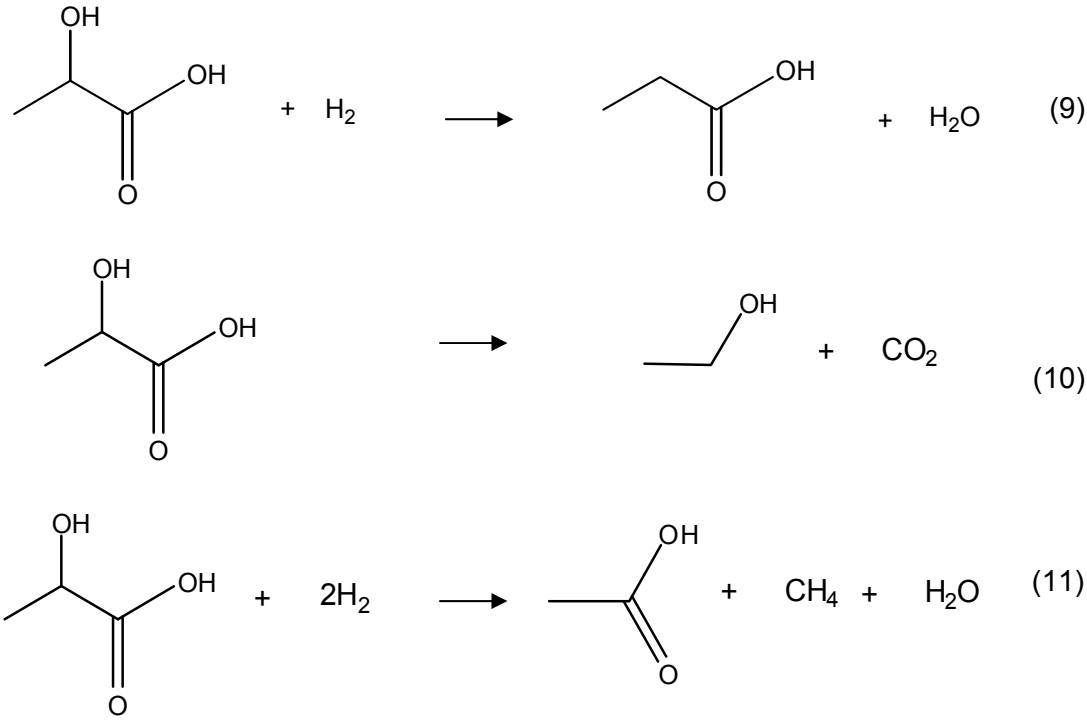

Route IV is the dehydration route of glycerol to 3-hydroxypropioaldehyde, which is rapidly hydrogenated in the presence of hydrogen to 1,3-propanediol [27]. However, only

minor concentrations of 1,3-propanediol were formed compared to 1,2-propanediol, which indicates that this route contributes to a much lesser extent to the formation of products compared to routes I to III.

The yield of the carbon based products as function of the conversion shows that the contribution of the various routes varies considerably with the conversion. At low conversion levels routes I, II and III proceed in parallel. At conversions higher than 50% the yields of 1,2-ethanediol, acids and aldehydes decrease significantly, while the yield of 1,2-propanediol did not further increase, which clearly shows that routes II and III dominate in the conversion of glycerol to ethanol (as secondary products). 1,2-ethanediol, acids and aldehydes are intermediate products, which are further converted to carbon dioxide as it increased sharply at higher conversion. Moreover, the ethanol and carbon dioxide yields increased steadily, while the yield to 1,2-propanediol was constant at conversion levels above 50%. The same trend was observed for the aqueous phase reforming of hydroxyacetone at high conversion levels indicating that ethanol is formed via decarbonylation of hydroxyacetone and 1,2-propanediol.

The hydrogen formation in the aqueous phase reforming reaction was found to be strongly influenced by the size of the metal particles. On the catalyst with the smallest Pt particles (particle size 1.1 nm) the rate to hydrogen formation was about 1.6 times higher compared to the catalyst with a Pt particle size 2.6 nm. It is known that the higher relative concentration of edges and kinks on the surface small Pt particles favors the cleavage of C-H bond [38] and C-C bonds [31-37]. Therefore, reactions proceeding via C-C and C-H cleavage, such as the formation of hydrogen, are enhanced on small Pt particles. Similarly, surface atoms on smaller crystallites also appear to bind $-CH_x$ more strongly resulting in a decrease of the C-H bond activation energy [38]. Therefore, the water gas shift reaction is faster on smaller particles and consequently smaller concentrations of CO were observed over the catalysts with the smaller metal particles. This agrees well with

reports of the structure sensitivity of the water gas shift reaction by Kuijper et al. [39] and Chinchen et al. [40].

In contrast to hydrogen and CO_2, enhanced rates to hydrogenated (e.g., alkanes) and oxygenated products (e.g., 1, 2-propanediol) increased with increasing particle size. Alkanes (methane, ethane and propane) were formed via the hydrogenation of CO and this reaction is typically favored by surface sites of high coordination (i.e., planar sites) [41-47]. The hydrogenation of the C=O bond of the dehydrated intermediate compounds (such as hydroxyacetone) appears to be enhanced by larger particles. Therefore, products such as 1, 2-propanediol are favored over the larger particles, while the hydrogenolysis of the C-C bond leading to methanol is preferred over the smaller Pt particles. This attributed to the fact that large particles interact less strongly with substrate and products. In addition, steric constraints favor the adsorption of the carbonyl bond thus enhancing hydrogenation of the C=O. Similar observations were made previously for the hydrogenation of crotonaldehyde [48].

With increasing pressure the formation of hydrogen, methanol and all carbon containing gaseous products decreased in agreement with refs. [15, 16]. With increasing pressure the coverage of the metal surface with hydrogen, which is available for the reactions in the liquid phase, increases [15]. This will directly enhance the rates for the hydrogenation reactions via routes II, II and IV and lead to increasing selectivities to oxygenated C2 and C3 products in the liquid phase. On the contrary, the trend for the formations of alkanes follows that of the hydrogen and CO_2, which clearly indicated that these products are formed via route I.

Increasing glycerol concentration enhances the rates for the formation of gaseous and liquid phase products. Previous publications on aqueous phase reforming of methanol and 1,2-ethanediol with concentrations up to 10 wt% reported the same trend in hydrogen rate [15]. As the reaction orders with respect to glycerol are positive an increase of the reactant concentration increases rates of liquid products. The similar

orders for gaseous products including hydrogen, carbon dioxide and alkane imply their formation via the same reaction route (route I). The reaction orders of the major liquid phase products formed via reaction route II and III are similar to the overall reaction order of glycerol indicating that these are the rate limiting reactions.

3.5 Conclusions

A reaction network consisting of four parallel routes was established for the aqueous phase reforming of glycerol based on the detection of glyceraldehydes, hydroxyacetone and CO as reaction intermediates by ATR-IR spectroscopy. In the reforming of glycerol hydrogen is produced by hydrogenolysis of the C-C and C-H bonds, the CO formed reacts further via a water-gas shift reaction to H_2 and CO_2 (route I). The generally low temperature of the reaction allows an almost complete conversion of CO, which resulted in favorably low CO concentrations in the gaseous products. For reactions of glycerol to liquid products three routes proceeding (Route II) via the dehydration to hydroxyacetone followed by hydrogenation to 1,2-propanediol (Route III) the dehydrogenation to glyceraldehyde, which is converted to lactic acid and finally reduced to propanoic acid or decarboxylated to ethanol were identified by utilizing hydroxyacetone and lactic acid as reactants in APR condition. The dehydration route from glycerol to 3-hydroxypropioaldehyde (Route IV) followed by hydrogenation to 1, 3-propanediol which formed in the small extent is postulated.

Reforming and water-gas shift are structure sensitive reactions favored by small metal particles, while the hydrogenation/dehydrogenation and hydration/dehydration reactions leading to the oxygenated products in the liquid phase are favored by larger particles. Increasing the overall pressure is speculated to increase the availability of hydrogen on the catalyst enhancing the formation of diols and acids.

Both effects can be advantageously combined for optimizing the catalyst and the process towards formation of hydrogen or liquid phase. Catalysts with small metal

clusters and reactions carried out at lower pressure favor the formation of hydrogen, while catalysts with larger particles and reactions carried out at higher pressure lead to an increased selectivity for products in the liquid phase. Particularly interesting for this type of coupled reactions is the fact that the hydrogen required for the hydrogenation reactions is directly formed by reforming a part of glycerol.

3.6 References

1. D. Wang, D. Montane, E. Chornet, Appl. Catal. A,143 (1996) 245.
2. S. Czernik , R. French, C. Feik , E. Chornet, Ind. Eng. Chem. Res. 41 (2002) 4209.
3. T. Hirai, N. Ikenaga, T. Miyake, T. Suzuki, Energy and Fuels 19 (2005) 1761.
4. B. Zhang, X. Tang, Y. Li, Y. Xu , W. Shen, J. Hydrogen Energy 32 (2007) 2367.
5. S. Adhikari, S. D. Fernando, S. D. T. Filip, M. Bricka, P.H. Steele , A. Haryanto, Energy and Fuels 22 (2008) 1220.
6. R. D. Cortright, R. R. Davda, J. A. Dumesic, Nature 418 (2002) 964.
7. R. R. Davda, J. W. Shabaker, G. W. Huber, R. D. Cortright, J. A. Dumesic, Appl. Catal. B Environmental 56 (2005) 171.
8. J. W. Shabaker, G. W. Huber, J. A. Dumesic, J. Catal. 222 (2004) 180.
9. G. W. Huber, J. W. Shabaker, J. A. Dumesic, Science 300 (2003) 2075.
10. G. W. Huber, J. A. Dumesic, Catal. Today 111 (2006) 119.
11. J. W. Huber, J. W. Shabaker, S. T. Evans , J. A. Dumesic, Appl. Catal. B Environmental 62 (2006) 226.
12. R. R. Davda, J. W. Shabaker, G. W. Huber, R. D. Cortright , J. A. Dumesic, Appl. Catal. B Environmental 43 (2003) 13.
13. J. W. Shabaker, G.W. Huber, R. R. Davda, R. D. Cortright , J. A. Dumesic, Catal. Lett. 88 (2003) 1.
14. J. W. Shabaker, D. A. Simonetti, R. D. Cortright , J. A. Dumesic, J. Catal. 231 (2005) 67.
15. J. W. Shabaker, R. R. Davda, G. W. Huber, R. D. Cortright , J. A. Dumesic, J. Catal. 215 (2003) 344.
16. J. W. Shabaker, J. A. Dumesic, Ind. Eng. Chem. Res. 43 (2004) 3105.
17. P. H. Lewis, J. Catal. 11 (1968) 162.

18. G. Vergeret, P. Gallezot, In: Ertl G, Knözinger H, J. Weitkamp (Eds.) Handbook of Heterogeneous Catalysis. VCH, Weinheim, 1997, Vol 2, p.439.

19. N. J. Harrick, Internal Reflection Spectroscopy, Interscience, New York, 1967.

20. D. Lin-Vien, N.B. Colthup, W.G. Fateley and G. Grasselli, Infrared and Raman Characteristic Frequencies of Organic Molecules, Academic Press: San Diego, 1991.

21. B. E. Hayden, A. M. Bradshaw, Surface Science 125 (1983) 787.

22. F. Kitamura, M. Takede, M. Takahashi, M. Ito, Chem. Phys. Lett. 142 (1987) 318.

23. J. Cunningham, B. K. Hodnett, M. Illyas, J. Tobin, E. L. Leahy and J. L. G. Fierro, J. Chem. Soc. Faraday Discuss. 72 (1981) 283.

24. K. Kunimatsu, H. Uchida, M. Osawa and M. Watanabe, J. Electroanal. Chem. 587 (2006) 299.

25. M. Marquevich, S. Czernik, E. Chornet, D. Montane, Energy and Fuels 13 (1999) 1160.

26. M. C. Ramos, A. I. Navascues, L. Garcia and R. Bilbao, Ind. Eng. Chem. Res. 46 (2007) 2399.

27. T. Miyazawa, K. Kunimori, K. Tomishige, J. Catal. 240 (2006) 213.

28. M. A. Dasari, P. Kiatsimkul, W. R. Sutterlin, G. J. Suppes, Appl. Catal. A: General 281 (2005) 225.

29. S. Wang, H. Liu, Catal. Lett. 117 (2007) 1.

30. C. Keresszegi, D. Ferri, T. Mallat, A. Baiker, J. Phys. Chem. B 108 (2005) 958.

31. A. E. T. Kuiper, J. Medema, J. J. G. M. Bokhoven, J. Catal. 29 (1973) 40.

32. J. R. Anderson, Y. Shlmoyama, Proc. Int. Congr. Catal. 5 (1972) 965.

33. J. K. A. Clarke, J. F. J. Taylor, J. Chem. Soc. Faraday Trans. 174 (1978) 174.

34. R. Maurel, G. Leclercq, J. R. Barbie, J. Catal. 37 (1975) 324.

35. J. Barbier, A. Morales, P. Marecot, R. Maurel, Bull. Sot. Chem. Beiges 88 (1979) 569.

36. J. P. Brunelle, A. Sugier, J. F. Le Page, J. Catal. 43 (1976) 273.

37. C. Corolleur, F.G. Gault, D. Juttard, G. Maire, J.M. Muller, J. Catal. 27 (1972) 466.

38. J. Wei, E. Iglesia, J. Phys. Chem. B 108 (2004) 4094.

39. E. G. M. Kuijpers, R. B. Tjepkema, W. J. J. van der Wal, Appl. Catal. 25 (1986) 139.

40. G. C. Chinchen, M. S. Spencer, Catal. Today 10 (1991) 293.

41. C. H. Bartholomew, R. B. Pannell, J. L. Butler, J. Catal. 65 (1980) 335.

42. C. S. Kellner, A. T. Bell, J. Catal. 75 (1982) 251.

43. M. Boudart, M. A. McDonald, J. Phys. Chem. 83(11) (1984) 2195.

44. R. C. Reuel, C. H. Bartholomew, J. Catal. 85 (1984) 63.

45. L. Fu, C. H. Bartholomew, J. Catal. 92 (1985) 376.

46. M. A. MacDonald, D. A. Storm, M. Boudart, J. Catal. 102 (1986) 386.

47. M. H. Al-Dahhan, M. P. Dudukovic, Chem. Eng. Sci. 51 (1996) 2139.

48. M. Englisch, A. Jentys, J.A. Lercher, J. Catal. 166 (1997) 25.

49. V. K. Jones, L. R. Neubauer, C. H. Bartholomew, J. Phys. Chem. 90 (1986) 4832.

Chapter 4

Influence of the nature of the supports on the reaction pathway

Abstract

The influence of catalyst support acid base and the redox properties on the activity and selectivity of noble metals based catalysts for aqueous phase reforming of glycerol is reported. Partially reducible supports such as ZrO_2 and TiO_2 enhance the selectivity to alkanes and lower the CO formation, whereas in absence of a polar support surface the selectivity towards CO is the highest among the catalysts investigated. The presence of Brønsted acid sites on silica alumina favors the formation of alcohols via enhancing dehydration and decarboxylation reactions. Catalysts containing Lewis acid and basic sites (Pt/ZrO_2 and Pt/ASA) form via Cannizzaro type reactions.

4.1 Introduction

The worldwide increasing production of bio-fuels from renewable sources leads to an overproduction of glycerol in an aqueous solution being the byproduct from the biodiesel transesterification process. To improve the overall economic situation of the bio-diesel production, reaction routes for utilizing glycerol, preferably in the aqueous phase without further purification, are required. One alternative is to produce hydrogen from glycerol, which can be used as clean energy source and for hydrogenation reactions in the chemical industry.

Another option is to utilize glycerol as feedstock for the production of commodity chemicals such as diols, alcohols and acids. Aqueous phase reforming provides the potential for both reaction routes. Suitable catalysts include supported metal catalysts and the reaction is carried out in the liquid phase at temperatures between 453 and 533 K and the pressure required to maintain liquid phase reaction conditions (10 – 50 bar) [1-11].

The influence of the metal particle size and the reaction conditions on the reaction pathways of aqueous phase reforming of glycerol to hydrogen and oxygenated liquid phase products over Pt/Al_2O_3 catalysts is described in chapter 3 [12]. The reaction network is composed of 4 parallel pathways as shown in Figure 4.1.

Route I describes the C-C bond cleavage to form H_2 and CO, which is further converted to CO_2 and H_2 via water gas shift and to alkanes via hydrogenation of oxygenates or surface hydrocarbon fragments. Most products formed via this route are gaseous. The other three pathways describe the reactions to liquid phase products. Route II is the dehydration of glycerol to hydroxyacetone followed by hydrogenation to 1, 2-propanediol. Ethanol, which is a secondary product in this route, is selectively formed via decarbonylation of hydroxyacetone and 1,2-propandiol. Route III is the dehydrogenation of glycerol to glyceraldehyde and lactic acid, which is further dehydrated, decarbonylated and decarboxylated to propanoic acid, acetic acid and ethanol, respectively. Reaction route IV is the dehydration of glycerol to 3-hydroxypropioaldehyde followed by hydrogenation to 1, 3-propanediol. These reactions have been explored previously with analogous polyols. The redox properties of the supports are expected to influence the hydrogenation of CO [13,14] and the water gas shift reaction [15,16] (reaction route I), while the dehydration of oxygenated compounds (route II and IV) is expected to be catalyzed by acid catalysts [9,17,18]. The activity of Pt supported on a series of supports including ZrO_2, C, TiO_2, SiO_2-Al_2O_3, CeO_2, ZnO and Al_2O_3 was already studied for the aqueous phase reforming of 1,2-ethanediol at 498 K and 29.4 bar [9]. The dehydration reaction route of 1,2-ethanediol to acetaldehyde and ethanol was described as an acid-catalyzed reaction. Moreover, hydrogenolysis of glycerol was studied over Ru supported on carbon mixed with Amberlyst (used as acid catalysts component), which provided high selectivity to 1, 2-propanediol (55%) at 13% conversion due to the combination of the high activity of Amberlyst for the dehydration of glycerol to hydroxyacetone and the activity of the metallic component for the

hydrogenation of hydroxyacetone to 1, 2-propanediol [19]. Basic sites catalyze the disproportionation of an aldehyde lacking a hydrogen atom in the alpha position (reaction route III) [20] to an acid such as lactic acid trough a Cannizzaro type reaction [17].

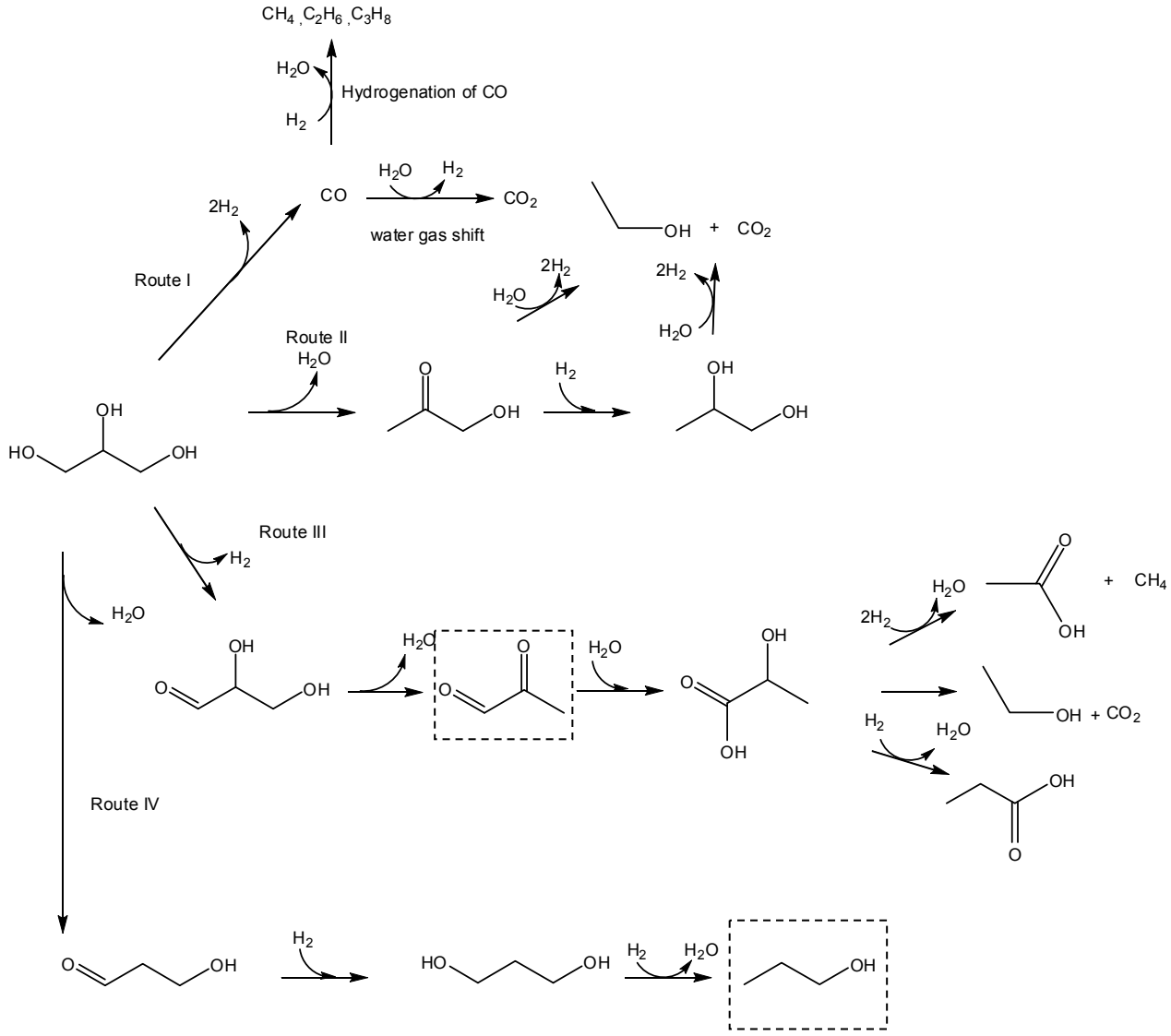

Figure 4.1: Proposed reaction network of aqueous phase glycerol reforming of glycerol hydrogenolysis adapted from Chapter 3. The species in dotted line are revised version.

The focus of the present contribution is related to the role of the acid, basic and redox sites of the support on the activity and selectivity to gaseous and liquid products in the aqueous phase conversion of glycerol.

4.2 Experimental Section

4.2.1 Catalysts preparation

The catalysts containing 3 wt % Pt were supported on carbon, ZrO_2, Al_2O_3, TiO_2 and ASA (amorphous silica-alumina) and prepared by incipient wetness impregnation using an aqueous solution of platinum(II)-ammonium nitrate (Strem chemicals) as Pt precursor. The supports were ZrO_2 (MEL Chemicals), activated carbon (Norit), Al_2O_3 (Aeroxide Alu C-Degussa), TiO_2 (Aldrich) and ASA (Aldrich, 14 wt% Al_2O_3). The ZrO_2 support was prepared from zirconium hydroxide by calcination in air at 673 K for 3 hours. After impregnation of the support the catalysts were dried under air at 393 K for 12 hours and subsequently calcined in synthetic air for 2 hours at 573 K (heating rate 1K/min). Prior to the kinetic tests the catalyst were reduced in H_2 at 623 K for 2 hours using a (heating rate 0.5 K/min).

4.2.2 Catalysts characterization

Atomic absorption spectroscopy (AAS)

The concentration of Pt was determined by atomic absorption spectroscopy using a UNICAM 939 AA-Spectrometer. Typically 20-40 mg of the sample was dissolved in a mixture of 0.5 ml of hydrofluoric acid (48%) and 0.1 ml of nitro hydrochloric acid at its boiling point (ca. 383 K).

Hydrogen chemisorption

The fraction of accessible Pt atoms was determined by H_2 chemisorption using a Sorptomatic 1990 Series sorptometer (Porotec Sorptomatic 1990 Automated BET). Approximately 1g of catalyst was reduced in H_2 at 588 K for 1 hour, followed by out gassing for 4 hours. The sorption isotherms were measured at 308 K. The amount of

chemisorbed hydrogen was obtained after removing physisorbed hydrogen from the sample by evacuation at 308 K. The metal dispersion was determined by assuming H/Pt ratio of 1 [21].

Nitrogen physisorption

The BET surface area and pore size distribution were determined by N_2 adsorption–desorption at 77 K using a Sorptomatic 1990 Series instrument after activation of the sample in vacuum at 573 K.

Temperature programmed desorption (TPD)

TPD of ammonia and carbon dioxide was performed in a 6 fold parallel reactor system using flow conditions. The catalysts were activated in He at 623 K for 1 hour using a heating rate from room temperature to 623 K of 5 K /min. Ammonia or carbon dioxide were adsorbed by adding 10 vol. % into in the He carrier gas (total flow 30 ml/min) at 423 K or 308 K, respectively. Subsequently, the samples were purged with He for 2 h in order to remove physisorbed molecules. For the temperature programmed desorption experiments the 6 samples were sequentially heated from 373 K to 1033 K for ammonia desorption and from 308 to 673 K for carbon dioxide desorption experiments with a rate of 10 K/min in helium (flowrate 30 ml/min). The species desorbing were monitored by mass spectrometry (Balzers QME 200). In each set of experiments a reference sample with known concentration of acid sites was used for the calibration of the MS signal. For quantification of the total acidity a standard with known acid site concentration was used. The response for the CO_2 signal was calibrated using the decomposition of $NaHCO_3$.

Pyridine adsorption followed by IR spectroscopy

IR spectra were measured from 4000 to 1100 cm^{-1} with a resolution of 4 cm^{-1} using a Perkin Elmer 2000 spectrometer. For the adsorption of pyridine, a self supporting wafer was pressed and activated at 623 K (increment 5 K/min) for 90 min. After cooling to 423 K, the spectrum of the activated sample was recorded. Pyridine was adsorbed at 423 K with a partial pressure of $2x10^{-2}$ mbar for 30 min and the sample was subsequently evacuated until the IR spectra remained constant. The concentration of Brønsted and Lewis acid sites was calculated according to the method published by Lercher et.al. [22].

4.2.3 Kinetic experiments

The activities of the catalysts for the aqueous-phase reactions of glycerol were studied in a micro reactor system as described in chapter 3. The reactor was a stainless-steel tubular reactor (1/4 inch-o.d.) containing a packed bed of 50-150 mg of the pressed and crushed catalyst with a particle size of 300 - 500 µm. The catalytic reactions were carried out at 498 K and 29 bar using an aqueous solution containing 20 wt.% glycerol prepared from glycerol in spectrometer grade, ≥99.5% (Aldrich) (H_2O/C = 6.81). The WHSV (gram of glycerol per gram of catalyst per hour) was varied between 7-15 hr^{-1} in order to maintain conversion levels below 10%, which allows using the differential model for treating the kinetic data. Prior to the reaction the catalysts were reduced in H_2 and before the reaction the system was purged and pressurized with nitrogen. To ensure stable state conditions, each experiment was carried out for 24 hours. The carbon products selectivities were calculated by as described in Equation 1. (The carbon balance was within ±5% errors).

$$Carbon\ Selectivity\ of\ species\ i\ (\%) = \frac{C\ atom\ in\ species\ i\ of\ products}{Converted\ glycerol\ based\ on\ carbon\ atom} \times 100 \qquad (1)$$

4.2.4 In situ ATR-IR spectroscopy during reactions

A trapezoidal crystal of ZnSe (size 27.7x10x2 mm with) with an angle of 60° (three active reflections) was used in a home-built stainless steel cell as described in chapter 3. The surface of internal reflection element (IRE area 4x16mm) was coated with an aqueous suspension of the 3 wt% Pt/γ-Al_2O_3 catalyst or with alumina powder (50 mg catalyst and 500 mg deinoized water prepared in an ultrasonic bath at 318 K). The water in the suspension was evaporated at room temperature for 6 hours and the thin film catalyst coated on the IRE was reduced in hydrogen at 513 K with 1K/min for 1 hour. The thickness of the film was around 4 μm (based on alumina density of 3.27 g/cm^3).

The IR spectra under reaction conditions were taken at a resolution of 4 cm^{-1} by accumulating 32 interferograms. After the reduction of catalysts, a liquid glyceraldehyde solution (20wt %) was pumped into the ATR cell with a HPLC pump at a rate of 0.01 ml/min. The pressure of the system adjusted to 29 bar and the temperature was increased from room temperature to 498 K with the rate of 3K/min.

4.3 Results

4.3.1 Catalysts characterization

The specific surface area, the metal dispersion and the concentration of acid/base sites of the Pt catalysts are summarized in Table 4.1. Pt/C has the highest specific surface area and dispersion followed by Pt/ASA, Pt/Al_2O_3, Pt/ZrO_2 and Pt/TiO_2. TPD of ammonia and carbon dioxide are shown in Figures 4.2 and 4.3, respectively. For ammonia on Pt/ASA and Pt/Al_2O_3 catalysts two distinct maxima were observed in the TPD, which indicate the presence of two sites with different acid strength sites, while for

the Pt/C, Pt/ZrO_2 and Pt/TiO_2 only one maximum was present. The CO_2 desorption of Pt/C, Pt/Al_2O_3, Pt/TiO_2 and Pt/ASA led to very small desorption peaks due to the small

amount of CO_2 retained except for Pt/ZrO_2. On all catalysts only one desorption maximum at 370 - 400 K was observed.

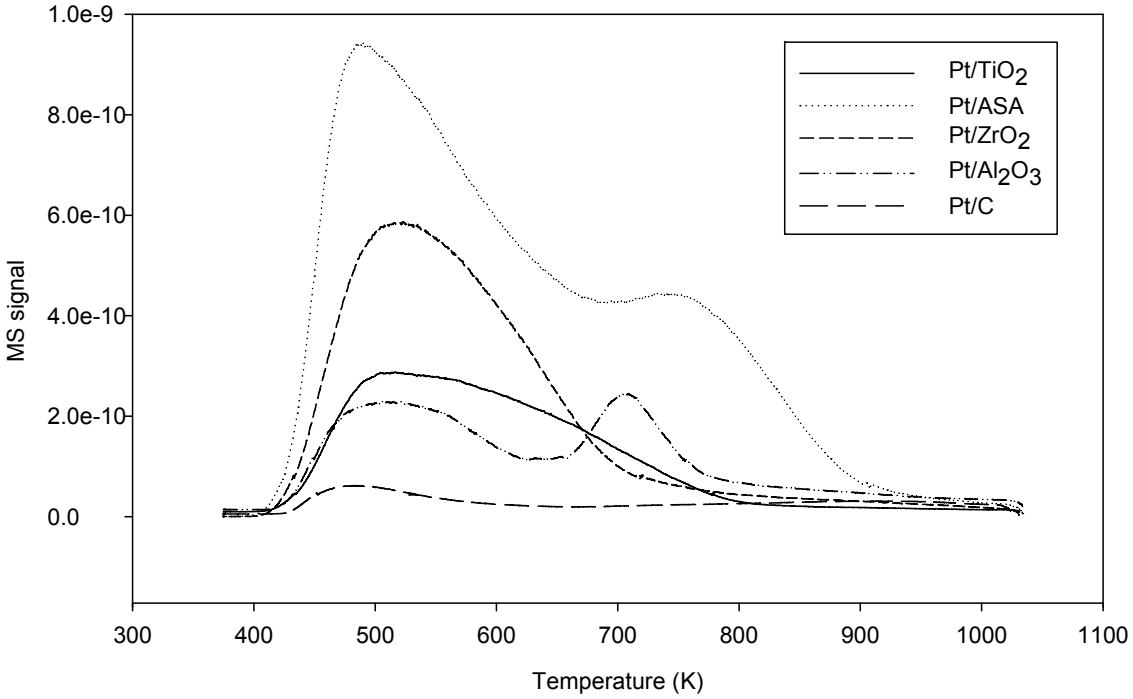

Figure 4.2: Temperature desorption of ammonia of Pt supported catalysts

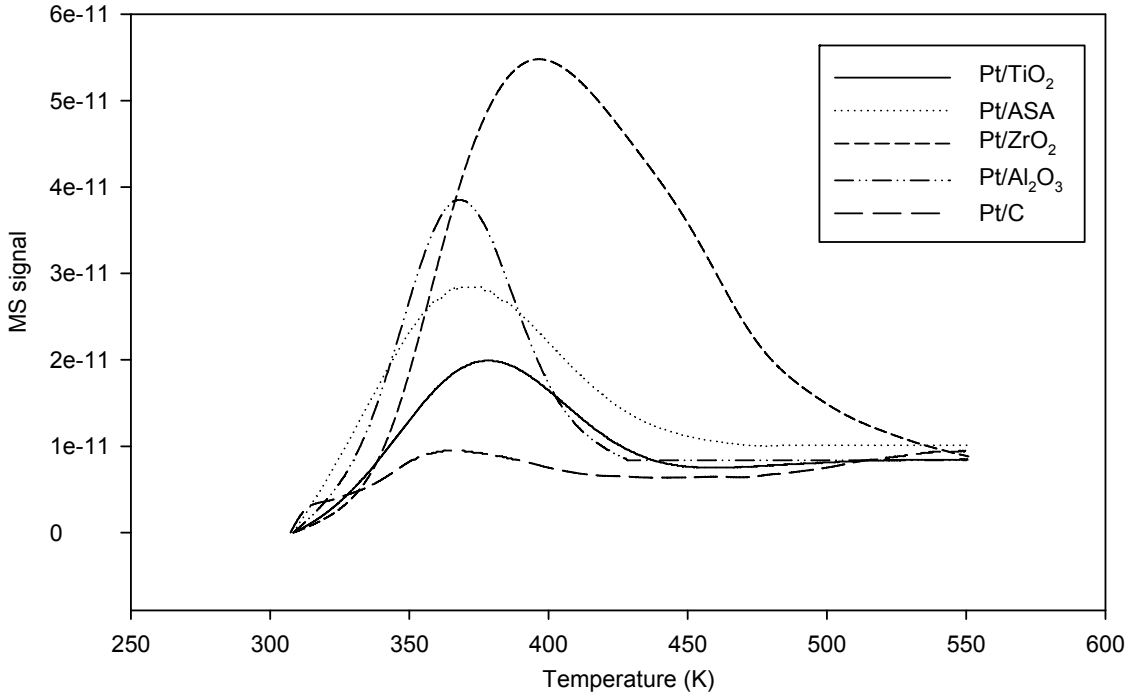

Figure 4.3: Temperature desorption of carbon dioxide of Pt supported catalysts

The type of acid sites present on the oxide samples was determined by IR spectroscopy using pyridine as probe molecule. The IR spectra of the oxide supported catalysts after adsorption of Pyridine and evacuation at 423 K are shown in Figure 4.4. Bands assigned to pyridine adsorbed on Brønsted acid sites (1544 cm^{-1}) were only observed with Pt/ASA, while pyridine adsorbed on Lewis acid sites (bands at 1455 cm^{-1}) was observed on all samples. The highest concentration of Lewis acid sites was observed on Pt/ASA followed by Pt/ZrO_2, Pt/Al_2O_3 and Pt/TiO_2. Comparing the results of desorption of ammonia and pyridine adsorption results, Pt/Al_2O_3 contained no Brønsted acid sites in stead there were two groups of Lewis sites on the surface (i.e., weak and strong ones) as two maxima peaks of ammonia desorption curve were observed. The concentrations of Brønsted and Lewis acid sites are summarized in Table 4.1 and showed perfect agreement with the concentration of acid sites determined by temperature programmed desorption of ammonia.

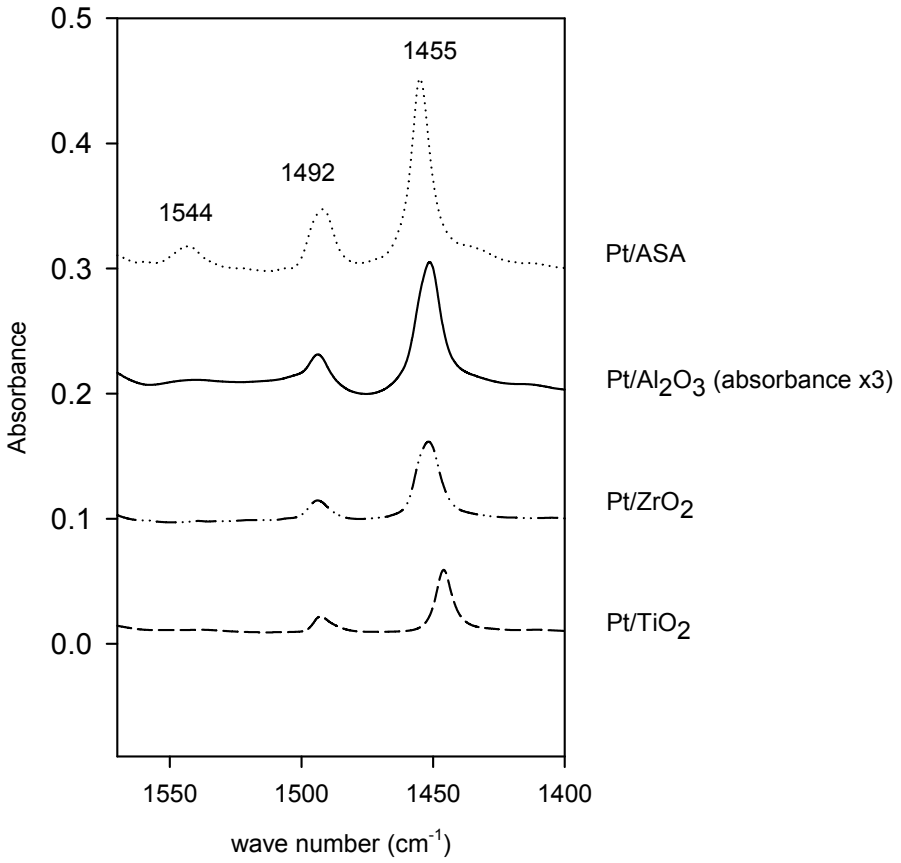

Figure 4.4: IR study of pyridine adsorbed on the series of Pt/ASA, Pt/alumina, Pt/TiO_2 and Pt/ZrO_2 at T = 423 K

Table 4.1: Catalysts characterization results

Catalysts	Surface area (m^2/g)	H/Metal ratio	Acidity ($mmolNH_3/g$)	Acidity (mmol/g) (Pyridine adsorption)		Basicity ($mmolCO_2/g$)
				Lewis	Brønsted	
Pt/ASA	439	0.75	0.60	0.46	0.11	0.05
Pt/Al_2O_3	104	0.75	0.15	0.14	-	0.05
Pt/TiO_2	55	0.76	0.16	0.16	-	0.03
Pt/ZrO_2	92	0.47	0.26	0.25	-	0.16
Pt/C	861	0.95	0.01	-	-	0.005

4.3.2 Catalytic activity

The gaseous products of the aqueous phase glycerol reforming over supported Pt catalysts were hydrogen, CO_2, CO and alkanes (C1-C3). The highest rate of hydrogen formation was achieved over Pt/Al_2O_3 catalysts followed by Pt/ASA, Pt/C, Pt/ZrO_2 and Pt/TiO_2 (see Figure 4.5). The selectivities to gas phase and liquid phase products are presented in Figure 4.6 and Table 4.2, respectively. The total amount of gaseous products was the highest on Pt/ZrO_2, followed by Pt/TiO_2, Pt/Al_2O_3 and Pt/ASA. Within the gaseous products Pt/ZrO_2 and Pt/TiO_2 catalysts had a higher selectivity to alkanes, while the selectivity to hydrogen was higher on the Pt/ASA and Pt/Al_2O_3 catalysts. Generally, low concentrations of CO were formed over the oxide based catalysts in the aqueous phase reforming reaction as summarized in Figure 4.7. The highest concentration of CO was formed over Pt/C (4600 ppm) followed by Pt/ASA and Pt/Al_2O_3 (about 450 ppm) and Pt/TiO_2 and Pt/ZrO_2 were the lowest concentration of CO (110 – 260 ppm) was observed.

The selectivities of the products formed in the liquid phase are summarized in Table 4.2. The selectivities of 1,2-propanediol and 1,3-propanediol are in a similar range

(~ 30 % for 1,2-propanediol and 0.3 - 0.9% for 1,3-propanediol). 1,2-Ethanediol was formed with a selectivity of ~ 10 % on carbon, ASA and Al_2O_3 supported catalysts, while

on Pt/ZrO_2 and Pt/TiO_2 the selectivity was lower (~6%). Alcohols (1-propanol and ethanol) and aldehydes (propanal and acetaldehyde) were obtained with higher selectivity over Pt/ASA and Pt/Al_2O_3. For lactic acid, propanoic acid and acetic acid, the highest selectivity was reached on Pt/ASA and Pt/ZrO_2 followed by Pt/TiO_2 and Pt/Al_2O_3.

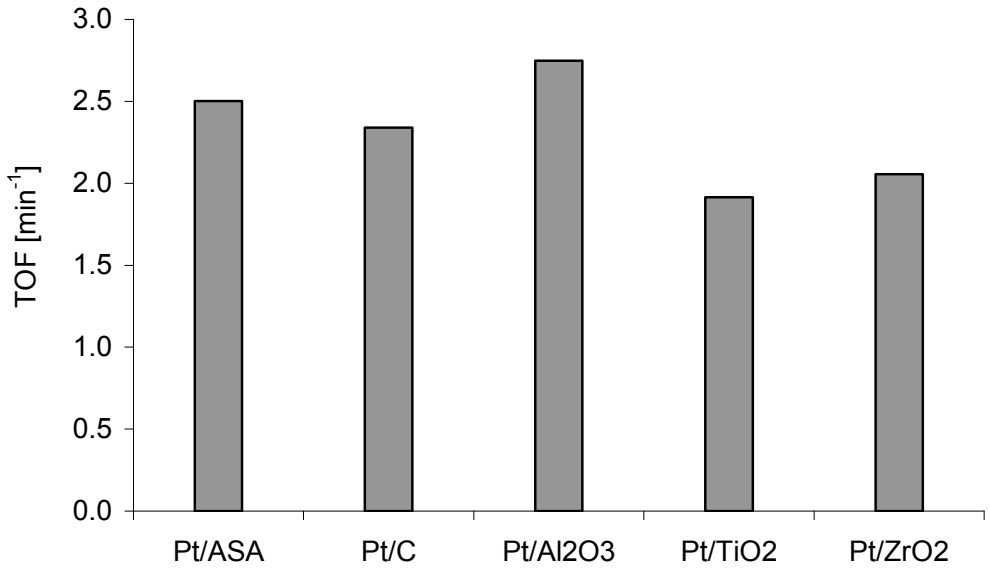

Figure 4.5: Hydrogen formation rate of Pt supported catalysts (Experimental conditions: T= 498 K, total pressure = 29 bar, Glycerol concentration = 20wt%, conversion at 10%)

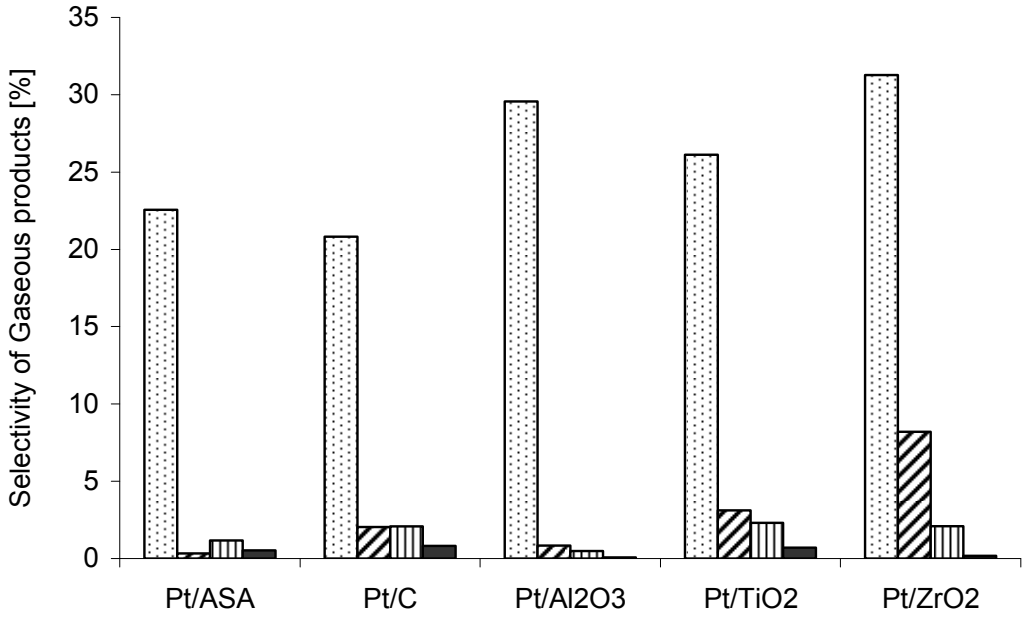

Figure 4.6: Gaseous products selectivity based on carbon atom carbon dioxide (⬚), methane (▨) ethane (▥) and propane (■). (Experimental conditions: T= 498 K, total pressure = 29 bar, Glycerol concentration = 20wt%, conversion at 10%)

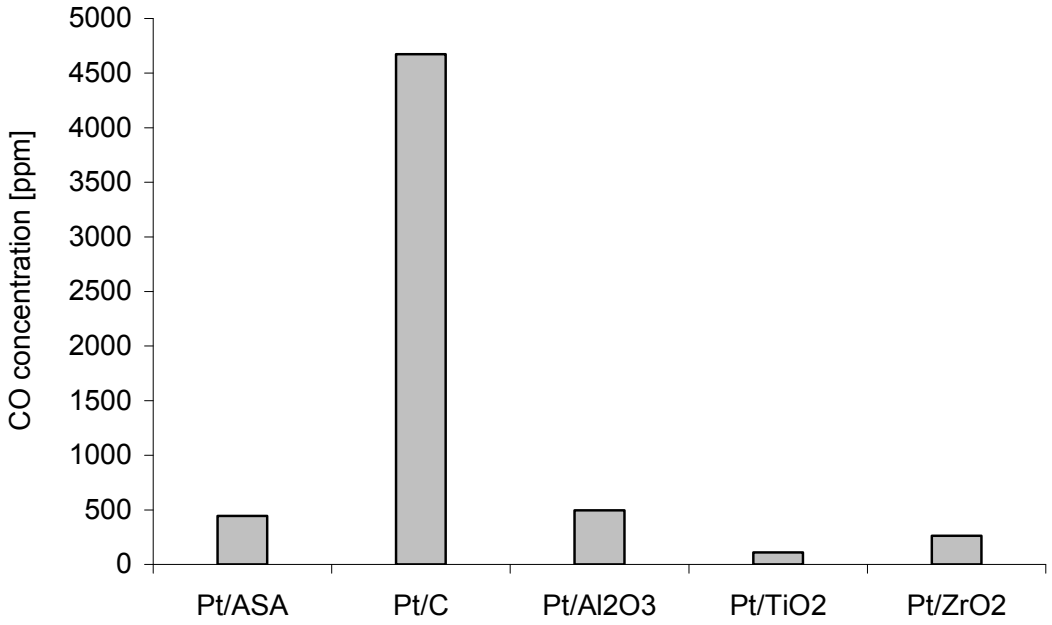

Figure 4.7: CO formation from metal supported catalysts (Experimental conditions: T= 498 K, total pressure = 29 bar, Glycerol concentration = 20wt%, conversion at 10%)

Table 4.2: Carbon containing products Selectivity based on carbon atom from Pt on different supports (Experimental conditions: T= 498 K, total pressure = 29 bar, Glycerol concentration = 20wt%, conversion at 10%)

Catalysts	Selectivity (%) based on carbon atom									
	PG	PD	EG	Acetol	Meth	Eth	Pro	Ald	Acid	Gas
Pt/ASA	28.9	0.1	10.1	6.2	0.9	18.7	3.4	1.3	3.7	25.4
Pt/C	28.8	0.7	9.4	11.6	2.5	10.0	1.8	2.3	2.0	26.0
Pt/Al_2O_3	31.9	0.9	11.4	6.0	2.2	12.0	2.8	1.0	2.1	31.0
Pt/TiO_2	34.8	0.2	5.6	10.8	0.1	10.1	1.1	0.6	2.4	32.2
Pt/ZrO_2	30.7	0.3	5.9	8.4	0.3	10.1	1.6	0.7	4.8	41.8

The symbols used in the table are described below:

PG: 1, 2-propanediol

PD: 1, 3-propanediol

EG: 1, 2-ethanediol

Acetol: hydroxyacetone

Eth: ethanol

Meth: methanol

Prop: propanol

Ald: Summation of acetaldehyde and propanal

Acid: Summation of acetic acid, propanoic acid and lactic acid

Gas: Summation of carbon dioxide, alkane (C1-C3) and carbon monoxide

4.3.3 Surface reaction study

The major product in liquid phase of all Pt catalyst was 1,2-propanediol, which did not vary as a function of the support used, while for the formation of acids and alcohols the acid/base properties of the support are crucial. To determine the reaction route for the formation of acids and alcohols (postulated to proceed via glyceraldehyde as intermediate after dehydrogenation of glycerol [12]) the reforming reaction of glyceraldehyde over Pt/Al_2O_3 was followed by *in situ* ATR-IR spectroscopy.

The reaction was carried out at 29 bar and temperatures from 303 K to 498 K, the IR spectra of the surface intermediates are shown in Figure 4.8. The wavenumbers of the IR bands of potential intermediates and products are summarized in Table 4.3. The bands of the carbonyl groups of glyceraldehyde, pyruvaldehyde and lactic acid at 1745, 1728 and 1717 cm^{-1}, respectively were used to differentiate among these compounds. The band at 1728 cm^{-1} (pyruvaldehyde) appears at 403 K. Increasing the temperature to 443 K led to bands at 1717 and 1456 cm^{-1}, which are assigned to carbonyl and carboxylic stretching vibrations of lactic acid. The negative band at 1170 cm^{-1} first present at 423 K, is attributed to an incomplete compensation of the band at 1129 cm^{-1} due to its shift to lower wavenumbers with increasing temperature.

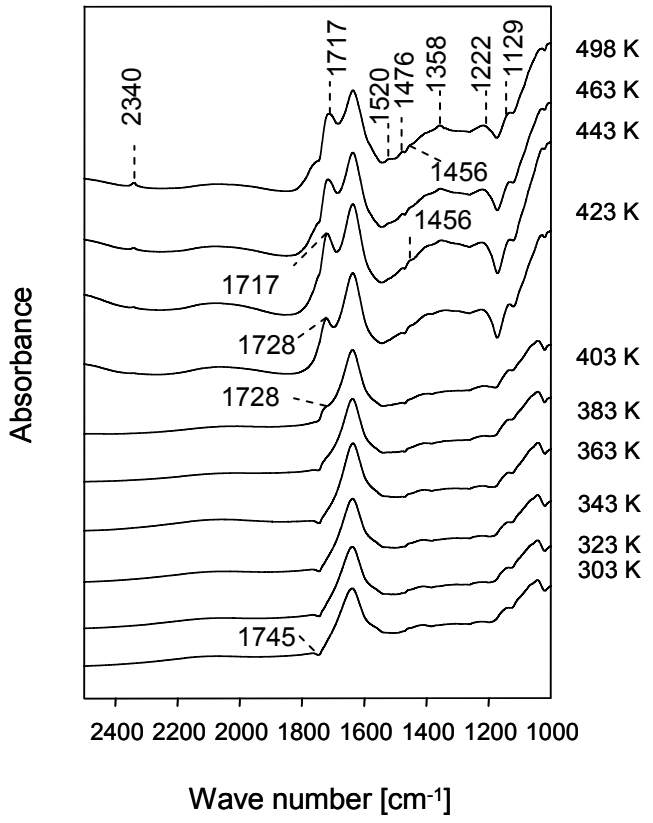

Figure 4.8: ATR-IR spectra of Pt/Al_2O_3 at different temperature at 29 bar with glyceraldehyde 20wt% in the range of wave number 2400 – 1000 cm^{-1}

Table 4.3 Band assignment of oxygenated compounds

Wave number (cm^{-1})			Bands Assignment
Glyceraldehyde 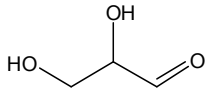	Pyrualdehyde 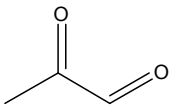	Lactic acid 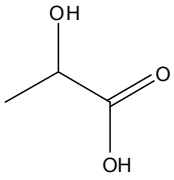	
1745	1728	1717	C=O stretching
-	-	1456	COO stretching
1402	-	-	COH deformation
-	1388	1376	CH_3 deformation
-	1362	1357	CH_3 deformation
1370	1268	1286	CH_2 twisting
1254	1245	1232	CH_2 twisting
-	1175	-	C=O(H) stretching
1142	-	1129	C-O stretching (α - hydroxyl)
-	1087	-	C=O(H) stretching
1038	-	1030	C-O stretching (β - hydroxyl)

At 463 K, a band at 2340 cm^{-1} is observed, which is assigned to CO_2 adsorbed on basic sites of alumina [23]. At 498 K, bands at appeared 1520 and 1476 cm^{-1} assigned to the asymmetric and symmetric stretching vibrations of carboxylate species formed after sorption of ethanol on alumina [24]. The bands at 1358, 1222 and 1129 cm^{-1} represent the deformation vibrations of CH_3, the twisting modes of CH_2 and stretching vibration of C-OH at alpha position in lactic acid. The product from the reaction at temperature 498 K was analyzed by GC-MS confirming that lactic acid and ethanol were formed.

4.4 Discussion

Gaseous products

The reaction network described in chapter 3 together with the intermediates identified by ART IR spectroscopy (which are presented in the dotted line) is shown in Figure 4.1. Hydrogen, carbon dioxide and methane were the main reaction products in the gas phase. These products were typically formed via reaction route I. After the C-C bond cleave of glycerol CO remains adsorbed on the Pt surface [12], which can react further via CO-hydrogenation and water gas shift reaction. On reducible supports the highest concentration of methane was formed. The strong metal support interaction of Pt/ZrO_2 and Pt/TiO_2 preferably activates the C=O bond at support-metal boundary site [13], which enhances the activity for hydrogenation. This additional reaction consumes hydrogen and, therefore, a lower hydrogen selectivity compared to Pt/ASA and Pt/Al_2O_3 was observed. Although SMSI effects are typically observed on catalysts calcined at higher temperatures, a certain degree of polarity on the particle parameter is already present even at lower temperatures [14].

The activity of Pt based catalysts for the water gas shift reaction is relatively high, therefore only small concentrations of CO were observed in the product [8, 15]. However, the thermodynamic equilibrium concentration of CO in the APR of glycerol at 498 K 29 bar is 7 ppm [25], which is significantly smaller than the observed CO concentration in the product and indicates that water gas shift reaction is not fully equilibrated. Pt supported on reducible carriers such as TiO_2 and ZrO_2 generally showed higher activity for the water gas shift reaction compared to Pt/Al_2O_3 and Pt/ASA. Over reducible supports the WGS reaction can proceed via an associative mechanism over formate intermediate species, which are formed by the reaction of CO initially adsorbed on Pt with hydroxyl groups of the reducible support at the metal-support interface [26]. The reducible supports such titanium dioxide and zirconium dioxide can decompose the intermediate formate species

thus enhancing the low temperature water gas shift reaction [15]. The activity for the water gas shift reaction at low temperature (473 – 523 K) showed that Pt on an irreducible support such as Al_2O_3) has a lower activity than on a reducible support such as TiO_2 [15,16]. Moreover, the hydrogen formation rates from the reducible supports (Pt/TiO_2 and Pt/ZrO_2) are lower which indicates that hydrogen is further consumed in the hydrogenation of CO. Thus, hydrogen production can be enhanced by the suppression of hydrogenation reactions of CO.

Liquid phase products

The major product in liquid phase 1,2-propanediol, small amounts of 1,3-propanediol were formed via reaction routes II and IV, which are not influenced by the support. Acid oxygenated products were produced in higher amounts on the catalysts with higher concentrations of Lewis acid and basic sites such as Pt/ZrO_2 and Pt/ASA. As previously shown in chapter 3, propanoic acid and acetic acid are converted from lactic acid via reaction route III, with lactic acid as product of a Cannizzaro type reacting of glyceraldehyde (shown in Figure 4.1). The dehydrogenation of glycerol to glyceraldehyde (reaction route III) is favored on catalysts with Lewis acid sites trough the abstraction of hydride ions [27] and the basic site catalyzed Cannizzaro type reaction [28,20].

The reaction pathway to lactic acid formation from glyceraldehyde over Pt/Al_2O_3 is reflected by the IR spectra of the adsorbed species during reaction. The stretching carbonyl band (1728 cm^{-1}) of pyruvaldehyde appeared at 403 K and the conversion to lactic acid at 423 K is indicated by the appearance of the stretching vibrations of carbonyl and carboxylic groups at 1717 and 1456 cm^{-1} (for the overall reaction see Equation 2). Glyceraldehyde is first dehydrated to pyruvaldehyde, which is subsequently converted to acids via Cannizzaro type reactions. Cannizzaro type reactions of aldehydes that do not have an α–hydrogen (such as benzaldehyde), were reported to form a mixture of carboxylic acids and alcohols in the presence of the basic sites [20]. Pyruvaldehyde is

selectively adsorbed on basic sites covalently bound to the oxygen as shown in Equation 3 and adsorbed on Lewis acid sites as shown in Equation 4 and can subsequently react to carboxylate and alcoholate species via hydride ion shift from adsorbed species (Equation 5).

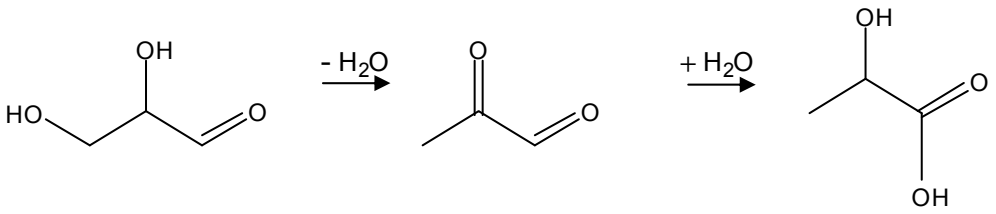

(2)

Glyceraldehyde Pyruvaldehyde Lactic acid

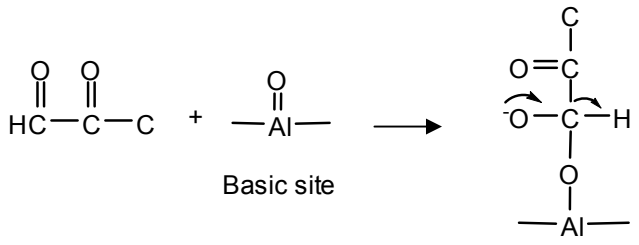

(3)

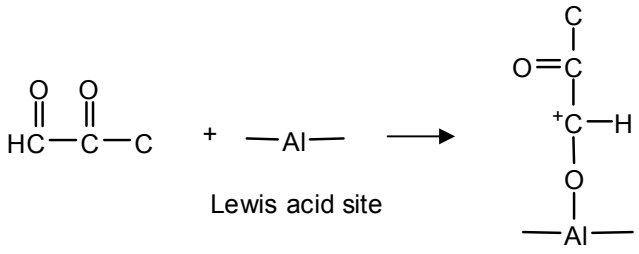

(4)

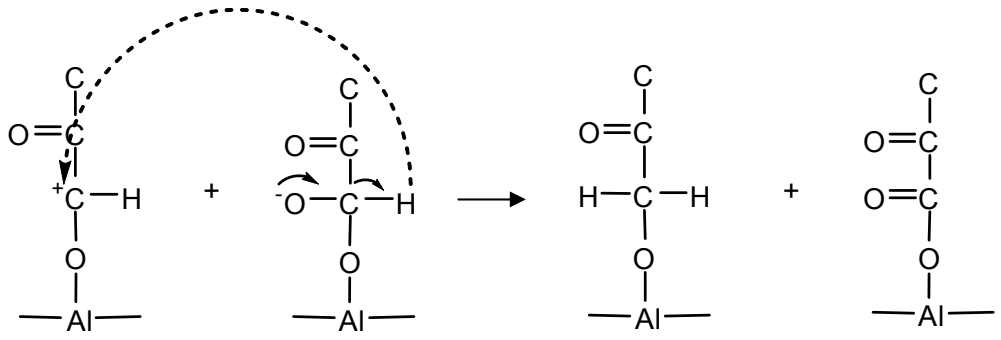

(5)

The adsorbed alcoholate and lactate species undergo further decarbonylation and decarboxylation reactions, respectively, to form ethanol (1520 and 1476 cm^{-1}) and carbon

dioxide (2340 cm^{-1}) which were observed to be adsorbed above 463 K on. Hydroxyacetone can undergo decarbonylation reactions (route II) whereas lactic acid further reacts via decarboxylation to ethanol (Route III). On catalysts containing Brønsted acid sites (Pt/ASA) and strong Lewis acid sites (Pt/Al_2O_3), it was observed that the higher the formation of ethanol the lower the amount of hydroxyacetone was produced. Previously it was described that decarbonylation and decarboxylation of oxygenated compound are enhanced by both Brønsted [29,30] and strong Lewis acid sites [30,31]. The proton is donated to the electron rich electron lone pair at the carboxyl/carbonyl oxygen thus weakening the C-C bond [30]. As the results, carbon dioxide and ethanol are produced (equation 6 and 7).

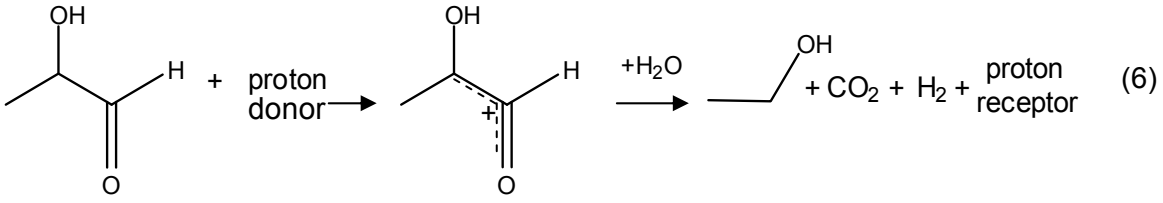

(6)

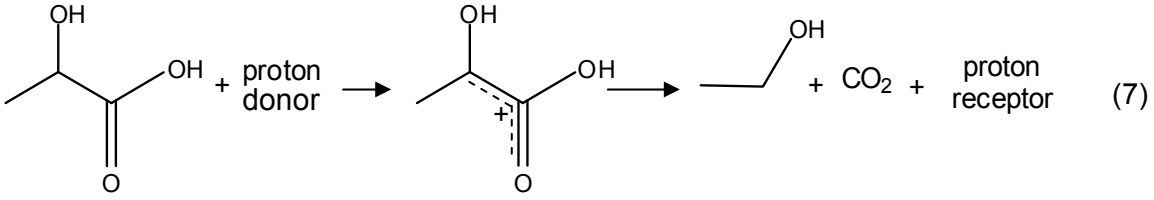

(7)

On the other hand, in the presence of strong Lewis acid site of Pt/Al_2O_3, it activated the C=O bond [32] of hydroxyacetone and lactic acid via the lone electron pair of the oxygen atom. Hydroxyacetone and lactic acid lose protons subsequently produced negatively charged at carbonyl and carboxyl ions which further undergo heterogeneous cleavage to form CO_2 and negatively changed ethanol ion which react with proton to from ethanol respectively.

In addition1-propanol is produced higher content from the Brønsted acidic on ASA supports as shown in Equation 8. A similar result for the dehydration of 1, 3-propanediol to propanol over Pt/ZSM5 was reported [33]

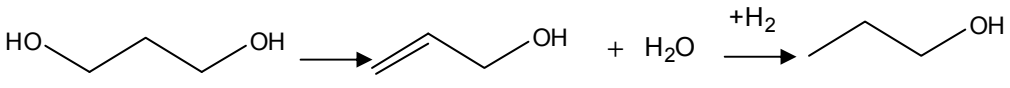

(8)

Only small concentrations of 1,2-ethanediol aldehyde, methanol and propanol observed on Pt supported on reducible oxides supports, while they produced higher amounts of alkanes via the activation of the C-O bond at the metal-support interface boundary [13] This further indicates that 1, 2-ethanediol aldehyde, methanol and propanol are precursors for the alkanes formation over Pt on reducible supports.

4.5 Conclusions

The activity and selectivity of supported precious metals in the aqueous phase reforming of glycerol to hydrogen and chemical intermediates is strongly influenced by the acid base and redox properties of the support. Pt supported on reducible supports such as TiO_2 and ZrO_2 formed the lowest amount of CO, while supports with weak interaction to the supported metal such as activated carbon led to the highest CO formation. This trend is explained by the fact that the redox properties and the polar interface at metal oxide boundary of TiO_2 and ZrO_2 weaken the carbonyl bond in CO which improves the CO hydrogenation and the water gas shift reaction. Brønsted acid sites present in ASA and strong Lewis acid sites on Al_2O_3 enhance the decarbonylation of hydroxyacetone, the decarboxylation of lactic acid to ethanol. The dehydration of 1, 3-propandiol to propanol is enhanced over Brønsted acid sites of Pt/ASA. The presence of Lewis acid-base sites (Pt/ZrO_2, Pt/Al_2O_3 and Pt/ASA) enhances the formation of acid oxygenated compounds through the dehydrogenation of glycerol to glyceraldehyde and the disproportionation of glyceraldehyde.

4.6 References

1. R. D. Cortright., R. R. Davda, J. A. Dumesic, Nature 418 (2002) 964.
2. J. W. Shabaker, G. W. Huber, R. D. Cortright., Ind. Eng. Chem. Res. 43 (2004) 3105.
3. J. W. Shabaker, G. W. Huber, J. A. Dumesic, J. Catal. 222 (2004) 180.
4. G. W. Huber, J. W. Shabaker, J. A. Dumesic, Science 300 (2003) 2075.
5. R. R. Davda, J. W. Shabaker, G. W. Huber, R. D. Cortright, J. A. Dumesic, Appl. Catal. B Environmental 56 (2005) 171.
6. G. W. Huber, J. A. Dumesic, Catal. Today 111(2006) 119.
7. G.W. Huber , J. W. Shabaker, S.T. Evans, J. A. Dumesic, Appl. Catal. B Environmental 62 (2006) 226.
8. R. R. Davda, J. W. Shabaker, G. W. Huber, R. D. Cortright, J. A. Dumesic, Appl. Catal. B Environmental 43 (2003)13.
9. J. W. Shabaker, G. W. Huber, R. R. Davda, R. D. Cortright., J. A. Dumesic, Cat. Lett. 88 (2003).
10. J. W. Shabaker, D. A. Simonetti, R. D. Cortright., J. A. Dumesic, J. Catal. Vol. 231 (2005) 67.
11. J. W. Shabaker, R. R. Davda, G. W. Huber, R. D. Cortright, J. A. Dumesic, J. Catal. 215 (2003) 344.
12. A. Wawrzetz, A. Hrabar, A. Jentys, A. A. Lemonidou, J. A. Lercher, PCCP submitted (2008).
13. K. Hayak, R. Kramer, Z. Paal, Appl. Catal. A General 162 (1997) 1.
14. E. V. Benvenutti, L. Franken, C. C. Moro, Langmuir 15 (1999) 8140.
15. H. Iida, A. Igarashi, Appl. Catal. A Genenal 298 (2006) 152.
16. P. Panagiotopoulou, D. I. Kondarides, Catal. Today 112 (2006) 49.
17. W. Turek, J. Haber, A. Krowiak, Appl. Sur. Sci. 252 (2005) 823.

18. N. Ichikawa, S. Sato, R. Takahashi, T. Sodesawa,
J. Mol. Catal A Chem. 256 (2006) 106.
19. T. Miyazawa, K. Kunimori, K. Tomishige, J. Catal. 240 (2006) 213.
20. C. Keresszegi, D. Ferri, T. Mallat, A. Baiker, J. Phys. Chem. B 109 (2005) 958
21. P. H. Lewis, J. Catal. 11 (1968) 162.
22. L. Ong, R. Olindo., J. A. Lercher, preparation for publication, PCCP (2009).
23. J. P. Peri, J. Phys. Chem. 70 (1966) 3168.
24. J. Cunningham, B. K. Hodnett, M. Ilyas, J. Tobin, E. L. Leahy, J. L. G. Fierro,
Faraday Discuss. Chem. Soc. 72 (1981) 283.
25. N. Luo, X. Zhao, F. Cao, T. Xiao, D. Fang, Energy and Fuels 21 (2007) 3505
26. G. Jacobs, L. Williams, U. Graham, D. Sparks D., B. H. Davis,
J. Phys. Chem. B 107 (2003) 10398.
27. W. L. Schuettea, A. E. Schweizer, Studies in Surf. Sci. and Catal. 134 (2001) 263.
28. W. L. Evans, Chem. Revs. 31 (1941) 537.
29. S. Vitolo, B. Bresci, M. Seggiani, M. G. Gallo, Fuel 80 (2001) 17.
30. A. Takemura, H. Nakamura, K. U. Taguchi,
Ind. Eng. Chem. Prod. Res. Dev. 22 (1985) 215.
31. A. Zecchina, S. Coluccia, C . Morterra, Appl. Spectrosc. Rev. 21(3) (1985) 259.
32. P. Gallezot, D. Richard, Catal. Rev. Sci. Eng. 40 (1998) 81.
33. K. Murata, I. Takahara, M. Inaba, React. Kinet. Catal. Lett. 93 (2008) 59.

Chapter 5

Summary

Summary

Glycerol is the biomass-derived byproduct formed during bio-diesel production. Nowadays the worldwide trend of increasing production of bio-fuels results in an overproduction of glycerol. The utilizing of glycerol to produce hydrogen and chemicals are the attractive alternative. This study focuses on hydrogen and oxygenated products formation via the aqueous-phase reforming process over Pt supported catalysts which carried out at relative low temperature (453 K – 533 K) and pressures (10 – 50 bar).

The selection of potential catalysts for the reforming of glycerol in the liquid phase is described in **Chapter 2**. The catalysts selection was done by firstly screening different metals supported on the alumina including Pt/Al_2O_3, Pd/Al_2O_3, Ni/Al_2O_3, Ru/Al_2O_3 and Rh/Al_2O_3. The hydrogen formation rate decreased in the order Pt > Pd > Rh > Ru > Ni at 498 K and 29 bar. The Pt catalyst exhibited the highest rate for H_2 formation (1.84 min^{-1}) with the lowest alkane selectivity (1%), the lowest formation of CO f (200 ppm) and high selectivtivity to 1,2-propanediol (32%). The selectivity of the metals for reactions to gaseous products were assigned to the different properties of the metal. The water gas shift reaction is favored on Pt, while Pd exhibited the lowest activity and consequently the highest amount of CO was formed. A high selectivity of saturated alkane C1-C3 with the selectivity about 10% was observed for Rh, Ru and Ni. In addition oxygenated liquid phase products were formed.. The major product is 1,2-propanediol (26-40% selectivity), the highest amount was formed over Ru, followed by Pt, Rh, Ni and Pd. On Pd acetic and propanoic acid were formed with a selectivity of 13%. The major reaction for 1, 2-propanediol formation was postulated trough the dehydration of glycerol to hydroxyacetone over the alumina support, which is subsequently hydrogenated to 1, 2-propanediol on the metal surface.

The detailed reaction network of aqueous phase reforming of glycerol on Pt/Al_2O_3 is described in **Chapter 3**. In order to understand the reaction pathways, the influences of the reaction conditions (pressure, space velocity and glycerol concentration) as well as

the effect of the metal particle size were examined. Furthermore the reaction of glycerol was investigated by ATR-IR spectroscopy to identify the reaction intermediates present In addition, aqueous phase reforming of the intermediates identified by ATR (i. e, hydroxyacetone and lactic acid) was done to further confirm the reaction route. In the aqueous phase reforming of glycerol H_2 is produced by hydrogenolysis of the C-C and C-H bonds, the CO formed reacts further via a water-gas shift reaction to H_2 and CO_2. The generally low temperature of the reaction leads to an almost complete conversion of CO, which resulted in favorably low CO concentrations in the gaseous products. For reactions of glycerol to liquid products three routes proceeding via the dehydration to hydroxyacetone followed by hydrogenation to 1,2-propanediol, the dehydrogenation to glyceraldehyde, which is converted to lactic acid and finally reduced to propanoic acid and selectively undergoing decarboxylation reaction to ethanol as well as the dehydration route from glycerol to 3-hydroxypropioaldehyde followed by hydrogenation to 1, 3-propanediol were identified.

The major factors influencing the selectivity are metal particle size and pressure. Catalysts with small metal clusters and reactions carried out at lower pressure favor the formation of hydrogen, while catalysts with larger particles and reactions carried out at higher pressure lead to an increased selectivity for products in the liquid phase. Particularly interesting in this reaction is that the hydrogen necessary for the hydrogenation reactions is formed by coupling with the reforming reaction, thus additional hydrogen in not required.

The influence of the support with respect to the acid/base and redox properties is discussed in **Chapter 4** using Pt supported on Carbon, SiO_2-Al_2O_3, ZrO_2, TiO_2 and Al_2O_3). Acidity and basicity were examined by pyridine adsorption and temperature programmed desorption of ammonia and carbon dioxide, respectively. The Brønsted acid sites present on SiO_2-Al_2O_3 enhanced the propanol formation via dehydration of 1,3-propanediol, while Lewis acid and basic sites favored the formation of oxygenated acid through Cannizzaro

reactions. Pt on reducible supports such as Pt/TiO_2, Pt/ZrO_2 shows a strong metal support interaction, which weakens the carbonyl bond in CO and subsequently improves CO hydrogenation and water gas shift reactions.

Chapter 6

Curriculum Vitae

List of publications and presentations

6.1 Curriculum Vitae

Aonsurang Wawrzetz (Boonyanuwat) was born in Si-Sa-Ket province, Thailand, on 19th Aug 1978. After finishing high school in Bangkok in 1996, she started her chemical engineering course at Mahidol University in May 1996 and received her bachelor degree in 2000. She went on to study further in Petrochemical technology department, Chulalongkorn University under the supervision of Professor Frank R. Steward. She finished her thesis, entitled “steam quality measurement in a high pressure system” and obtained master degree of science in 2002. She was employed as process engineer at Thai Industrial Gases Company (Linde group) until 2005. She joined the Chemical Technology department of Prof. J.A. Lercher at the Technical University Munich in March 2005 to start research on aspects of aqueous phase reforming of glycerol over supported catalysts.

6.2 List of publications

1. A. Wawrzetz, A. Jentys and J.A. Lercher, Proceedings of the DGMK-Conference "Synthesis Gas Chemistry", Dresden, Germany, Hydrogen production by aqueous-phase reforming of glycerol on supported metal catalysts, ISBN 3-936418-57-8, 2006.
2. A. Wawrzetz, A. Hrabar, A. Jentys, A. A. Lemonidou, J. A. Lercher, ready for submission to Physical Chemistry Chemical Physics, influence of metal particle size and reaction conditions on the reaction pathway, 2008.
3. A. Wawrzetz, A. Jentys and J.A. Lercher, ready for submission to Journal of molecular catalysis A, Aqueous phase reforming of Glycerol over Pt/Al_2O_3: influence of the nature of the supports on the reaction pathway, 2008.

6.3 List of presentations

1. DGMK-Conference "Synthesis Gas Chemistry", October 4 - 6, 2006, Dresden, Germany.
   A. Wawrzetz, A. Jentys, J.A. Lercher, oral presentation.

2. 40 Jahrestreffen Deutscher Katalytiker, March 14 - 16, 2007, Weimar, Germany.
   A. Wawrzetz, A. Jentys, J.A. Lercher, poster presentation.

3. IDECAT - Catalysis for Renewable conference, May 16 - May 18, 2006, Rolduc, Kerkrade, The Netherlands.
   A. Wawrzetz, A. Jentys, J.A. Lercher, poster presentation.

4. 41 Jahrestreffen Deutscher Katalytiker, Febraury 27 - 29, 2008, Weimar, Germany.
   A. Wawrzetz, A. Jentys, J.A. Lercher, poster presentation.